Pseudo-lignin Chemistry in Pretreatment of Biomass for Cellulosic Biofuel Production

A Dissertation
Presented to
The Academic Faculty

by

Fan Hu

In Partial Fulfillment
of the Requirements for the Degree
Doctor of Philosophy in the
School of Chemistry and Biochemistry

Georgia Institute of Technology
December 2014

Pseudo-lignin Chemistry in Pretreatment of Biomass for Cellulosic Biofuel Production

Approved by:

Dr. Art Ragauskas, Advisor
School of Chemistry and Biochemistry
Georgia Institute of Technology

Dr. Yulin Deng
School of Chemical and Biomolecular Engineering
Georgia Institute of Technology

Dr. Charles Liotta
School of Chemistry and Biochemistry
Georgia Institute of Technology

Dr. Preet Singh
School of Molecular Science and Engineering
Georgia Institute of Technology

Dr. Seth Marder
School of Chemistry and Biochemistry
Georgia Institute of Technology

Date Approved: July 09, 2014

ACKNOWLEDGEMENTS

Without the love, care, support, and sincere advice from many individuals, this dissertation was impossible to complete. I would like to say “thank you” to all of them. First of all, I would like to express my respectful gratitude to Professor Art Ragauskas for his guidance, mentoring, encouragement and financial support throughout my doctoral research. Under Dr. Ragauskas’ guidance, I have learned and accomplished far more than I had imagined at the beginning of my studies. Not only will the knowledge I gained from him greatly help me in my future endeavors, but also his diligence, dedication and professionalism will always be my model during my career development. In addition, I would also like to thank my thesis committee, Dr. Charles Liotta, Dr. Seth Marder, Dr. Preet Singh, and Dr. Yulin Deng, for their insightful comments and support from the initial to the final stage of my research.

I would like to thank the members from the Ragauskas group, past and present, for their friendship, helpful discussions, and collaborations. My special sincere thanks go to Dr. Yunqiao Pu, Dr. Fang Huang, Dr. Haoxi Ben, Dr. Reichel Samuel, Dr. Seokwon Jung, Xianzhi Meng and Qining Sun. I am also thankful to Dr. Cam Tyson and Michele Yager for their guidance and supports. I also acknowledge the financial support from BioEnergy Science Center at U.S. Department of Energy and the Paper Science & Engineering (PSE) Fellowship program at Institute of Paper Science & Technology (IPST) at Georgia Institute of Technology.

Most importantly, I owe my deepest gratitude to my ex-girlfriend and also the best friend, Karen Tse, for her love, support, and the appearance in my life. Finally I would like to thank myself for the persistence and endeavors during the toughest stage in my life so far.

TABLE OF CONTENTS

LIST OF TABLES

LIST OF FIGURES

LIST OF ABBREVIATIONS

AFEX	Ammonia Fiber Explosion
BSA	Bovine Serum Albumin
CBHI	Cellobiohydrolase
CEL	Cellulolytic Enzyme Lignin
CP/MAS	Cross Polarization/Magic Angle Spinning
CrI	Crystallinity Index
CSF	Combined Severity Factor
DAP	Dilute Acid Pretreatment
DEPT	Distortionless Enhancement by Polarization Transfer
DMSO	Dimethyl Sulfoxide
DP	Degree of Polymerization
EMAL	Enzymatic Mild Acidolysis Lignin
G	Guaiacyl Lignin Unit
GHG	Greenhouse Gas
GPC	Gel Permeation Chromatography
H	*p*-Hydroxyphenyl Lignin Unit
HPLC	High Pressure Liquid Chromatography
HMF	5-Hydroxymethyl Furfural
HSQC	Heteronuclear Single Quantum Correlation
HW	Hardwood
LCC	Lignin–Carbohydrate Complex
LODP	Leveling-off Degree of Polymerization

MWL	Milled Wood Lignin
NA	Not Available
ND	Not Determined
NMR	Nuclear Magnetic Resonance
RFS	Renewable Fuel Standard
RT	Room Temperature
S	Syringyl Lignin Unit
SW	Softwood
SEM	Scanning Electron Microscope
XRD	X-Ray Diffraction

SUMMARY

Bioethanol has been a popular choice as a renewable energy source to supplement fossil fuels because of its high octane number, heat of vaporization, and compatibility with modern motor vehicles. Abundant and renewable lignocellulosic biomass containing large amounts of structural polymeric sugars can play a significant role in the production of fuels and chemicals. To accomplish this, a number of process steps must be applied, with pretreatment being essential to overcome the natural resistance of plant cell walls to decomposition from microbes and enzymes. In general, acid pretreatment does not result in significant delignification; instead, it has been reported of the formation of a lignin-like material termed pseudo-lignin after acid pretreatment from literature. The understanding of fundamental chemistry surrounding pseudo-lignin formation is extremely important from the perspective of bioethanol production because pseudo-lignin may inhibit enzymatic deconstruction of biomass just like native lignin.

The first objective of this thesis focuses on the investigation of the chemistry of pseudo-lignin formation. Various analytical tools such as GPC, FT-IR and ^{13}C NMR were utilized to characterize pseudo-lignin extracted from holocellulose and cellulose treated at various dilute acid pretreatment conditions. The molecular weight and chemical structure information from these characterizations can provide valuable and precious mechanistic insights into the mechanisms of pseudo-lignin formation during pretreatment. The presence and structure of pseudo-lignin is important since this study shows that pseudo-lignin inhibits the enzymatic conversion of cellulose.

The second objective of this thesis aims to further investigate the effects of carbohydrate-derived pseudo-lignin on cellulose saccharification with the purpose of providing plausible mechanisms accounting for enzymatic hydrolysis retardation by pseudo-lignin. Due to the complex structure of cellulosic biomass, the wet chemistry method for compositional analysis defined by National Renewable Energy Laboratory (NREL, Golden, CO) does not distinguish between acid-insoluble lignin (Klason lignin) naturally found in biomass and pseudo-lignin resulting from carbohydrate degradation during pretreatment. Therefore, to avoid the complexity often encountered with interpretation of results for real biomass, pure Avicel cellulose alone or mixed with pure xylan or xylose sugar was pretreated with dilute sulfuric acid over the range of pretreatment severities often found to give the best conversion results. Following pretreatment, the solids were subjected to enzymatic hydrolysis, physical and chemical characterizations to elucidate the effects of pseudo-lignin on enzymatic hydrolysis and support identification of possible mechanisms to explain the results.

The third objective provides a detailed comparison of chemical structures between pseudo-lignin and native lignin after a mild dilute acid pretreatment. As native lignin is one of the major factors contributing to biomass recalcitrance, it is important to evaluate the inhibition effects of pseudo-lignin to enzymatic hydrolysis of cellulose in comparison to lignin. Enzymatic mild acidolysis lignin (EMAL) was isolated from hybrid poplar after a mild dilute acid pretreatment. This EMAL lignin isolation protocol was chosen because of its greater isolation yield compared to milled wood lignin (MWL) and cellulolytic enzyme lignin (CEL) protocols. More importantly, EMAL protocol has been shown to offer access at lignin samples that are more representative of the overall lignin present in

milled wood. The results of the third study revealed that pseudo-lignin is not derived from native lignin, but is even more detrimental to enzymatic hydrolysis of cellulose than dilute acid-treated lignin, thus its formation during acid pretreatment should be avoided. The last part of this thesis focuses on optimization of dilute acid pretreatment conditions to effectively reduce pseudo-lignin formation without significantly changing pretreatment severities. Although lowering pretreatment severity can suppress pseudo-lignin formation, it cannot effectively enhance biomass digestibility. Therefore, dilute acid pretreatment conditions that can reduce pseudo-lignin formation and increase biomass digestibility are essential to biorefining industry. Pseudo-lignin analysis showed that the addition of dimethyl sulfoxide (DMSO) to dilute acid pretreatment reaction medium significantly reduced pseudo-lignin formation, which is attributed to DMSO preferentially solvating and stabilizing the key intermediate, 5-hydroxymethyl furfural (HMF), to prevent it from further reactions to form pseudo-lignin.

CHAPTER 1

INTRODUCTION

As global energy consumption is continuing to rise, the world is pursuing the development of renewable energy sources to address vital strategic, economic and environmental issues related to the depleting fossil fuels [1]. Future reductions in fossil fuel consumptions will reside in a multifaceted approach including nuclear, solar, hydrogen, wind, and particularly biofuels such as bioethanol, which many countries have already initiated by advancing research and development programs [2]. At present, bioethanol production largely represents the first-generation biofuel which is produced from readily processable bioresources such as starch from corn and simple sugars from sugar cane [3,4]. However, as the demand for food resources increases, the search for renewable nonfood resources to displace substantial amounts of biofuels based food resources rests largely on low-cost lignocellulosic biomass [5]. Lignocellulosic biomass, such as wood, grass, and agricultural and forest residues, are the most abundant renewable feedstocks on the planet, with approximately 200 billion tons produced annually in the world [6]. Compared to grain, oil seed, or sugar crops, lignocellulosics have a higher productivity per hectare and require less input per unit of biomass produced than food based sugars and oils [7]. More importantly, lignocellulosic biomass can be acquired from agricultural and forest residues which complement current farm and forest products practices.

According to Renewable Fuel Standards (RFS) which represents a hybrid approach that superimposes a performance-based standard on a set of volumetric targets, the minimum

of volumetric requirement for cellulosic biofuel represents 60% GHG (greenhouse gas) reduction [8]. On November 8 2013, EPA released its proposed rulemaking for the 2014 Renewable Fuel Obligation. The revised cellulosic biofuel mandate was reduced from 1.75 billion gallon to 17 million gallon due to its limited availability [8]. This clearly indicates the need to research and develop technologies to boost cellulosic biofuel production.

To biologically convert lignocellulosic biomass to biofuels, a number of steps must be applied with pretreatment being critical to reduce biomass recalcitrance via altering cell wall structural features so that the polysaccharide fractions (mainly cellulose) locked in the intricacy of plant cell walls can become more accessible and amenable to enzyme attack [9]. Several leading thermochemical pretreatment technologies have been reported to enhance biomass enzymatic digestibility significantly [10]. Dilute acid pretreatment (DAP) is such a representative leading technology, which often results in higher acid-insoluble lignin content than the untreated material [11,12,13,14]. This phenomenon has been hypothesized to be due, in part, to the formation of a lignin-like material termed pseudo-lignin [15,16].

The first part of this thesis (Chapter 4) verified this hypothesis and further demonstrated that pseudo-lignin can be generated from biomass polysaccharides without significant contribution from native lignin during DAP. Pseudo-lignin generated from dilute acid-treated poplar holocellulose and cellulose was isolated, and its molecular weight, chemical structure and morphology were characterized. Equally important, the study in Chapter 4 showed that the presence of pseudo-lignin on the surface of pretreated biomass dramatically lowered cellulose digestibility. To illustrate this inhibition effect caused by

pseudo-lignin while avoiding the complexity encountered with interpretation of results for real biomass, Avicel cellulose alone or mixed with Beechwood xylan or xylose was pretreated with dilute sulfuric acid over a range of optimal conditions that often give the best cellulose-to-glucose conversion yields (Chapter 5). The pretreated solids were then subjected to enzymatic hydrolysis, physical and chemical characterizations to provide possible mechanisms to explain the inhibition effect. During enzymatic hydrolysis, lignin acts as a physical barrier to prevent enzyme access to the carbohydrate fraction of biomass and tends to unproductively bind to enzymes. Therefore, it is essential to compare the inhibition effect of lignin after DAP with that of pseudo-lignin. The study in Chapter 6 was conducted with this purpose, and the results revealed that pseudo-lignin is not derived from native lignin but it is even more detrimental to enzymatic hydrolysis of cellulose compared to dilute acid-treated lignin, clearly indicating the formation of pseudo-lignin during DAP should be avoided. Chapter 7 developed a method to optimize DAP conditions to effectively reduce pseudo-lignin formation without significantly lowering pretreatment severity. Unfortunately, this method could not change the pseudo-lignin molecular weight or any of its structural features significantly. Nevertheless, the study in Chapter 7 is the first demonstration that the amount of pseudo-lignin formed during DAP can be reduced, which contributes to further optimization of DAP technology.

CHAPTER 2

LITERATURE REVIEW

2.1 Cellulosic Ethanol

Biofuels are fuels that contain energy from geologically recent carbon fixation. Due to the rising oil price and the need for energy security, biofuels have increased in popularity. Bioethanol is one of the most important liquid forms of biofuel and is an alcohol made by fermentation. At present, bioethanol is mostly produced from carbohydrates derived from starch crops such as corn or sugarcane, representing the first-generation of biofuel. The U.S. production of the first-generation bioethanol has increased dramatically since 1980 (Figure 2.1) [17]. However, as continued growth in food price and in the number of starving people, first-generation biofuel is threatening food supplies and biodiversity [3,4]. Alternatively, bioethanol can be produced from non-food sources such as lignocellulosic biomass which represents one of the most abundant, renewable and sustainable resource one the plant. This second-generation bioethanol or cellulosic ethanol can help solve the problems of first generation biofuel and can supply a larger proportion of fuel supply sustainably, affordably, and with greater environmental benefits.

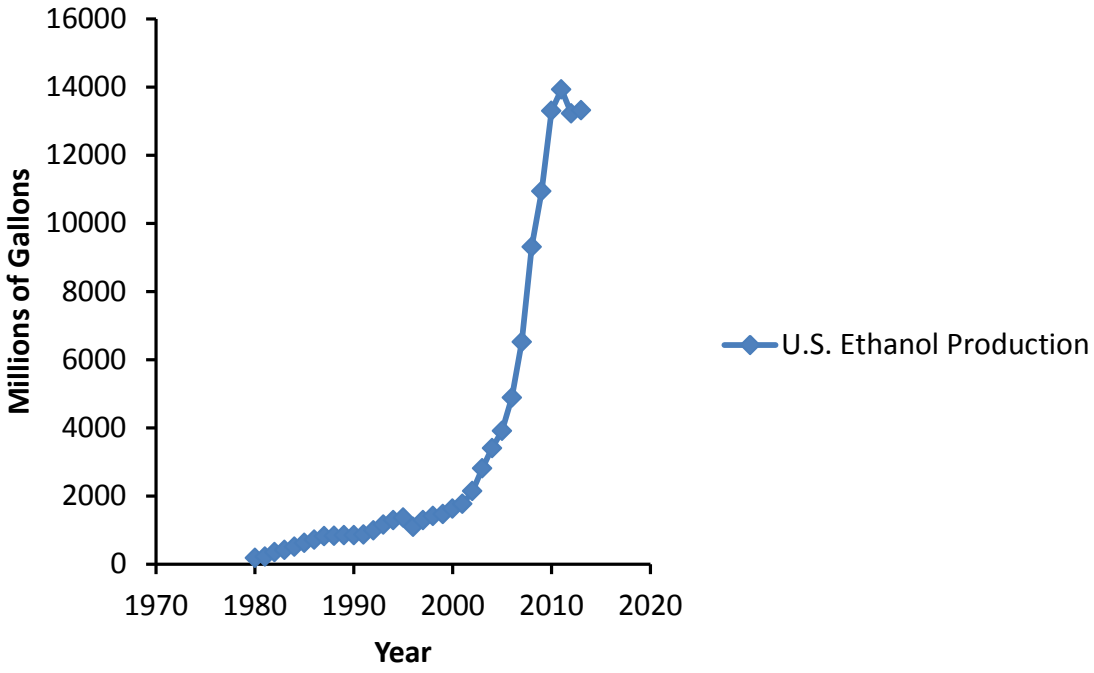

Figure 2.1 The U.S. ethanol production from 1980 to 2013

Production of cellulosic ethanol generally requires more complex processes compared to the first-generation bioethanol (Figure 2.2). For the first generation bioethanol production, the sugar extracted from sugar-rich crops is directly fermented to ethanol. To convert lignocellulosic biomass into cellulosic ethanol, a pretreatment step is usually required to overcome lignocellulosic recalcitrance. The pretreated biomass is then amenable to be accessed by cellulolytic enzymes to convert cellulose to glucose. Subsequently, simple sugars are fermented to ethanol followed by a distillation process separating and purifying ethanol to meet fuel specifications.

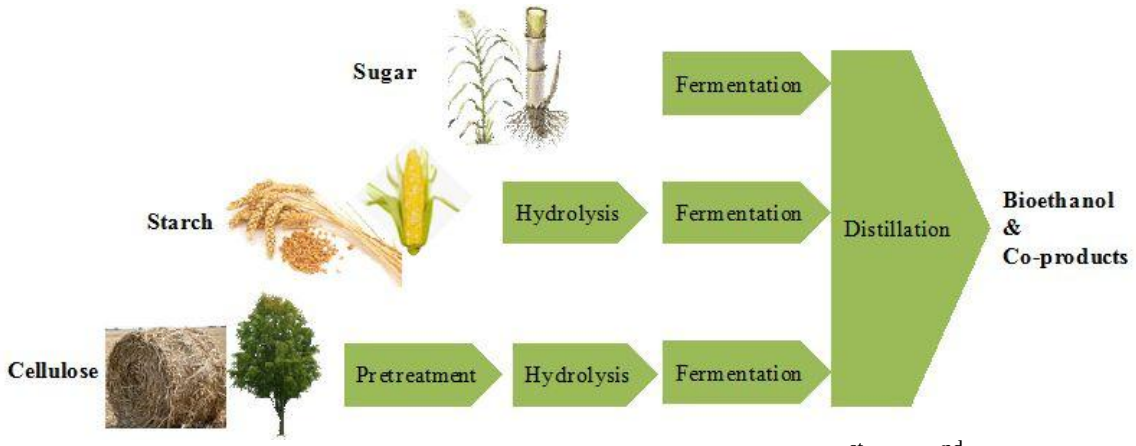

Figure 2.2 An overview of the production process of bioethanol: 1st and 2nd generation bioethanol [18]

2.2 Ligocellulosic Biomass

Most terrestrial lignocellulosics are primarily composed of three major components: cellulose (38–50%), hemicellulose (23–32%), and lignin (10–25%), as well as smaller amounts of pectin, protein, extractives and ash [5,19]. These components together form a complex and rigid structure, leading lignocellulosic biomass to be resistant to biological and chemical deconstruction [6]. Table 2.1 summarizes average contents of these three major components from several common biofuel crops.

Table 2.1 The average contents of major components from common biofuel crops

	Composition (%, dry basis)			Reference
	Cellulose	Hemicellulose	Lignin	
Switchgrass	45	30	12	20
Poplar	45	21	24	21
Miscanthus	48	30	12	22
Corn stover	40	25	17	20
Wheat straw	38	27	20	23
Rice straw	37	34	12	24
Sugarcane bagasse	40	24	25	20
Cotton stalk	31	11	28	25

2.2.1 Cellulose

Cellulose is a linear polymer made up of β-D-glucopyranosyl units linked with 1→4 glycosidic bonds with cellobiose as the repeating unit. The size of cellulose molecule is typically defined by the average number of monomer (glucose) units referred as the degree of polymerization (DP), which can be determined by various analytical techniques including gel permeation chromatography (GPC), light scattering intrinsic viscosity measurements and viscometric methods [26]. The DP of cellulose in plants depends on cellulose origin, cellulose isolation method and even the measurement technique, and the value is typically in the range of 1510 to 5500 (Table 2.2) [26]. Cellulose DP value is very important because it profoundly influences the mechanical, solution, biological, and physiological properties of cellulose.

Table 2.2 the DP of native cellulose from plants [26]

Plant species	DP
Southern pine	1450
Corn kernels	1693
Cotton stalks	1820
Jute fiber	3875
Wheat straw	2660
Rice straw	1820
Corn stover	2520
Poplar	3500
Aspen	4581

Cellulose has a strong tendency to form intra- and inter-molecular hydrogen bonds by the large number of hydroxyl groups on the cellulose chains. These hydrogen bonds stiffen cellulose chains and promote aggregation into a crystalline structure [27]. The most common crystalline form of native cellulose is cellulose I that has parallel glucan chains and strong intramolecular hydrogen bonds. In nature, cellulose I exists as two crystalline suballomorphs, cellulose I_α and I_β. Cellulose I_α has a one-chain triclinic unit cell while cellulose I_β has a monoclinic two-chain unit cell [28]. The relative amounts of cellulose I_α

and I_β have been found to vary between samples from different origins. Whereas cellulose I_α has been found rich in the cell wall of primitive microorganisms such as some algae and in bacterial cellulose, cellulose I_β has been found rich in higher plants such as cotton, wood, and ramie fibers [28]. Cellulose I_α is meta-stable in nature and can be converted to the thermodynamically more stable allomorph (cellulose I_β) by annealing [29,30]. Nishiyama *et al*. [30] proposed that slippage of the glucan chains is the most likely mechanism for conversion of cellulose I_α to cellulose I_β. Both chains in cellulose I_α and I_β are organized in sheets packed in a parallel-up fashion, with the hydroxymethyl groups in the *tg* conformation [30]. Amorphous cellulose can be divided into accessible fibril surface portion and inaccessible fibril surface portion. Accessible fibril surfaces are those in contact with water, while the inaccessible fibril surfaces are fibril-fibril contact surfaces and surfaces resulting from distortions in the fibril interior [11]. In addition to the crystalline and amorphous regions, some researchers used CP/MAS ^{13}C NMR technique to reveal that cellulose also contains a para-crystalline portion, which is less ordered than crystalline cellulose I_α and I_β, but more ordered than the amorphous region [31,32]. Table 2.3 lists the relative contents of crystalline, para-crystalline and amorphous portion of cellulose from three popular biomass feedstocks determined by CP/MAS ^{13}C NMR.

Table 2.3 The relative contents (%) of crystalline, para-crystalline and amorphous portion of cellulose from Populus, Loblolly pine and Switchgrass

Biomass feedstock	I_α	$I_{\alpha+\beta}$	Para-crystalline	I_β	Accessible fibril surface	Inaccessible fibril surface	Reference
Populus	5.0	14.2	31.1	19.8	10.2	18.3	33
Loblolly pine	0.1	30.7	24.8	6.9	33.1	15.6	11
Switchgrass	2.3	8.8	27.3	4.5	5.7	51.3	34

2.2.2 Hemicellulose

Hemicellulose is the second most common polysaccharide in nature [20]. It is amorphous and hydrophilic in the fiber wall and acts as an interfiber bonding agent serving as support for cellulose microfibrils. Unlike cellulose, hemicellulose is composed of combinations of pentoses (xylose and arabinose) and/or hexoses (mannose, galactose, and glucose), and it is frequently acetylated and has side chain groups such as uronic acid and the 4-*O*-methylester. Other sugars such as rhamnose and fucose are also sometimes present in small amounts. The DP of hemicellulose is typically in the range of 50 to 300 [27], which is much lower than that of cellulose.

The chemical nature of hemicellulose is dependent on the source. In general, the dominant component of hemicellulose from hardwoods is glucuronoxylan, while galactoglucomannan or arabinoglucuronoxylan is prevalent for softwoods (Table 2.4) [27]. Xylan is a heteropolysaccharide with a homopolymeric backbone chain of 1,4-linked β-D-xylopyranosyl units [20]. The branches of xylan vary from species to species, which may contain arabinose, glucuronic acid, or the 4-*O*-methyl ether, acetic, ferulic, and *p*-coumaric acids. For example, the C2-OH and C3-OH of hardwood glucuronoxylan are partially acetylated (i.e., 3.5 – 7.0 acetyl groups/10 xylose), whereas softwood xylan polymer is not acetylated and typically is branched with (1→2)-linked pyranoid 4-*O*-methyl-β-D-glucuronic acid and (1→3)-linked β-L-arabinofuranosyl units with an arabinose:uronic acid:xylose ratio of ~1:2:8 [35]. Galactoglucomannan is comprised of (1→4)-linked β-D-glucopyranosyl and D-mannopyranosyl units which are partially acetylated at the C2-OH and C3-OH and partly substituted by (1→6)-linked α-D-galactopyranosyl units [35]. There are generally two different types of

galactoglucomannans in softwoods: one being highly branched with a ~1:1:3 ratio of galactose:glucose:mannose and another that is less branched with a ~0.1:1:3 ratio galactose:glucose:mannose [35]. On the other hand, the glucomannan polymer in hardwoods has little or no branching with a typical glucose:mannose ratio of ~1:1.5 [35]. Table 2.5 summarizes hemicellulose composition and its DP in several hardwood and softwood species.

Table 2.4 The major hemicellulose component in softwood (SW) and hardwood (HW) [27,36,37]

Wood type	Hemicellulose type	Amount (% on wood)	Composition			DP
			Unit	Major ratio	Linkage	
SW	Galactoglucomannan	10-15	β-D-Man*p*	4	1→4	100
			β-D-Glc*p*	1	1→4	
			β-D-Gal*p*	0.1	1→6	
			Acetyl	1		
	Arabinoglucuronoxylan	7-10	β-D-Xyl*p*	10	1→4	100
			4-*O*-Me-α-D-Glc*p*A	2	1→2	
			β-L-Ara*f*	1.3	1→3	
HW	Glucuronoxylan	15-30	β-D-Xyl*p*	10	1→4	200
			4-*O*-Me-α-D-Glc*p*A	1	1→2	
			Acetyl	7		
	Glucomannan	2-5	β-D-Man*p*	1-2	1→4	200
			β-D-Glc*p*A	1	1→4	

Table 2.5 Hemicellulose composition and its DP in several biomass feedstocks [38,39]

		Carbohydrate composition of the hemicellulose		
Biomass	Hemicellulose	Sugar residues	Molar ratio	DP
Birch	Glucuronoxylan	4-*O*-MeGlcA:Xyl	5:100	101-122
Aspen	Glucuronoxylan	4-*O*-MeGlcA:Xyl	9:100	101-122
Spruce	Arabinoglucuronoxylan	Ara: 4-*O*-MeGlcA:Xyl	6:13:100	107-145
	Galactoglucomannan	Gal:Glu:Man	16:24:100	118-132
Pine	Arabinoglucuronoxylan	Ara: 4-*O*-MeGlcA:Xyl	10:16:100	107-145
	Galactoglucomannan	Gal:Glu:Man	9:22:100	118-132
Larch	Arabinoglucuronoxylan	Ara: 4-*O*-MeGlcA:Xyl	10:12:100	107-145
	Galactoglucomannan	Gal:Glu:Man	8:26:100	118-132
Wheat straw	Arabinoglucuronoxylan	Ara: 4-*O*-MeGlcA:Xyl	6:22:100	107-132

2.2.3 Lignin

Lignin is an amorphous, cross-linked, and three-dimensional phenolic polymer. Three types of phenylpropanoid units are generally considered as major precursors for biosynthesis of lignin: coniferyl, sinapyl, and p-coumaryl alcohol (Figure 2.3), which give rise to guaiacyl (G), syringyl (S) and *p*-hydroxyphenyl (H) units respectively in its structure [40]. Generally, lignin in softwoods is mainly composed of guaiacyl units with small amounts of *p*-hydroxyphenyl units existed, while lignin in hardwoods primarily consists of both guaiacyl and syringyl units including a minor amount of *p*-hydroxyphenyl units. Lignin in grasses typically contains all the three types of monolignol units, with peripheral groups (i.e., hydroxycinnamic acids) incorporating into its core structure [40]. Table 2.6 summarizes the typical G/S/H lignin ratio from several common biofuel crops. Lignin is biosynthesized from the three monolignols, and the polymerization process is initiated by the oxidation of the monolignol phenolic hydroxyl groups. The oxidation has been shown to be catalyzed via an enzymatic route [27,41], and it is believed that both peroxidases and laccases are involved in lignin synthesis, where laccase is primarily responsible for the initial polymerization of monolignols to oligolignols, while peroxidases catalyze the reactions of oligolignols leading to the extended lignin macropolymer [41]. The enzymatic dehydrogenation is initiated by an electron transfer that yields reactive monolignol species with free radicals (Figure 2.4). A monolignol with a free radical can then couple with another monolignol with a free radical to generate a dilignol. Subsequent nucleophilic attack by water, alcohols, or phenolic hydroxyl groups on the benzyl carbon of the quinone methide intermediate will restore the aromaticity of the benzene ring [41]. The generated dilignols will then

undergo further polymerization to form aryl ether bonds (β-*O*-4) being the most common and important interunit linkage. Other common interunit linkages include resinol (*β*-*β*), phenylcoumaran (*β*-5), biphenyl (5-5), and 1,2-diaryl propane (*β*-1) (Figure 2.5). An example of a radical coupling is shown in Figure 2.6 [41]. Typical proportions of lignin interunit linkages in softwood and hardwood are summarized in Table 2.7.

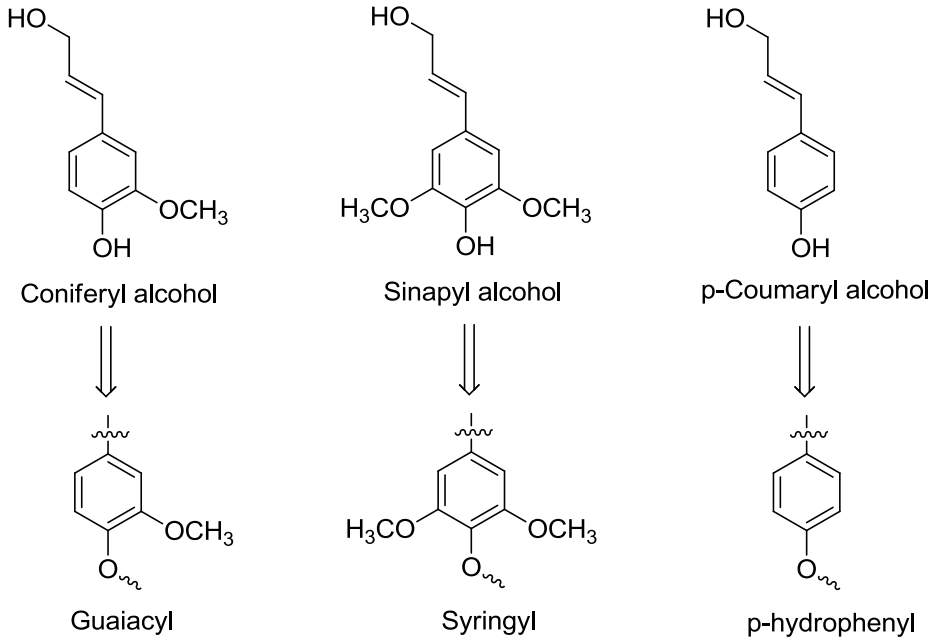

Figure 2.3 Typical phenylpropanoid precursors employed in the biosynthesis of lignin in plant biomass [9]

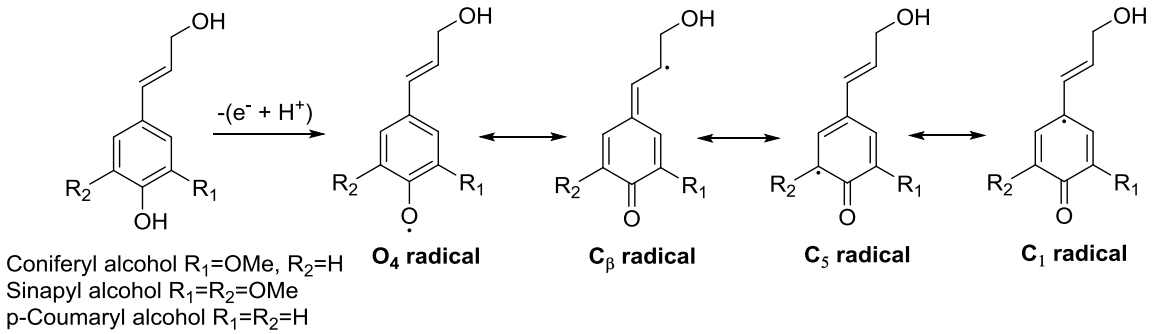

Figure 2.4 Resonance stabilized phenoxy radical during lignin biosynthesis

Table 2.6 The G/S/H lignin ratio from several common biofuel crops

	G lignin (%)	S lignin (%)	H lignin (%)	Reference
Switchgrass	51	41	8	42
Poplar	29	61	10 (as *p*-hydroxybenzoate)	43,44
Miscanthus	52	44	4	45
Corn stover	51	3.6	46	46
Wheat straw	49	46	5	47
Rice straw	45	40	15	47
Sugarcane bagasse	30	37	33	48

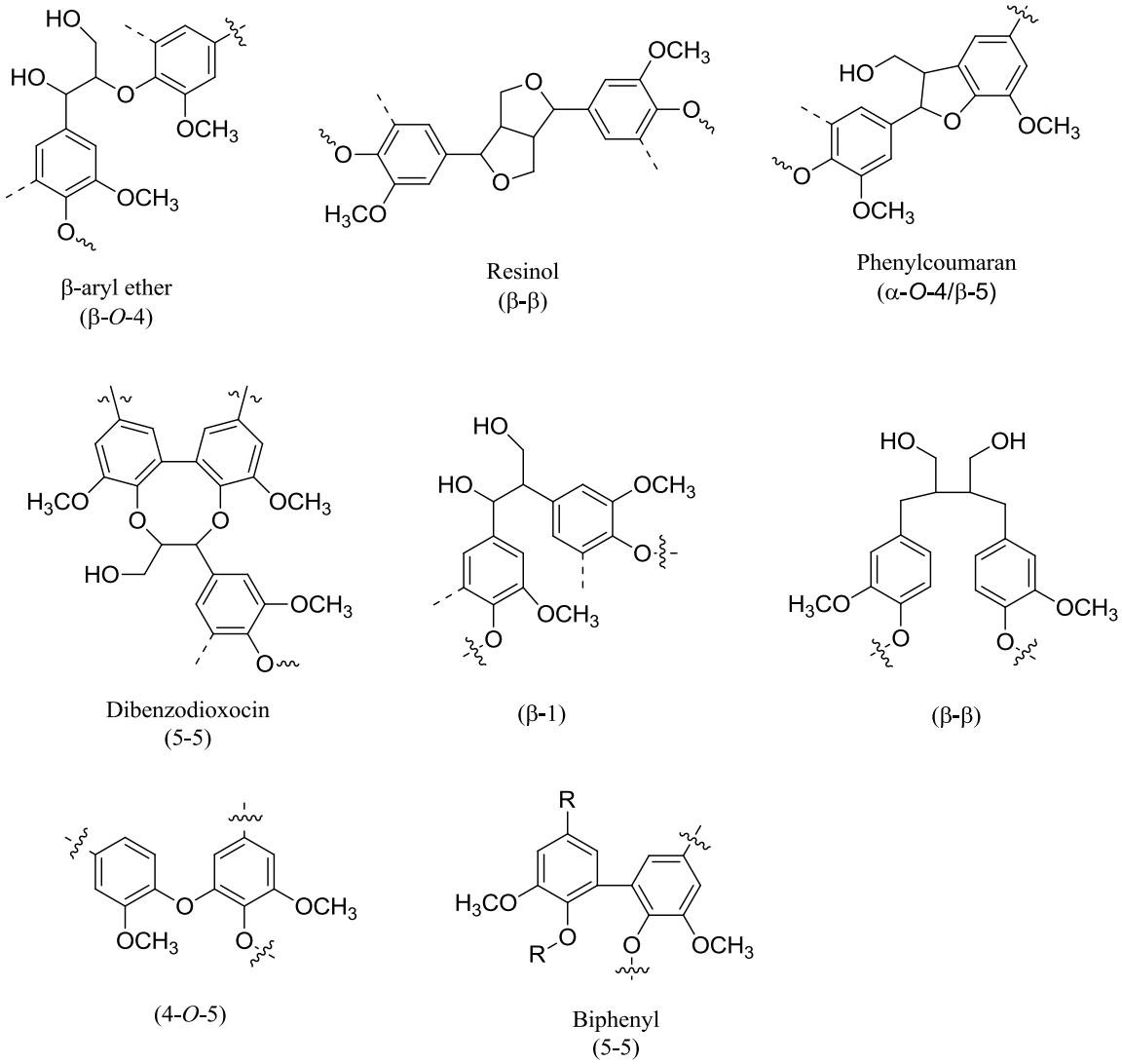

Figure 2.5 Some common interunit linkages found in lignin [47]

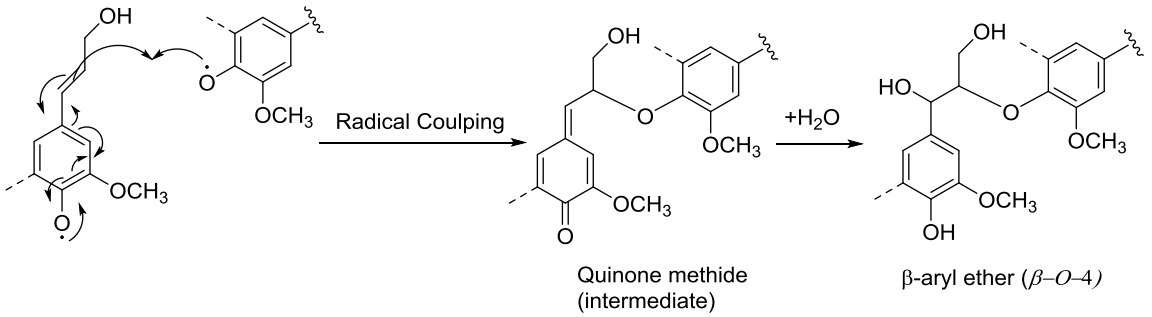

Figure 2.6 Formation of *β*-O-4 interlinkage via radical coupling

Table 2.7 Proportions of different types of lignin linkages in softwood and hardwood [49]

Linkage type	Percentage of total linkage	
	Spruce lignin (%)	Eucalyptus lignin (%)
β-O-4	45	61
α-O-4	16	N.D.
β-β	2	3
β-5	9	3
5-5	24-27	3
β-1	1	3
4-O-5	N.D.	9
Dibenzodioxocin	7	N.D.

Lignin is relatively hydrophobic and covalently linked to hemicelluloses to create cross-links. These cross-links are also called lignin-carbohydrate complexes (LCCs), which are believed to include phenyl glycoside bonds, esters, and benzyl ethers (Figure 2.4) [50]. LCCs can be isolated as water-soluble entities and divided into three classes based on molecular weight. Lignin carbohydrate bonds are presumed to exist in higher molecular weight lignin fractions which are water insoluble. In softwood LCCs, carbohydrate portions are mainly composed of galactomannan, arabino-4-*O*-methylglucuronoxylan, and arabinogalactan, which are linked to lignin at benzyl positions [51,52]. On the other hand, hardwood and grass LCCs are exclusively composed of 4-*O*-methylglucuronoxylan and arabino-4-*O*-methylglucuronoxylan, respectively [53].

The biosynthesis pathway for the ether and ester linkages of lignin-carbohydrate covalent bonds has been proposed to involve a nucleophilic addition of the hemicelluloses to the quinone methide intermediate formed from the dehydrogenative polymerization of coniferyl alcohol (Figure 2.7) [54]. According to the quantum mechanics calculation, the coupling between phenoxy radicals and β-radicals is the most favored, and thus the *β*-O-4 linkage is the most abundant in lignin structure. The quinone methide-like structure which is the intermediate of the β-*O*-4 linkage formation reaction contains an electrophilic α-position and it can be attacked by water, alcohol, or carboxyl groups, resulting in the formation of benzyl alcohols, benzyl ethers, and benzyl esters. On the other hand, the biosynthesis of glycosidic and acetal LCCs is not fully discovered yet.

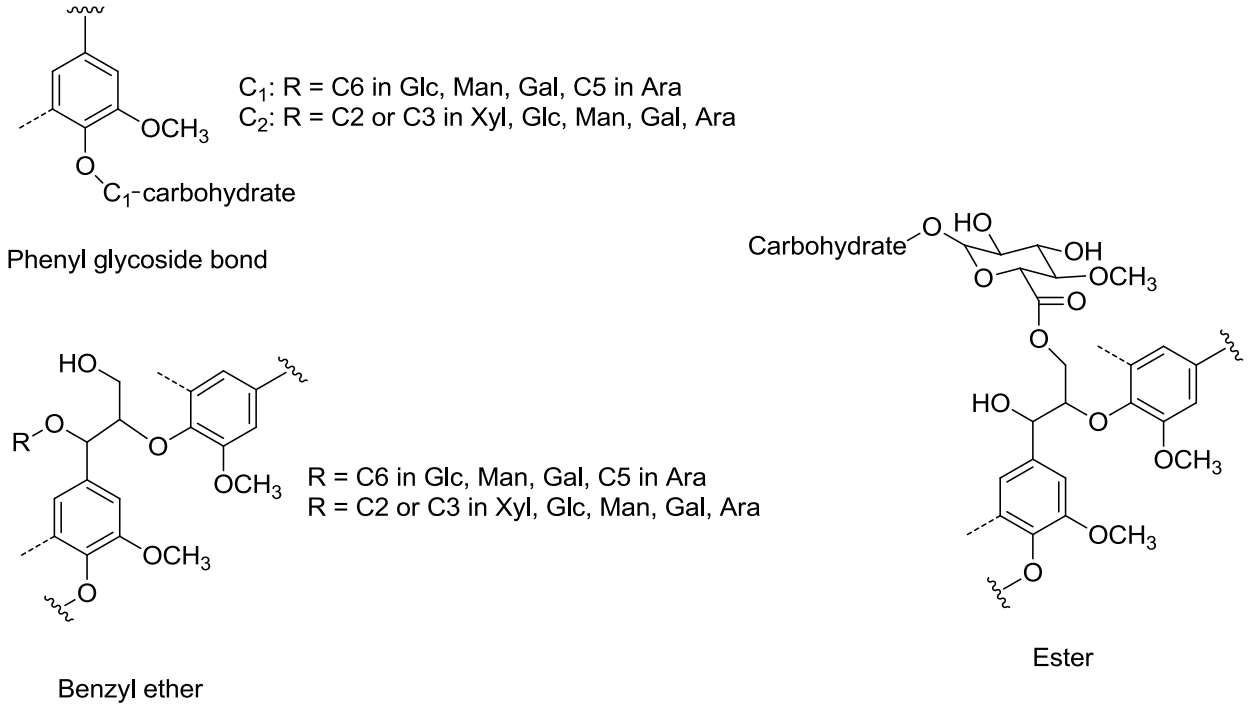

Figure 2.7 Lignin-carbohydrate complexes linkages

2.3 Lignocellulosic Recalcitrance and Pretreatment Technologies

2.3.1 Lignocellulosic Recalcitrance

To date, it is generally accepted that the plant cell wall microstructure is a lignin and polysaccharides matrix in which these biopolymers are intimately associated with each other [9,55]. In addition, plant cell walls generally are composed of three layers of anatomical regions including the middle lamella, the primary wall, and the secondary wall as shown in Figure 2.8. The structural complexity of plant cell walls causes plant biomass to be resistant to enzymatic and microbial deconstruction, which is defined as lignocellulosic recalcitrance [1]. Several factors are believed to contribute to this recalcitrance, which include the structure and content of lignin, acetylated hemicelluloses, LCCs, cellulose crystallinity and DP, pore size/volume, and specific surface area of cellulose [7].

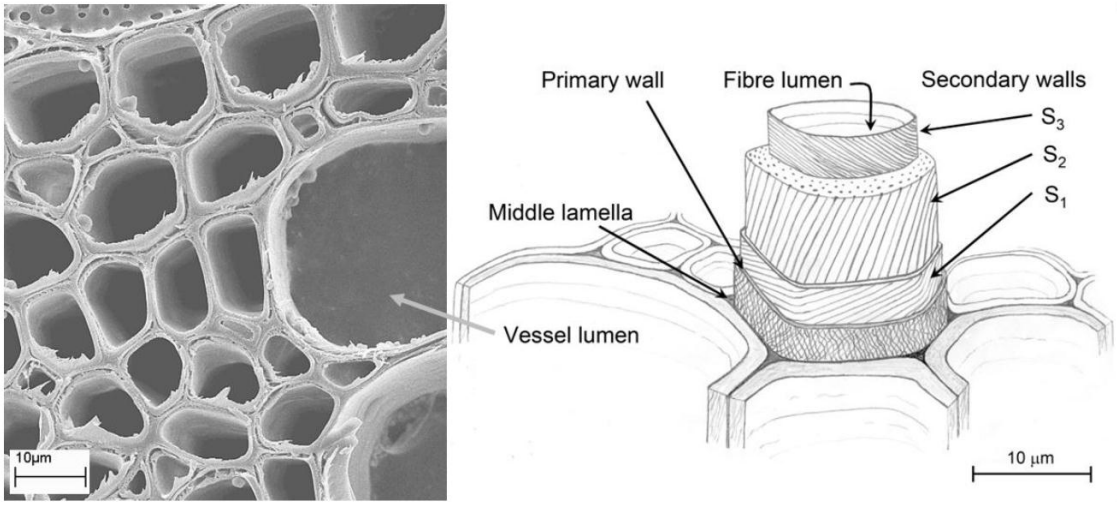

Figure 2.8 Electron microscope and schematic diagram of wood cell wall structure [56]

Lignin is considered the most recalcitrant component of the major plant cell wall biopolymers, and it acts as a physical barrier to prevent enzyme access to the carbohydrate fraction of lignocellulosics. Although the detailed mechanism that explains the protective effect of lignin against enzymatic hydrolysis is still unclear, the cross-linkages between lignin and carbohydrate, the structure and distribution of lignin in

lignocellulosics are believed to be significant [57]. In addition, during enzymatic hydrolysis, enzymes tend to irreversibly bind to lignin through hydrophobic interactions that cause a loss in their activities [58]. Such nonproductive binding of enzymes to lignin has been suggested to be responsible for the requirement of high enzyme loadings [59,60,61,62].

Hemicelluloses sheath cellulose microfibrils and the acetyl groups of hemicelluloses are believed to sterically hinder enzyme attack [7]. Unbranched hemicelluloses (xyloglucan, homoxylan, and mannan) form hydrogen bonds with the surface of cellulose fibrils, whereas hemicelluloses and the side chains of branched hemicelluloses (uronic acid and arabinose) may be covalently bonded to lignin to create enzyme-impenetrable LCCs [63]. LCCs are thought to be the major impediments to enzyme access to cellulose [63]. Therefore, hydrolysis of hemicellulose and cleavage of LCCs can also open the plant cell wall structure. Sierra *et al.* [7] suggested that moderate hemicellulose removal (>50 %) is required to significantly increase the enzymatic digestibility of cellulose [64]. Furthermore, removal of hemicelluloses increases the mean pore size and the specific surface area of cellulose [65] that are influential structural features related to noncomplexed cellulase adsorption on the cellulose surface and subsequent enzymatic deconstruction [62] since cellulases must bind to the surface of cellulose before hydrolysis can take place. One of the impacts of pretreatment is to enlarge pore sizes to create more surface area and enhance cellulase penetration into biomass. Meng *et al.* [66] utilized a modified Simons' stain method along with several NMR techniques to measure the cellulose accessibility/porosity of several poplar samples after DAP and steam explosion. They revealed that pretreated poplar has larger pore size distributions and

specific surface area when compared to an untreated sample. The Simons' stain method showed that DAP is more effective than steam explosion in terms of the specific surface area increase, and that DAP increases specific surface area as a function of pretreatment severity. On the other hand, NMR relaxometry and diffusometry indicated that pore expansion for DAP pretreatment occurs primarily in first 10 min of pretreatment, but steam explosion is more effective at pore expansion for the cell wall water pools detected by changes in relaxation times [66]. Zeng and coworkers [67] demonstrated that an increased surface area results in more exposed cellulose, thereby increasing the initial enzymatic hydrolysis rate of cellulose.

The effect of cellulose crystallinity on the overall cellulose-to-glucose conversion has been an issue for extensive studies. The degree of cellulose crystallinity is expressed in terms of the crystallinity index (CrI) according to the data from X-ray diffraction (XRD) technique, and is defined as follows:

$$CrI = 100 \times \left[\left(I_{002} - I_{amorphous} \right) / I_{002} \right]$$

- I_{002} is the intensity for the crystalline portion of cellulose at about $2\theta = 22.5°$
- $I_{\text{amorphous}}$ is the minimum intensity corresponding to the amorphous portion at about $2\theta = 18°$

In addition to the XRD peak height method that has been used in about 70 to 85 % of the studies [68], the CrI can also be determined from the areas of the crystalline and amorphous C4 signals using the following formula, based on solid-state NMR analysis (Figure 2.9) [69]:

$$CrI = 100 \times \left[A_{86–92ppm} / \left(A_{79–86ppm} + A_{86–92ppm} \right) \right]$$

- $A_{86\text{-}92\ ppm}$ is the area of the crystalline C4 signal

- $A_{79\text{-}86\ ppm}$ is the area of the amorphous C4 signal

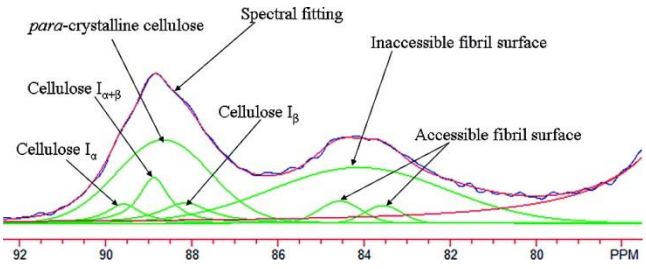

Figure 2.9 Spectral fitting for the C4 region of the CP/MAS ^{13}C NMR spectrum of cellulose [70]

Furthermore, it has been shown that different measurement techniques give different CrI values, but the order of crystallinity is relatively consistent within each measurement technique [68]. Zhang and Lynd [71], Sannigrahi *et al.* [72], Zhu *et al.* [73], Yoshida [74], Mittal *et al.* [75], and Ioelovich and Morag [76] have suggested that the degree or rate of enzymatic hydrolysis of cellulose declines with increasing cellulose crystallinity (Table 2.8). Pu *et al.* [77] observed that Cellulose I_{α}, para-crystalline, and non-crystalline regions of cellulose are more susceptible to enzymatic hydrolysis than cellulose I_{β} during the initial phase, thereby leading to an increase in cellulose crystallinity during the initial phase of hydrolysis.

On the other hand, Puri [78], Grethlein [79], and Thompson *et al.* [80] did not observe this strong correlation between cellulose crystallinity and hydrolysis rate/degree. During enzymatic hydrolysis of organosolv pretreated switchgrass, Cateto *et al.* [81] showed that cellulose crystallinity remained approximately constant, and this was explained by the "peeling-off" type mechanism - the effect of the synergistic action of cellulases on the removal of the outer layers of the cellulose crystallite in order to gain access to the inner

layers. It has been reported that the initial enzymatic hydrolysis rate of different cellulose allomorphs decreases in the following order: amorphous>III_I>II>I, which has been attributed to the enhanced specific surface areas compared to cellulose I [82]. The slower hydrolysis rate of native crystalline cellulose (cellulose I) is attributed to the presence of strong interchain hydrogen bonding between adjacent chains in a cellulose sheet and weaker hydrophobic interactions between cellulose sheets, resulting in the stability of crystalline cellulose nanofibers that strongly resist chemically or biologically catalyzed degradation [83,84]. In addition, Weimer *et al.* [82] stated that the increased enzymatic hydrolysis rate of cellulose III_I was due to its lower crystallinity, lower packing density, and higher distances between hydrophobic surfaces compared to cellulose I.

Hall *et al.* [85] demonstrated that the initial enzymatic hydrolysis rate of cellulose decreases linearly as crystallinity increases. Additionally, differences in the adsorption properties of cellulases on crystalline and amorphous cellulose are also believed to be related to the reactivity difference between crystalline and amorphous cellulose [86,87]. Hall *et al.* [85] have observed that the amount of adsorbed enzymes appeared to decrease linearly with crystallinity only at CrI above 45 %, whereas a constant amount of adsorbed enzymes leading to higher hydrolysis rate was observed at lower degrees of crystallinity (i.e., CrI < 45 %). They inferred that the adsorbed enzymes on the cellulose with low degrees of crystallinity are more active at the same overall concentration, which is owing to a more open cellulose structure that hinders enzymes from residing on neighboring chains from hindering one another [88]. Exo-cellulases may also locate a chain end faster with an open structure so that hydrolysis may occur quicker. However, the hydrolysis rate is limited to the high degrees of crystallinity because the internal surface of highly

crystalline cellulose is poorly accessible to enzymes, leading to low enzyme adsorption. Based on the conflicting results from the literature, further studies are needed to determine whether cellulose crystallinity provides a clear indication of enzymatic digestibility of cellulose.

Table 2.8 Cellulose conversion yield versus crystallinity for different substrates

Sample	Crystallinity index (%)	Extent of enzymatic hydrolysis (%)	Enzymes loadings	Reference
*Ground high lignin poplar	60.2	3.5 in 1 h	30 FPU/g for cellulase from Spezyme CP	73
Ground high lignin poplar	25.9	25.0 in 1 h	10 FPU/g for cellulase from Spezyme CP	73
Ground high lignin poplar	16.4	29.8 in 1 h	10 FPU/g for cellulase from Spezyme CP	73
Ground high lignin poplar	8.2	31.9 in 1 h	10 FPU/g for cellulase from Spezyme CP	73
Ground low lignin poplar	66.1	14.8 in 1 h	10 FPU/g for cellulase from Spezyme CP	73
Ground low lignin poplar	32.0	42.1 in 1 h	10 FPU/g for cellulase from Spezyme CP	73
Ground low lignin poplar	17.5	53.3 in 1 h	10 FPU/g for cellulase from Spezyme CP	73
Untreated Miscanthus	54.2	12.0 in 72 h	328 U/g for cellulase from Celluclast 1.5 L and 268 U/g for β-glucosidase from Novozyme 188	74
Untreated Miscanthus	41.9	16.2 in 72 h	328 U/g for cellulase from Celluclast 1.5 L and 268 U/g for β-glucosidase from Novozyme 188	74
Untreated Miscanthus	24.8	27.9 in 72 h	328 U/g for cellulase from Celluclast 1.5 L and 268 U/g for β-glucosidase from Novozyme 188	74
Ground delignified Miscanthus	55.9	65.8 in 72 h	328 U/g for cellulase from Celluclast 1.5 L and 268 U/g for β-glucosidase from Novozyme 188	74
Ground delignified Miscanthus	53.0	79.8 in 72 h	328 U/g for cellulase from Celluclast 1.5 L and 268 U/g for β-glucosidase from Novozyme 188	74

Table 2.8 continued				
Ground delignified Miscanthus	45.7	82.3 in 72 h	328 U/g for cellulase from Celluclast 1.5 L and 268 U/g for β-glucosidase from Novozyme 188	74

*Note: hybrid poplar was ground to 0.4 mm.

The DP of cellulose has also been postulated to play a role in its susceptibility to enzymatic deconstruction of cellulose. During enzymatic hydrolysis, endo-cellulases are involved in cleaving internal β (1→4) linkages of cellulose chains, decreasing the DP of cellulose and exposing reactive ends that can be attacked by exocellulases [55, 56]. Exo-cellulases are known to have a marked preference for substrates with lower DP [71], thus it is expected that reduction in the DP of cellulose would produce more chain ends with higher enzyme accessibility to cellulose. Furthermore, it has been shown that cellulose with shorter chains is more amenable to enzymatic deconstruction due to the absence of strong hydrogen bonding [89,90,91]. One of the earliest studies focusing on the effect of the DP of cellulose on enzymatic saccharification (Table 2.9) [78] suggested that the DP of cellulose may play an important role in the enzymatic degradation of cellulose, especially in the initial rate of hydrolysis. However, Sinistyn and co-workers [92] showed that reduction in the DP of cotton linters while keeping the crystallinity index constant had negligible impact on the enzymatic hydrolysis rate. Zhang and Lynd [93] observed that a decrease in cellulose DP was less effective in accelerating enzymatic hydrolysis than an increase in the accessibility of β-glycosidic bonds. Such results suggest that the understanding of the impact of cellulose chain length on enzymatic hydrolysis is still developing.

Table 2.9 DP versus extent of enzymatic hydrolysis for different substrates [78]

Substrate	Treatment	DP	Extent of enzymatic hydrolysis (%)
Bagasse	Untreated	925	28
	CO_2 explosion, 5 min at 200 °C and 3.45 MPa	572	78
	Alkali explosion, 5 min at 200 °C and 3.45 MPa with 8% NaOH	550	85
Wheat straw	Untreated	1045	29
	CO_2 explosion, 5 min at 200 °C and 3.45 MPa	698	81
	Alkali explosion, 5 min at 200 °C and 3.45 MPa with 6% NaOH	662	85
E. regnans	Untreated	1510	9
	Ozone treatment, 15% ozone charge and 50% solids in water	1065	86
P. radiata	Untreated	3063	3
	Ozone treatment, 15% ozone charge and 50% solids in water	2900	87
Cotton linters	Untreated	3170	38
	Ball-milling for 15 min	2214	57

2.3.2 Pretreatment Technologies

The pretreatment of lignocellulosic biomass is probably the most critical step as it has a huge impact on all the rest steps in the process of cellulosic ethanol production [94]. A large number of pretreatment approaches have been investigated on a wide variety of feedstock types, which can typically be divided into physical, chemical and biological methods [64]. Physical pretreatment such as ball-milling can enlarge the surface area of biomass thereby increasing the enzyme absorption or further pretreatment accessibility, but the performance is economically poor. Biological pretreatment has been considered as an environmentally friendly approach because it has low chemical and energy requirement to enhance cellulose enzymatic digestibility. It uses microorganisms such as fungi to selectively degrade lignin and hemicellulose but very little of cellulose [95]. It

seems to be conceptually ideal pretreatment method, but the controllable, cost effective, and rapid system has not been discovered to date [96]. As a result, chemical pretreatment is currently the most promising and widely applied method, which utilizes chemical treatment to alter the physicochemical structural and compositional properties of lignocellulosic biomass, making cellulose more accessible to enzymes during hydrolysis step [64,97]. Among various chemical pretreatments, dilute acid pretreatment, hydrothermal pretreatment, and ammonia fiber explosion pretreatment are the major techniques being developed [5]. This section will review these leading chemical pretreatment technologies following the acid-neutral-alkaline order.

2.3.2.1 Dilute Acid Pretreatment

Dilute acid pretreatment can significantly reduce lignocellulosic recalcitrance and it has been successfully applied to a wide range of feedstocks, including softwoods, hardwoods, herbaceous crops, and agricultural residues [98,99,100,101,102]. It is usually performed over a temperature range of 120 to 210 °C, with acid concentration typically less than 4 wt%, and residence time from a few seconds to an hour in different types of reactors such as batch [103], plug flow [104], percolation [105], countercurrent [106], and shrinking-bed reactors [106,107,108]. Although a variety of acids such as hydrochloric acid, nitric acid, phosphoric acid and peracetic acid have been employed, sulfuric acid has been most widely used since it is inexpensive and effective [109]. Table 2.10 summarizes DAP results for different substrates.

Table 2.10 Summary of DAP conditions for different substrates

Substrate	Pretreatment conditions	CS	Cellulose conversion yield (%)	Enzymes loadings	Reference
Corn stover	121 °C, 2.0% H_2SO_4, 120 min	2.01	75.6 in 72 h	40 FPU/g for cellulase from Celluclast 1.5 L, and 8 CBU/g for β-glucosidase from Novozym 188	98
	121 °C, 2.0% H_3PO_4, 120 min	1.28	56.0 in 72 h	40 FPU/g for cellulase from Celluclast 1.5 L, and 8 CBU/g for β-glucosidase from Novozym 188	98
Cotton stalk	121 °C, 2.0% H_2SO_4, 60 min	1.71	23.9 in 72 h	40 FPU/g for cellulase from Celluclast 1.5 L, and 70 CBU/g for β-glucosidase from Novozym 188	25
Aspen	175 °C, 0.25% H_2SO_4, 30 min	2.10	42.3 in 72 h	60 FPU/g for cellulase from Spezyme CP and 120 CBU/g for β-glucosidase from Novozyme 188	99
	170 °C, 1.10% H_2SO_4, 30 min	2.60	88.0 in 72 h	7.5 FPU/g for cellulase from Celluclast 1.5 L and 11.25 CBU/g for β-glucosidase from Novozyme 188	100
Switchgrass	140 °C, 1.0% H_2SO_4, 40 min	1.79	75.0 in 72 h	15 FPU/g for cellulase from Spezyme CP and 30 CBU/g for β-glucosidase from Novozyme 188	101
Sweet sorghum bagasse	180 °C, 1.0% H_2SO_4, 20 min	2.67	53.9 in 60 h	20 FPU/g for cellulase	102

The combined severity (CS) factor is used for an easy comparison of pretreatment conditions and for facilitation of process control, which relates the experimental effects of temperature, residence time and acid concentration [110].

$$CS = \log\left\{t \exp\left[\left(T - T_{ref}\right)/14.7\right]\right\} - pH$$

- t is the pretreatment time (min)
- T is the pretreatment temperature (°C)
- T_{ref} is 100 °C.

A primary effect of DAP is to hydrolyze hemicelluloses and to disrupt the lignin structure so that the treated biomass has increased enzyme access to cellulose fraction. Hemicellulose, mainly xylan, is hydrolyzed to fermentable sugars during DAP, as glucomannan is relatively stable in acid [65]. In general, less xylan remains in the pretreated solid residues at higher severity pretreatment conditions [111,112,113,114,115,116,117] as shown in Figure 2.10. At lower CS, most of the released xylan is accumulated in the liquors in the form of xylose, whereas, at higher CS, the released xylan in the liquors is partially converted to furfural [112,113]. Kabel *et al.* [113] demonstrated that the amount of furfural and the xylan loss increased as both CS increased and the percentage of residual xylan decreased.

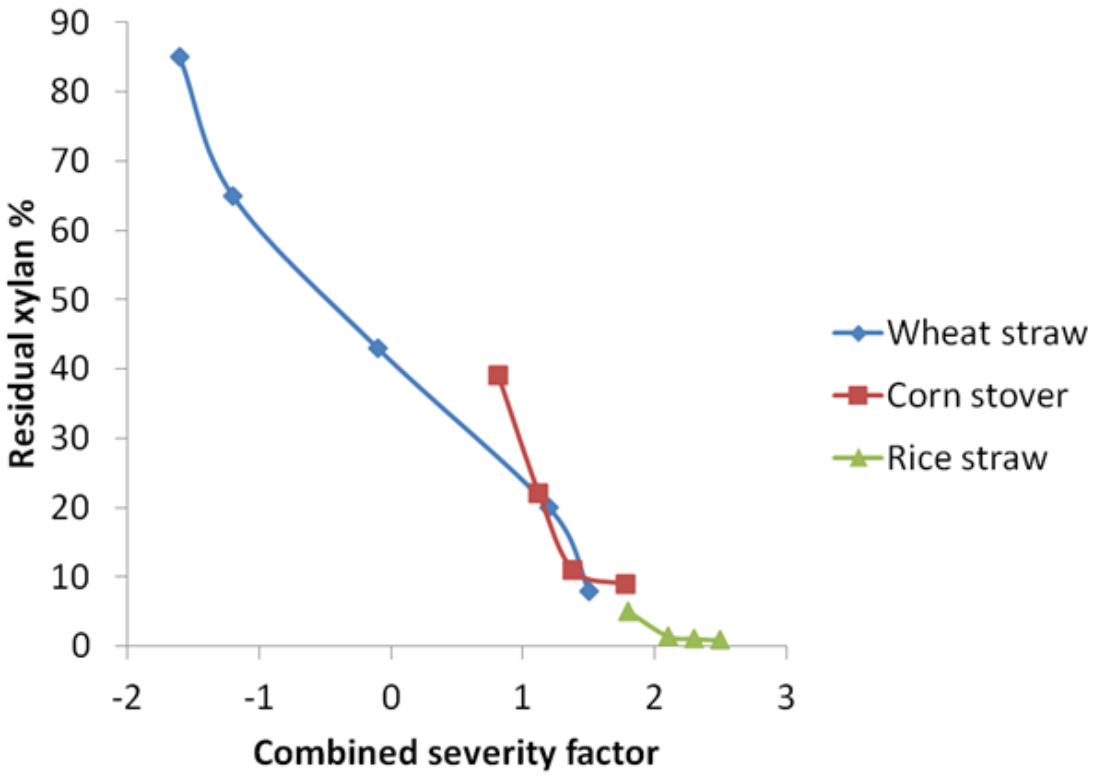

Figure 2.10 Residual xylan content versus pretreatment severity for different feedstocks [5]

During DAP, the hydrolyzed acetyl groups become an in-situ source of acetic acids that further catalyzes xylan depolymerization, whereas another fraction of the acetyl esters remains covalently linked to the xylan backbone and are released from the residue together with the xylan as esterified xylo-oligosaccharides [113]. This latter fraction is believed to be stronger inhibitor to cellulases than pure xylo-oligosaccharide owing, in part, to the steric hindrances of the acetyl groups. Furthermore, it has been hypothesized that xylan is dissolved in the reaction media first as high M_w (DP > 25) material followed by cleavage of more and more bonds between xylose residues upon higher severity pretreatment conditions [112]. This hypothesis was confirmed by Kabel *et al.* [113]. Their work showed that the more severe the pretreatment the more low M_w (DP < 9) xylans and the less high M_w xylans were detected in the liquor. Additionally, the

proportions of medium M_w (DP 9-25) xylans first increased slightly upon a medium severity (CS -0.4 to 1.2), but then decreased rapidly at higher severity in favor of low M_w xylans formation.

The majority of the hemicelluloses (xylose, mannose, arabinose and galactose) from substrate including hardwood (such as poplar), agricultural residue (such as corn stover) and grass (such as switchgrass) are removed during DAP. The hydrolyzation of cellulose and subsequent solubilization of glucose would take place if the pretreatment conditions are too severe [114,115,116,118,119,120,121]. Foston and Ragauskas [118] stated that the degradation of cellulose is an acid catalyzed and thermally accelerated chain scission mechanism. The reaction takes place within the fibril structure from within either a crystalline or amorphous region of cellulose. This process consists of two major stages; an initial rapid hydrolysis of the more solvent accessible amorphous region, and a latter much slower hydrolytic attack of the crystalline portion [122,123].

In general, the crystallinity of cellulose increases throughout the process of DAP as shown in Table 2.11. Foston and Ragauskas [118] have observed that para-crystalline content of cellulose from poplar and switchgrass appears to increase with pretreatment temperature based on solid-state ^{13}C CP/MAS NMR studies. They suggested that the majority of the increase in crystallinity and para-crystalline percentage is primarily due to localized hydrolyzation and removal of cellulose in the amorphous regions. The more solvent accessible amorphous regions are more prone to degradation during pretreatment at higher temperature because cellulose hydrolysis is thermally accelerated.

Table 2.11 Crystallinity index (CrI) before and after DAP for different substrate

Substrate	Pretreatment conditions	CrI (%) before pretreatment	CrI (%) after pretreatment	Reference
Corn stover	160 °C, 0.5% H_2SO_4, 20 min	50.3	52.5	119
Poplar	160 °C, 1.0% H_2SO_4, 5 min	49.9	70.5	118
	190 °C, 2.0% H_2SO_4, 70 s	49.9	50.6	119
Sugarcane bagasse	80 °C, 50% peracetic acid, 2 h	42.6	63.0	124
Loblolly pine	180 °C, 0.5% H_2SO_4, 10 min	62.5	69.9	11

In addition, the relative proportion of both the crystalline and para-crystalline forms can also be affected by ultrastructural transformation mechanisms and/or hydrolyzation at crystalline surfaces. For example, it has been observed that the relative intensity of the cellulose I_α form decreases while the relative intensity for the other crystalline allomorphs increases with residence time for both poplar and switchgrass during DAP [118]. This data suggests the cellulose I_α form is susceptible to either selective degradation by acidic hydrolyzation and/or transformation to other crystal allomorphs during pretreatment. In fact, conditions in DAP could promote cellulose annealing [11,125,126] of cellulose I_α into cellulose I_β crystal. This transformation is attributed to the metastable properties of the triclinic one-chain crystal structure of cellulose I_α [123,127]. It has been suggested that during DAP cellulose I_α is primarily converted to pare-crystalline cellulose, followed by conversion to cellulose I_β while simultaneously a small fraction of para-crystalline cellulose slowly transforms into crystalline cellulose [118].

Interestingly, Sannigrahi *et al.* [11] observed a large increase in the relative proportion of cellulose I_β accompanied by a decrease in the relative proportions of both cellulose I_α and

para-crystalline region from dilute acid pretreated pine. This suggests that the types of lignocellulosic materials and exact pretreatment conditions influence cellulose crystalline allomorphs and para-crystalline contents during DAP.

DAP leads to the reduction in the DP of cellulose especially at high severity pretreatment conditions, which increases enzymatic digestibility of cellulose. The DP of cellulose from different substrates decreases gradually until reaching a nominal value namely the leveling-off degree of polymerization (LODP) throughout the course of DAP [111,128]. The initial faster DP reduction phase is believed to represent the hydrolysis of the reactive amorphous region of cellulose; whereas the slower plateau rate phase corresponds to the hydrolysis of the slowly reacting crystalline fraction of cellulose [128].

In summary, DAP is one of the most important chemical pretreatment technologies because of its high hemicellulose solubilization and recovery, and high yields in subsequent enzymatic deconstruction of cellulose. However, DAP is still among the most expensive steps in biomass conversion to fuels [129], primarily owing to the additional costs for acid, special reactor material and acid-neutralization step.

2.3.2.2 Hydrothermal Pretreatment

Hydrothermal pretreatment refers to the use of water in the liquid or vapor phase to pretreat lignocellulosic materials under high pressure. Pressure is utilized to maintain water in the liquid state at elevated temperatures of 160-240 °C [130]. Table 2.12 summarizes pretreatment results for different substrates. Hydrothermal pretreatment can be performed in co-current, countercurrent or flow-through reactors. In the co-current process, the water-lignocellulosics slurry is heated to pretreatment conditions and held for

the required residence time. In the countercurrent process, the water and lignocellulosics flow in the opposite directions. In the flow-through process, hot water flows through a stationary bed of lignocellulosics [7]. This pretreatment technology is particularly promising because of several potential advantages including no requirement for catalysts, or special reactor materials or preliminary feedstock size reduction [131].

Table 2.12 Hydrothermal pretreatment results for different substrates

Substrate	Pretreatment conditions	Cellulose conversion yield (%)	Enzymes loadings	Reference
Wheat straw	200 °C, 40 min	95.8 in 72 h	15 FPU/g for cellulase from Celluclast 1.5 L, and 15 IU/g for β-glucosidase from Novozyme 188	132
	195 °C, 20 min	87.5 in 72 h	15 FPU/g for cellulase from Celluclast 1.5 L, and 15 IU/g for β-glucosidase from Novozyme 188	133
	195 °C, 40 min	81.2 in 72 h	15 FPU/g for cellulase from Celluclast 1.5 L, and 15 IU/g for β-glucosidase from Novozyme 188	133
Corn stover	190 °C, 15 min	69.6 in 168 h	15 FPU/g for cellulase from Spezyme CP, and 65 IU/g for β-glucosidase from Novozyme 188	67
Switchgrass	200 °C, 10 min	77.4 in 48 h	49 FPU/g for cellulase from Celluclast 1.5 L, and 40 IU/g for β-glucosidase from Novozyme 188	134

The goal of hydrothermal pretreatment is to solubilize hemicelluloses and to increase cellulose digestibility. During pretreatment, water acts as a weak acid and releases the hydronium ion, which causes depolymerization of hemicellulose by selective hydrolysis of glycosidic linkages, liberating *O*-acetyl group and other acid moieties from hemicellulose to form acetic and uronic acids. The release of these acids has been

postulated to catalyze hydrolysis of hemicelluloses and oligosaccharides from hemicelluloses [135,136,137,138]. However, this postulate was challenged since it cannot explain the large difference in the performance of flow through reactor that removes much more hemicellulose especially at high flow rate (Figure 2.11). This is because the large amount of water used in a flow through reactor quickly dilutes and removes organic acids, which lowers the organic acids concentrations and minimizes the time for them to act on the solid hemicellulose.

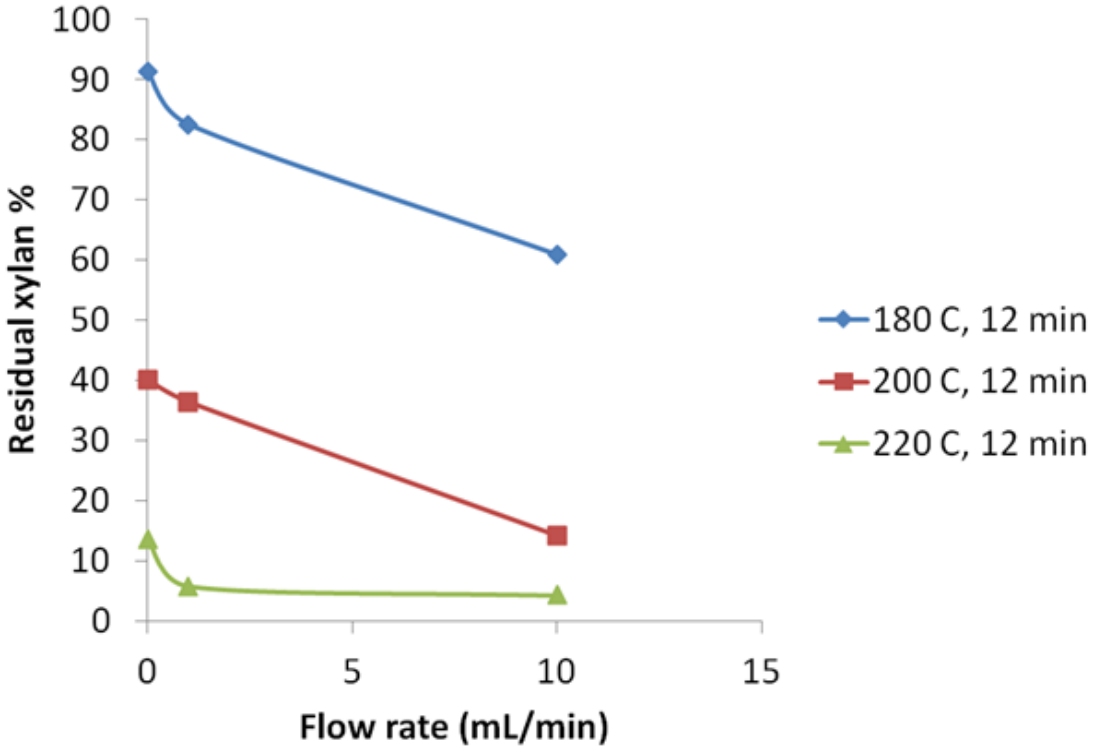

Figure 2.11 Flow rate versus xylan removal for hydrothermal pretreatment of corn stover

Liu and Wyman [139] postulated that the long-chain hemicellulose oligomers and unreacted hemicellulose could form hydrogen bonds with water molecules to form an "ice-like" layer that slows the access of water to hemicellulose during hydrothermal pretreatment. Additionally, it was hypothesized that the flow of liquid would enhance removal of less-soluble oligomers and disturb the "ice-like" layer, leading to reduce the

thickness of the stagnant fluid layer surrounding the solid particles and to lower the resistance to penetration of water into the solids for hydrolysis and diffusion of oligomers into solution [139]. Therefore, hemicellulose hydrolysis is controlled by both chemical reaction (i.e. temperature and acid concentration) and mass transfer effect [139]. At relatively high acid concentration condition, mass transfer is insignificant since the hydronium ions would rapidly hydrolyze long-chain oligomers to more rapidly dissolving short-chain species and then to monomers. This is why hemicellulose solubilization is mainly controlled by temperature and acid concentration in DAP, while mass transfer is believed to play a more important role in hydrothermal pretreatment [139], where most of hemicellulose sugars are released as oligomers [112,139,140,141,142]. However, the detailed mechanism accounting for the enhanced hemicellulose removal with flow rate is still not fully understood [143]. Furthermore, it was found that lignin-hemicellulose-oligomers and their solubility might significantly affect the rates and yields of hemicellulose solubilization [143].

It has been observed that hemicellulose is easily dissolved in water together with a considerable part of lignin at approximately 180 ºC [139,144,145,146], and solubilization of hemicellulose increases significantly with pretreatment severity (i.e. temperature and time). Garrote *et al.* [137] and Vegas *et al.* [138] showed that the medium molecular weight (DP 9-25) xylo-oligosaccharides were predominant in hydrothermal pretreatment, and their proportions decreased slightly with severity due to the increased decomposition. The amount of low molecular weight (DP < 9) fraction increased with severity while the proportion of high molecular weight (DP > 25) fraction declined with severity. These

authors concluded that the majority of xylan-derived products in hydrothermal pretreatment corresponded to xylo-oligosaccharides with DP less than 25 [137,138]. Hydrothermal pretreatment results in preserving most of the cellulose in the solid form, and the amount of glucan retained is greater than in DAP [132]. Yu and Wu [147] investigated the hydrolysis behavior of amorphous and crystalline cellulose in hydrothermal pretreatment. The minimal temperature required to rupture the glycosidic bonds in the chain segments within the amorphous portion of cellulose appears to be approximately 150 ºC whereas for crystalline portion of cellulose it is 180 ºC. Furthermore, low-DP glucose oligomers are produced at 180 °C, whereas large-DP glucose oligomers are released at temperatures above 200 ºC. Clearly, this difference in the hydrolysis behavior between amorphous and crystalline cellulose is due to the significant ultrastructural differences in the amorphous and crystalline portions of cellulose. Therefore, amorphous cellulose is more reactive than crystalline cellulose and several researchers have reported that the crystallinity index of cellulose increased after hydrothermal pretreatment [119,148], although no significant change in cellulose crystallinity has also been observed when the pretreatment severity is low [149]. The DP of cellulose decreases progressively until reaching LODP during hydrothermal pretreatment [111,128], which is similar to those reviewed for DAP.

To summarize, hydrothermal pretreatment without adding any catalyst is attractive due to much lower cellulose degradation and significant reduction in the chemical and materials of construction costs compared to DAP, but it also produces large amounts of hemicellulose oligosaccharides that must be further hydrolyzed to fermentable

monosaccharides. Furthermore, higher water input in hydrothermal pretreatment demands more energetic requirements, which is not favorable for developing at commercial scale.

2.3.2.3 Ammonia Fiber Explosion Pretreatment

Ammonia, a non-corrosive chemical, is a desirable pretreatment reagent because it can effectively swell lignocellulosic material; has high reaction selectivity with lignin over carbohydrates, and is easy to recover and recycle due to its high volatility [150]. During ammonia fiber explosion (AFEX) pretreatment, the lignocellulosic material is treated with liquid ammonia at temperatures between 60 and 100 °C and high pressure for a variable period of time (such as 30 min), and then the pressure is released. Due to the design of commercial-scale AFEX process requires adequate ammonia contacts with moist biomass followed by removing adequate ammonia with minimal costs, the conventional approach to perform AFEX is to treat moist biomass (0.1-2 g H_2O/g dry biomass) with liquid ammonia (0.3-2 g NH_3/g dry biomass) while heating (40-180 ºC) the biomass-water-ammonia mixture for a period of time (5-60 min) before rapidly releasing the pressure. This swift pressure release leads to a rapid expansion of the ammonia gas that causes swelling and physical disruption of biomass fibers. In addition, about 95% of the ammonia can be recovered in the gas phase and recycled, with a small amount of ammonia that remains in the lignocellulosics might serve as a nitrogen source for the microbes in the fermentation process [151]. AFEX has been applied to various lignocellulosic materials including rice straw, corn stover and switchgrass. However, it is not effective on lignocellulosics with high lignin content such as softwood [19,152]. Table 2.13 summaries AFEX pretreatment results for various substrates.

Table 2.13 AFEX pretreatment results for different substrates

Substrate	Pretreatment conditions	Cellulose conversion yield (%)	Enzymes loadings	Reference
Switchgrass	100 °C, 1:1 ammonia to biomass loading, 80% moisture content, 5 min	93 in 168 h	15 FPU/g for cellulase from Spezyme CP, and 40 IU/g for β-glucosidase from Novozyme 188	153
Coastal Bermuda grass	90 °C, 1:1 ammonia to biomass loading, 60% moisture content, 5 min	87.1 in 48 h	30 FPU/g for cellulase from *Trichoderma reesei*	154
	100 °C, 1:1 ammonia to biomass loading, 60% moisture content, 5 min	89.0 in 48 h	30 FPU/g for cellulase from *Trichoderma reesei*	154
	80 °C, 1:1 ammonia to biomass loading, 60% moisture content, 30 min	97.3 in 48 h	30 FPU/g for cellulase from *Trichoderma reesei*	154
Corn stover	90 °C, 1:1 ammonia to biomass loading, 60% moisture content, 5 min	93 in 168 h	60 FPU/g for cellulase from Spezyme CP	155
	90 °C, 1:1 ammonia to biomass loading, 60% moisture content, 5 min	93 in 168 h	31 mg/g for cellulase protein from Spezyme CP, and 33 mg/g for β-glucosidase protein from Novozyme 188	156
Poplar	180 °C, 2:1 ammonia to biomass loading, 233% moisture content, 30 min	93 in 168 h	125 mg/g for cellulase protein from Spezyme CP, and 33 mg/g for β-glucosidase protein from Novozyme 188	156

In AFEX, the combination of chemical and physical effects leads to partially solubilization of hemicelluloses and the disruption of the cell wall complex structure thereby increasing the accessibility of cellulose and hemicellulose to enzymes [151,155].

Removal of acetyl groups from hemicellulose results in the formation of acetamide and acetic acid, but it is reported that AFEX removes the least amount of acetyl groups from lignocellulosic material compared to other leading pretreatment technologies [119]. AFEX can be considered as a 'dry to dry' process since dry mass recovery following AFEX treatment is almost 100% [155]. Although results from the literature have suggested that the physical removal of hemicellulose and lignin from plant cell walls into separate liquid phases is necessary to enhance enzymatic digestibility of cellulose, AFEX can still achieve more than 90% conversion of cellulose and hemicellulose to fermentable sugars at optimal conditions (Table 7). Furthermore, enzymatic digestibility of AFEX-treated material at low enzyme loadings is very high comparing to other pretreatment technologies [157]. These all suggest that ammonia may affect hemicellulose differently from other chemicals.

Several researchers reported subtle changes in the inner cell wall localization of the lignin and hemicelluloses during AFEX pretreatment account for the increase in cellulose accessibility [158,159,160]. During AFEX pretreatment, ammonia causes a series of ammonolysis (amide formation) and hydrolysis reactions (acid formation) in the presence of water, which cleave LCC ester linkages such as diferulates cross-linking arabinose side-chains of xylan [159]. Cleavage of these lignin-hemicellulose ester linkages facilitates the solubilization and removal of lignin and hemicellulose oligomers thereby exposing the embedded cellulose microfibrils [159]. Furthermore, the rapid pressure release leading to the expansive decompression of ammonia at the end of pretreatment would form large pores at the middle lamella. Chundawat *et al.* [159] stressed that these large pores would greatly facilitate the accessibility of cellulases because the radius of

gyration of exo-cellulase Cel7A from *Trichoderma reesei* is smaller than the pore size. In addition, increasing the cell wall porosity without extensively extracting of lignin and hemicellulose could prevent collapse and aggregation of cellulose microfibrils, thereby preserving pretreatment effectiveness [158,161]. The mechanism discussed above partially explains how AFEX pretreatment reduces lignocellulosic recalcitrance.

AFEX pretreatment has a much lower impact on the DP of cellulose than other leading pretreatment technologies such as DAP [119]. Another major chemical effect of AFEX is cellulose decrystallization [119,162,163] that allows cellulose to be more easily degraded in the enzymatic hydrolysis process. In general, lower moisture content in AFEX pretreatment tends to produce less crystalline samples [162]. This is probably owing to the high moisture in the biomass promotes the formation of ammonia hydroxide [153] that hydrolyzes more hemicellulose and lignin, thereby increasing the relative crystallinity of cellulose. The reduction in cellulose crystallinity after AFEX pretreatment may be attributed to the generation of more amorphous cellulose [119].

2.4 Lignin Globules and Pseudo-lignin Formation during Dilute Acid Pretreatment

It has been observed that lignin is translocated and redistributed during DAP, leading to the formation of lignin droplets of various morphologies [158,164,165,166,167,168,169]. Pingali *et al.* [14] proposed that lignin aggregates are present within the bulk pretreated material prior to the formation of larger lignin droplets resulting from lignin redistribution at a later stage. Furthermore, high temperature exceeding the lignin phase transition temperature (ranging from 120 ºC to 200 ºC) is required for such aggregates to form. Further studies revealed that once the lignin phase transition temperature is

reached, lignin becomes fluid and then coalesce to form droplets within the cell wall matrix. The hydrostatic pressures within the cell wall layers force a fraction of this lignin to the outer face, which in turn contacts with the pretreatment bulk and deposits back onto the plant cell wall surface during DAP [165,167,168]. By using confocal and fluorescence lifetime imaging microscopy, Coletta *et al.* [170] observed DAP results in a disorder in the arrangement of lignin and its accumulation in the external border of the cell wall. This relocation and redistribution of lignin is more pronounced with higher acid concentration and/or temperature, which overlays the cell wall surfaces and potentially blocks enzymes further access to cell wall components [171].

Similar to the re-deposit lignin droplets, Sannigrahi *et al.* reported that pseudo-lignin which is formed during DAP has spherical structures and deposits on the cell-wall surface of dilute acid-treated biomass (Figure 2.12) [109,172]. The formation of pseudo-lignin also accounts for the relatively comparable or even higher lignin content observed in the dilute acid-treated biomass. It is well-known that DAP alone is not efficient for lignin removal [11,42,173]. For instance, a study by Cao *et al.* [174] reported lignin contents (~ 24.4-25.9%) in the pretreated poplar similar to the untreated control (24.6%) after DAP at 170 °C over the range of 0.3-26.8 min. An increase in lignin content by ~ 2-6% was observed in poplar after treating with dilute acid at 140 –180°C [13]. Similarly, Samuel *et al.* [42] documented a 10% increase in lignin content in switchgrass after DAP at 190°C with the residence time of 1 min. These results can be mostly attributed to the concomitant loss of polysaccharides. Under DAP conditions, undesired by-products such as furfural and 5-hydroxylmethyl furfural (HMF) are formed from xylose and glucose, respectively via acid-catalyzed dehydration reactions (Figure 2.13) [5]. Further

rearrangements of furfural and/or HMF can produce aromatic compounds, which undergo further polymerization and/or polycondensation reactions to form pseudo-lignin. Therefore, the formation of pseudo-lignin during pretreatment is unfavorable due to it comes from carbohydrate degradation and more importantly, it may be detrimental to enzymatic hydrolysis of cellulose just like native lignin.

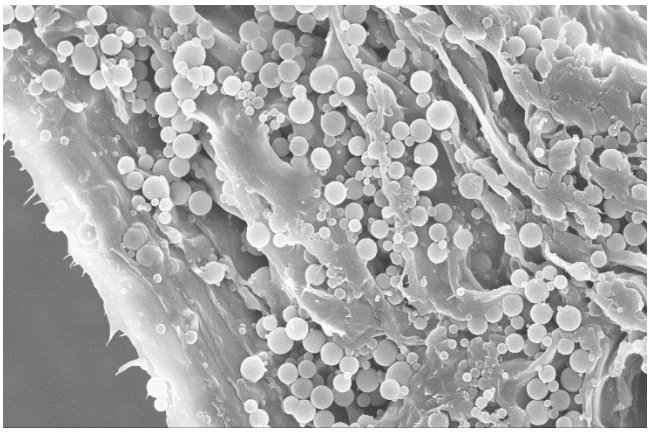

Figure 2.12 SEM image of pseudo-lignin deposition on surface of poplar holocellulose after dilute acid pretreatment [9]

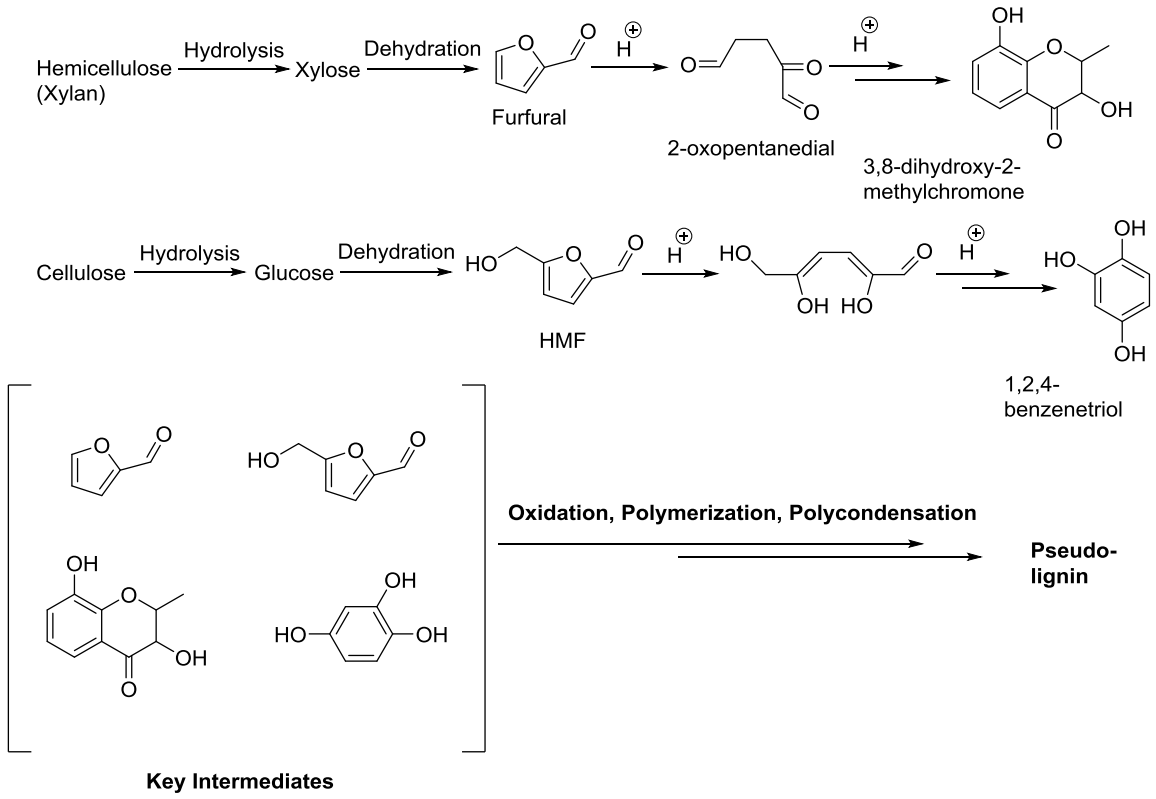

Figure 2.13 Reaction pathways of undesired by-products generated from carbohydrates under DAP conditions

CHAPTER 3

Experimental Materials and Procedures

3.1 Materials

3.1.1 Chemicals and Materials

All chemicals were purchases either from Sigma-Aldrich (St. Louis, MO) or VWR (West Chester, PA), and used as received except for *p*-dioxane, which was distilled over sodium borohydride prior to use. All gases were purchased from Airgas (Radnor Township, PA). Pure cellulose (Avicel1 PH 101; Lot No.1316179) was purchased from FMC Biopolymer (Philadelphia, PA). Beechwood xylan (Catalog No. X-4252; Batch No. 017K0688) and xylose (99% purity; Batch No. 069K0115) were from Sigma-Aldrich (St. Louis, MO. *Accellerase 1500* cellulase (Batch No.1681198062) and *Multifect* xylanase (Lot No.301-04021-015) were provided by Genencor, a division of Danisco A/S (now DuPontTM Genencor1 Science, Palo Alto, CA). Protein contents of cellulase and xylanase, as determined by the standard BCA method [175], were 82 and 42 mg/mL, respectively. The specific activity of *Accellearse 1500*, as reported elsewhere [176], was about 0.5 FPU/mg protein, consistent with values typically noted for commercial cellulase preparations. CBHI purified to homogeneity (single band on SDS gel, 18.5 mg/mL as determined by BCA method) from Genencor *Spezyme1 CP* (lot 301-04075-034; 59±5 FPU/mL, 123±10 mg protein/mL) cellulase was prepared by Protein Labs (San Diego, CA) by following standard protocols [177].

3.1.2 Biomass Substrate

Hybrid poplar (*Populus trichocarpa x deltoides*) was obtained from Oakridge National Laboratory, TN and Wiley milled to pass a 2-mm screen. The sample was air-dried and stored at -20 ºC.

3.2 Experimental Procedures

3.2.1 Soxhlet Extraction

Extractive-free poplar was prepared with sequential 24 h Soxhlet extractions according to TAPPI method T 204 cm-07 [172]. Extractives were removed by placing the samples into an extraction thimble in a Soxhlet apparatus. The extraction flask was filled with ethanol/toluene (1/2, v/v) and then refluxed with boiling rate of 24 solvent cycles per h. The extractive-free solids were air-dried overnight.

3.2.2 Holocellulose Pulping

Poplar holocellulose was isolated from the extractive-free poplar by removing lignin following literature procedures [178]. Extractive-free sample was subjected to an oxidative treatment with $NaClO_2$ (1.30 g/g dry weight sample) and acetic acid in a sealed plastic pouch (Kapak Corporation). The pouch was then placed in a reciprocating water bath at 70 °C for 1 h. The oxidative treatment was repeated three more times to produce holocellulose. The holocellulose was recovered by filtration and washed thoroughly with deionized (DI) water, and air-dried overnight.

3.2.3 α-Cellulose Isolation

α-Cellulose was isolated from poplar holocellulose following Tappi method T-203 cm-09 with a slight modification [172]. Holocellulose was suspended in 17.5 wt% NaOH solution at room temperature (RT) for 1 h. DI water was then added to the slurry to dilute

NaOH solution to 8.75 wt%. The slurry was allowed to stir for another 30 min, and then filtered through a filter funnel. The solids were washed with excess DI water until the pH of the filtrate was close to 7, and air-dried overnight.

3.2.4 Dilute Acid Pretreatment

Two-step dilute acid pretreatments were applied to both poplar holocellulose and α-cellulose. The samples were soaked in 0.10 M sulfuric acid (5% solids) while stirring at RT for 4 h. The presoaked slurry was filtered through a filter funnel and the solids were washed with excess DI water, added to 0.10 or 0.20 M sulfuric acid (5% solids) and transferred to a Parr 4560 mini pressure reactor (600 mL) for the second pretreatment step under various conditions. The reactor was heated to the desired temperature from RT with constant stirring at a heating rate of ~6 ºC/min. After pretreatment, the reactor was cooled to RT in an ice-water bath. The slurry was filtered through a filter funnel and the pretreated solids were washed with excess DI water.

3.2.5 Pseudo-lignin Preparation

Poplar holocellulose or α-cellulose samples recovered from various DAP conditions were refluxed with *p*-dioxane–water (9:1, v/v), under nitrogen following a literature method [179]. The samples were filtered and washed with *p*-dioxane, and the combined filtrates were concentrated under vacuum and then dissolved in DI water to precipitate pseudo-lignin. Finally, the precipitated pseudo-lignin was freeze-dried and vacuum dried at 40 ºC.

3.2.6 Enzymatic Mild Acidolysis Lignin (EMAL) Preparation

Dilute acid-treated poplar (pretreatment conditions: 170 °C, 0.5% H_2SO_4, 8 min; combined severity factor (CSF): 1.97) was ball-milled for one week in a porcelain jar

using ceramic balls under nitrogen. Ball-milled dilute acid-treated poplar powder (dry weight: 21.42 g;) was subjected to enzymatic hydrolysis by Cellulysin cellulase at an enzyme loading of 40 mg/g of biomass. The enzymatic hydrolysis was carried out at 35 °C over a period of 48 h at pH 5.0 (20 mM acetate buffer solution) and a consistency of 3%. After enzymatic hydrolysis, the impure enzymatic hydrolysis lignin was centrifuged and washed twice with acidic deionized water at pH 2.0 (0.01 M HCl) and freeze-dried. Impure enzymatic hydrolysis lignin (dry weight: 16.26 g) was suspended in 326.00 mL *p*-dioxane/acidified deionized water solution 85:15 v/v, containing 0.01 M HCl and stirred at 87 °C under N_2 for 2 h. The obtained solution was filtered, and the lignin solution was collected. The solid residue was sequentially washed with fresh *p*-dioxane/deionized water solution (85:15 v/v) 2-3 times. The total filtrates solution was neutralized with sodium bicarbonate and stirred for 3 h. The neutralized solution was then rotary-evaporated until a thick solution was obtained. This thick solution was carefully dropped into a large quantity of acidified deionized water (0.01 M HCl), and the precipitated lignin was isolated by centrifugation, washed, and freeze-dried.

3.2.7 Lignocellulosic Samples Preparation

Pseudo-lignin or dilute acid-treated lignin was added to poplar holocellulose to produce various lignocellulosic samples. In brief, various amounts of pseudo-lignin or dilute acid-treated lignin was dissolved in p-dioxane/water (10/1, v/v). A sample of poplar holocellulose (dry weight: 0.50 g) was added to the solution, and the mixture was stirred in dark at RT for 2 h under N_2 protection. The slurry was then transferred to an aluminum weigh dish and allowed to air-dry in fumehood.

3.2.8 Enzymatic Hydrolysis

Cellulase from *Trichoderma reesei ATCC 26921* and Novozyme 188 (β-glucosidase) from *Aspergillus niger* were purchased from Aldrich−Sigma and used as received. The activities of cellulase and β-glucosidase were determined to be 91.03 FPU/ml and 387.70 CBU/ml, respectively, according to the literature methods [180]. Enzymatic hydrolysis of different samples was performed at a consistency of 1% (w/v) in 50 mM citrate buffer (pH 4.8) with cellulase and β-glucosidase loadings of 20 FPU/g and 40 CBU/g, respectively. The mixture was incubated at 50 °C under continuous agitation at 150 rpm. A sample of the hydrolysis liquid (1.00 mL) at various time intervals was withdrawn, and the hydrolysis was quenched by submersion for 10 min in a vigorously boiling water bath. The liquid samples were then immediately frozen at -20 °C until analysis on an Agilent 1200 series high-performance liquid chromatography (HPLC) system (Agilent Technologies) equipped with an autosampler and an Aminex HPX-87H column and precolumn (Bio-Rad Laboratories). The analysis was carried out at 65 °C using 10 mM nitric acid solution as eluent at a flow rate of 0.6 mL min^{-1} and with refractive index detection. The calibration of the system was performed with glucose standards.

3.3 Analytical Procedures

3.3.1 Carbohydrate and Acid-insoluble (Klason) Lignin Analysis

Samples for carbohydrate constituents and acid-insoluble lignin analysis were prepared using a two-stage acid hydrolysis protocol based on Tappi method T-222 om-88 [172] with a slight modification. The first stage utilized a severe pH and a low reaction temperature (72% H_2SO_4 at 30 ºC for 1 h). The second stage was performed at lower acid concentration and higher temperature (3% H_2SO_4 at 121 ºC for 1 h) in a MED12

autoclave. The resulting solution was cooled to RT and filtered through a G8 glass fiber filter (Fisher Scientific, USA). The remaining residue, considered as acid-insoluble lignin, was oven-dried and weighed to obtain the acid-insoluble lignin content. The filtered solution was analyzed for carbohydrate constituents by high-performance anion-exchange chromatography with pulsed amperometric detection (HPAEC-PAD) using Dionex ICS-3000 (Dionex Corp., USA) equipped with an IonPac AG15 AS15 5-µm column using 200 mM NaOH solution at a flow rate of 0.3 mL min^{-1}.

3.3.2 Molecular Weight Analysis

Dry pseudo-lignin (20 mg) was acetylated by stirring with 1:1 (v/v) acetic anhydride/pyridine mixture (2.00 ml) at RT for 72 h. The reaction was quenched by anhydrous methanol (1.00 ml) and the solvent mixture was removed under reduced pressure at 50 ºC. The acetylated lignin was dissolved in chloroform (50 ml) and washed with water (20 ml). The chloroform phase was dried over anhydrous $MgSO_4$ and then concentrated under reduced pressure. Prior to gel permeation chromatography (GPC) analysis, the dried acetylated pseudo-lignin samples were dissolved in tetrahydrofuran (1.00 mg/ml), filtered through a 0.45 µm filter and placed in a 2 ml auto-sampler vial. The molecular weight distributions of the acetylated pseudo-lignin samples were analyzed by Agilent GPC SECurity 1200 system equipped with four Waters Styragel columns (HR0.5, HR2, HR4, HR6), Agilent refractive index (RI) detector and Agilent UV detector (270 nm). Tetrahydrofuran was used as the mobile phase (1.0 ml/min) and the injection volume was 30.0 µl. A calibration curve was constructed based on 10 narrow polystyrene standards ranging in molecular weight from 1.2×10^3 to 5.5×10^4 g/mol. Data collection and processing were performed by Polymer Standards Service

WinGPC Unity software (Build 6807). The number-average and weight-average molecular weights (M_n and M_w) were calculated by the software relative to the universal polystyrene calibration curve.

3.3.3 Fourier Transform Infrared (FT-IR) Spectroscopy

Spectrum One FT-IR system (Perkin Elmer, Wellesley, MA) with a universal attenuated total reflection (ATR) accessory was used to characterize the isolated pseudo-lignin samples. Each sample was pressed uniformly and tightly against the diamond surface using a spring-loaded anvil. FT-IR spectra were obtained by averaging 64 scans from 4,000 to 650 cm^{-1} at 4 cm^{-1} resolution. Baseline and ATR corrections for penetration depth and frequency variations were carried out using the Spectrum One software supplied with the equipment.

3.3.4 Nuclear Magnetic Resonance (NMR) Spectroscopy

3.3.4.1 Quantitative ^{13}C NMR Characterization

NMR experiments were performed using a Bruker AMX-400 spectrometer operating at a frequency of 100.61 MHz for ^{13}C NMR analysis. Quantitative ^{13}C NMR spectrum was acquired using dimethylsulfoxide (DMSO)-d_6 (450 µL) as the solvent for the samples (120 mg) at 298 K with an inverse-gated decoupling sequence, 90° pulse angle, 12-s pulse delay, 8000 scans, 10.0 Hz line broadening, and no zero filling.

3.3.4.2 ^{13}C-^{1}H 2D Heteronuclear Single Quantum Coherence (HSQC) NMR Characterization

2D heteronuclear single quantum coherence (HSQC) correlation NMR analysis was performed using a Bruker AMX-400 spectrometer. 2D HSQC spectrum was acquired using dimethylsulfoxide (DMSO)-d_6 (450 µL) as the solvent for the samples (120 mg) at

298 K. The conditions were 13-ppm spectra width in F2 (^{1}H) dimension with 1024 data points (95.9-ms acquisition time), 210-ppm spectra width in F1 (^{13}C) dimension with 256 data points (6.1-ms acquisition time); a 3-s pulse delay; a $^{1}J_{C\text{-}H}$ of 145 Hz; and 32 scans. The central DMSO-d_6 solvent peak (δ_C 39.5 ppm; δ_H 2.5 ppm) was used for chemical shifts calibration [181]. Spectra processing used a typical squared sine apodization in F2 and F1. NMR data were processed using the TopSpin 2.1 software (Bruker BioSpin).

3.3.4.3 Distortionless Enhancement by Polarization Transfer (DEPT-135) ^{13}C NMR Characterization

Distortionless enhancement by polarization transfer (DEPT) NMR spectra were recorded by a Bruker AMX-400 spectrometer using dimethylsulfoxide (DMSO)-d_6 (450 µL) as the solvent for the samples (120 mg) at 298 K with a 135º pulse angle, 3-s pulse delay, 12000 scans, 10.0 Hz line broadening, and no zero filling.

3.3.4.4 Solid-state ^{13}C CP/MAS NMR Characterization

The ground samples (~ 30% moisture) were packed in 4mm zirconia rotors fitted with kel-F caps and measured at 10 KHz spinning speed. The NMR experiments were performed with a Bruker Advance-400 spectrometer operating at a ^{13}C frequency of 100.6 MHz. CP/MAS experiments utilized a 5 µs (90º) proton pulse, 1.5 ms contact pulse, 4 s recycle delay with 8000 scans, 15.0 Hz line broadening, and zero filling of 2048. The line-fitting analysis was done using NUTS NMR Data Processing software (Acorn NMR, Inc.).

3.3.5 Scanning Electron Microscopy (SEM)

All cross-sectioned samples were mounted onto a stage and then coated with gold for 2 min by EM350 sputter. Images were acquired via a JEOL-1530 Thermally-Assisted Field

Emission (TFE) Scanning Electron Microscope (SEM) (JEOL, Peabody, MA) at various resolving powers under 5 kV.

3.4 Error Analysis

The experiments of the carbohydrate and acid-insoluble lignin analysis were performed in triplet, and the results represented the mean values of three independent experiments. The standard deviation associated with the carbohydrate and acid-insoluble lignin measurements were ± 0.2-2.8%, and ± 0.1-0.7%, respectively. All enzymatic hydrolysis experiments were performed in duplicate, and the results represented the mean values of two independent experiments. The standard deviation associated with the glucose yield at each time interval was in the range of ± 0-10%. For solid-state NMR analysis, error analysis was conducted by three individual line-fit data processing analyses.

Chapter 4

PSEUDO-LIGNIN FORMATION AND ITS IMPACT ON ENZYMATIC HYDROLYSIS[1]

4.1 Introduction

Increasing global energy demand, unstable and expensive petroleum resources and concern over global climate changes have led to the development of renewable energy sources such as cellulosic ethanol that can supplement fossil fuels [1,2]; however, the yield of ethanol production from native lignocellulosic materials is relatively low due to the natural resistance of plant cell walls to decomposition from microbes and enzymes [1]. Dilute acid pretreatment has been proven to successfully hydrolyze hemicelluloses and disrupt the lignocellulosic structure thereby reducing its recalcitrance for a wide range of feedstocks including softwoods, hardwoods, herbaceous crops, agricultural residues, wastepaper and municipal solid waste. Dilute acid pretreatment does not lead to significant delignification. Instead, several studies have found that the acid-insoluble (Klason) lignin content of dilute acid pretreated material is often higher than that of the starting material [11,12,13,14]. This phenomenon has been hypothesized to be due to repolymerization of polysaccharides degradation products (such as furfural) and/or polymerization with lignin to form a lignin-like material termed pseudo-lignin [15,16]. Sannigrahi *et al.* [109] demonstrated that pseudo-lignin can be generated from carbohydrates without significant contribution from lignin during dilute acid

[1] This manuscript was accepted for publication in Bioresource Technology, 2012. It is entitled as – Pseudo-lignin Formation and Its Impact on Enzymatic Hydrolysis. The other authors are Seokwon Jung and Art Ragauskas from School of Chemistry and Biochemistry at Georgia Institute of Technology.

pretreatment, especially under high severity pretreatment conditions. Scanning electron microscopy (SEM) studies on dilute acid pretreated holocellulose revealed the presence of spherical droplets on the surface of pretreated holocellulose, which were attributed to pseudo-lignin. ^{13}C CP/MAS NMR analysis of pretreated holocellulose indicated significant peaks originating from carbonyl, aromatic, methoxy and aliphatic structures and attributed to the structure of pseudo-lignin. Furthermore, the intensities of these peaks increased as pretreatment severity increased, suggesting an acid-catalyzed disproportionation mechanism accompanying pseudo-lignin formation.

Although the generation of pseudo-lignin has been proposed by many researchers [16,182,183,184,185], there has been a lack of understanding of the fundamental chemistry surrounding pseudo-lignin. The objective of this study is to characterize pseudo-lignin isolated from dilute acid pretreated hybrid poplar holocellulose and α-cellulose, in order to give an insight into the chemical structure and formation mechanism of pseudo-lignin. More importantly, the interaction between pseudo-lignin spheres and cellulases was investigated in order to determine whether the presence of pseudo-lignin may be detrimental to enzymatic hydrolysis of cellulose.

4.2 Experimental Section

4.2.1 Materials

Samples were prepared as described in Chapter 3 (3.1.2 Biomass Substrate). Hybrid poplar (*Populus trichocarpa x deltoides*) was obtained from Oakridge National Laboratory, TN and Wiley milled to pass a 2-mm screen. The sample was air-dried and stored at -20 ºC.

4.2.2 Extractive-free poplar, poplar holocellulose and cellulose preparation

Samples were prepared as described in Chapter 3 (3.2.1-3.2.3). All the results from the analyses were calculated based on the oven dry weight of biomass that was determined by measuring the moisture content using a moisture analyzer.

4.2.3 Dilute acid pretreatment

Two-step dilute acid pretreatments with two different conditions for the second step were applied to both poplar holocellulose and α-cellulose (Table 4.1). The samples were soaked in 0.10 M sulfuric acid (5% solids) while stirring at RT for 4 h. The presoaked slurry was filtered through a filter funnel and the solids were washed with excess DI water, added to 0.10 or 0.20 M sulfuric acid (5% solids) and transferred to a Parr 4560 mini pressure reactor (600 mL) for the second pretreatment step. The reactor was heated to the desired temperature with constant stirring at a heating rate of ~6 ºC/min. After pretreatment, the slurry was filtered through a filter funnel and the pretreated solids were washed with excess DI water.

Table 4.1 Conditions for treatment (2nd step) of poplar holocellulose and a-cellulose following initial 1st step treatment of soaking (5% solids) while stirring in 0.10 M H_2SO_4 at RT for 4 h

Sample	2^{nd} step condition
Holocellulose (0.1M)	180 °C, 0.1 M H_2SO_4, 40 min
Holocellulose (0.2M)	180 °C, 0.2 M H_2SO_4, 60 min
α-cellulose (170C)	170 °C, 0.1 M H_2SO_4, 20 min
α-cellulose (180C)	180 °C, 0.1 M H_2SO_4, 40 min

4.2.4 Pseudo-lignin Preparation

Pseudo-lignin samples isolated from dilute acid-treated poplar holocelulose and cellulose were prepared as described in Chapter 3 (3.2.5 Pseudo-lignin Preparation).

4.2.5 Lignocellulosic Samples Preparation

Hybrid poplar was subjected to a two-step dilute acid pretreatment with the same protocol as applied to holocellulose A. Pretreated poplar holocellulose was isolated from dilute acid pretreated poplar using the same method as described in Chapter 3 (3.2.2 Holocellulose Pulping). Pseudo-lignin extracted from pretreated holocellulose was added to pretreated poplar holocellulose to produce pseudo-lignin on holocellulose samples. In brief, the appropriate amount of pseudo-lignin (10%, 20% and 40% of acid-insoluble lignin value of pretreated poplar, Table 4.2) was dissolved in *p*-dioxane/water (10/1, v/v). A sample of pretreated poplar holocellulose (0.50 g dry weight) was added to pseudo-lignin solution, and the mixture was allowed to stir in dark at RT under N_2 protection for 2 h. The slurry was transferred to an aluminum weigh dish and allowed to air-dry in a fumehood.

Table 4.2 The quantities of pseudo-lignin (based on acid-insoluble lignin value of pretreated poplar) and holocellulose addition for the pseudo-lignin on holocellulose preparation

Sample	Pseudo-lignin extracted from holocellulose pretreated at	Pseudo-lignin addition level (%)	Pseudo-lignin addition (g)	Holocellulose addition (g)	Total mass (g)
a	180 °C, 0.1 M H_2SO_4, 40 min	10	0.07	0.50	0.57
b	180 °C, 0.2 M H_2SO_4, 60 min	10	0.07	0.50	0.57
c	180 °C, 0.1 M H_2SO_4, 40 min	20	0.14	0.50	0.64
d	180 °C, 0.2 M H_2SO_4, 60 min	20	0.14	0.50	0.64
e	180 °C, 0.1 M H_2SO_4, 40 min	40	0.28	0.50	0.78
f	180 °C, 0.2 M H_2SO_4, 60 min	40	0.28	0.50	0.78
Pretreated holocellulose	NA	NA	NA	0.50	0.50
Pretreated poplar	NA	NA	NA	NA	1.26

4.2.6 Carbohydrate and Acid-insoluble Lignin Analysis

Carbohydrate profiles and acid-insoluble lignin content in various samples were determined as described in Chapter 3 (Chapter 3.3.1 Carbohydrate and Acid-insoluble Lignin Analysis).

4.2.7 Molecular Weight Measurement of Pseudo-lignin

The molecular weights of pseudo-lignin samples were determined as described in Chapter 3 (Chapter 3.3.2 Molecular Weight Analysis).

4.2.8 FTIR Spectroscopic Analysis

Samples were characterized by FT-IR according to the procedures described in Chapter 3 (Chapter 3.3.3 Fourier Transform Infrared (FT-IR) Spectroscopy).

4.2.9 ^{13}C NMR Spectroscopic Analysis

Quantitative 13C NMR and DEPT-135 NMR experiments were performed according to the procedures described in Chapter 3 (3.3.4.1 and 3.3.4.3).

4.2.10 Scanning Electron Microscopy

SEM characterization was performed according to the procedures described in Chapter 3 (3.3.5 Scanning Electron Microscopy (SEM)).

4.2.11 Enzymatic Hydrolysis

Enzymatic hydrolysis experiments were performed as described in Chapter 3 (3.2.8 Enzymatic Hydrolysis). A sample of hydrolysis liquid (1.00 mL) at time intervals of 0.5, 1, 1.5, 2, 2.5, 3, 4, 6, 7, 24 and 48 h was withdrawn and the hydrolysis was quenched by submersion for 10 min in a vigorously boiling water bath. The liquid samples were then stored and analyzed as described in Chapter 3 (3.2.8 Enzymatic Hydrolysis).

4.3 Results and Discussion

4.3.1 Pseudo-lignin Extraction Yields

The lignin and carbohydrate contents of untreated and pretreated α-cellulose and holocellulose are summarized in Table 4.3. In general, the acid-insoluble lignin content of pretreated samples is higher than that of the starting material, indicating the formation of pseudo-lignin during pretreatment. The proportion of acid-insoluble lignin or pseudo-lignin in the pretreated solids increased as the pretreatment severity increased, while the proportion of carbohydrates retained in the solids showed the inverse trend. Compared to untreated α-cellulose, the increase in acid-insoluble lignin content of α-cellulose pretreated at the least severe conditions (170 ºC, 0.1 M H_2SO_4, 20 min) was not significant, leading to no significant amount of isolated pseudo-lignin. Whereas the acid-insoluble lignin content of α-cellulose B increased by more than seven times, and its glucan value declined by 19% compared to untreated α-cellulose. At the most severe conditions (180 ºC, 0.2 M H_2SO_4, 60 min), holocellulose B has the highest proportion of pseudo-lignin and the least amount of glucan retained compared to untreated holocellulose. Furthermore, pretreated holocellulose generated higher proportion of pseudo-lignin than pretreated α-cellulose, even under the same pretreatment conditions. Additionally, no significant amount of xylan was retained for all samples after pretreatment. These results suggest that pseudo-lignin can be produced from both acid pretreated cellulose and hemicellulose, and its proportion increases as the pretreatment severity increases.

Table 4.3 Lignin and carbohydrate contents of holocellulose and α-cellulose (based on oven-dried samples)

Sample	Acid-insoluble lignin (%)	Xylan (%)	Glucan (%)	Recovery from pretreatment (%)	Pseudo-lignin extraction yield (isolated pseudo-lignin/total acid-insoluble lignin x 100%)
α-cellulose	2.3	1.0	99.4	NA	NA
α-cellulose (170C)	6.6	0	94.0	62.7	0
α-cellulose (180C)	20.0	0	80.4	31.7	44.6
Holocellulose	4.7	22.0	68.1	NA	NA
Holocellulose (0.1M)	37.5	0	65.3	28.8	51.3
Holocellulose (0.2M)	86.9	0	7.0	19.2	33.7

4.3.2 Molecular Weight Analysis of Isolated Pseudo-lignin

The molecular weights of isolated pseudo-lignin are shown in Table 4.4. In general, the molecular weights of isolated pseudo-lignin were much lower than those of milled wood lignin (M_n ~4060 g/mol; M_w ~10002 g/mol) from poplar [186]. Furthermore, pseudo-lignin extracted from holocellulose pretreated at different conditions had similar molecular weights, which were larger than those of pseudo-lignin extracted from pretreated α-cellulose.

4.3.3 Structural Characterization of Isolated Pseudo-lignin

The FT-IR spectra of a-cellulose, holocellulose, pseudo-lignin extracted from pretreated a-cellulose, holocellulose A and holocellulose B are presented in Figure 4.1. The FT-IR spectra of all isolated pseudo-lignin samples show similar profiles but different intensities of the absorption bands, which are significantly distinct from those of the starting materials (α-cellulose and holocellulose). Based on FT-IR characterization, pseudo-lignin consists of hydroxyl, carbonyl and aromatic structures. The hydroxyl stretching peaks at

~3238 cm^{-1} are strong and broad, indicating the presence of hydrogen-bonding in isolated pseudo-lignin. The strong bands at ~1697 cm^{-1} and ~1611 cm^{-1}, together with the band at ~1512 cm^{-1} can be attributed to C=O (carbonyl or carboxylic) conjugated with aromatic ring, whereas the bands in the 1320-1000 cm^{-1} region correspond to C-O stretching (in alcohols, ethers or carboxylic acids). These observations indicate dehydration and aromatization reactions of carbohydrates take place during the formation of pseudo-lignin. In addition, the peak at ~867 cm-1 arising from C-H out-of-plane bending suggests the benzene rings of pseudo-lignin are 1,3,5-trisubstituted. The above peak assignments are summarized in Table 4.4.

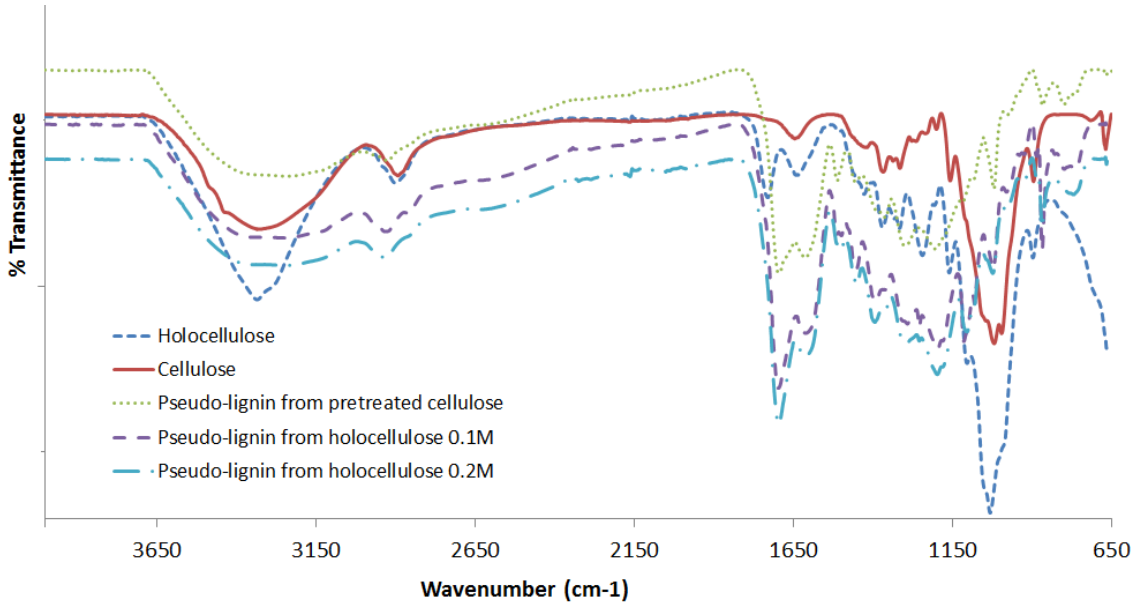

Figure 4.1 FT-IR spectra of cellulose, holocellulose, pseudo-lignin extracted from pretreated α-cellulose, holocellulose (0.1M) and holocellulose (0.2M)

Table 4.4 Peak assignments for FT-IR spectra of pseudo-lignin [187]

Wavenumber (cm^{-1})	Assignment
3238	O-H stretching in alcohols, phenols or carboxylic acids
2923	Aliphatic C-H stretching
1697	C=O stretching in carboxylic acids, conjugated aldehydes or ketones
1611, 1512	Aromatic C=C stretching (in ring)
1360	Aliphatic C-H rocking
1299, 1203, 1020	C-O stretching in alcohols, ethers, or carboxylic acids
867, 800	Aromatic C-H out-of-plane bending

To further characterize the functional groups in pseudo-lignin, ^{13}C NMR spectra of isolated pseudo-lignin were obtained and this data is summarized in Figure 4.2. A primary qualitative assignment based on literature is proposed in Table 4.5. The ^{13}C NMR spectra are predominantly comprised of signals from carbonyl, carboxylic, aromatic and aliphatic structures, which do not contain significant signals from cellulose or xylan. The peaks centered at 208-205 ppm and 203-185 ppm can be attributed to C=O in ketones and C=O in aldehydes, respectively. Whereas the peaks centered at 178-172 ppm correspond to C=O in carboxylic acids. This is consistent with FT-IR characterization, indicating the presence of carbonyl and carboxylic groups in pseudo-lignin. In addition, the intensities of carbonyl and carboxylic peaks are stronger for pseudo-lignin extracted from pretreated holocellulose B compared to other samples, which implies more degradation reactions of carbohydrates occur at the more severe conditions. The ^{13}C NMR spectra of isolated pseudo-lignin also present common peaks in the aromatic region (δ 155-96 ppm). The peaks in the 155-142 ppm region are characteristic of aromatic C-O bonds. Whereas the peaks in the 142-125 ppm and 125-96

ppm regions represent aromatic C-C bonds and aromatic C-H bonds, respectively. Among the aromatic signals, aromatic C-O bonds are the most predominant, and the signal at ~66 ppm was due to *p*-dioxane which could not be fully removed after extended time in a vacuum oven. To obtain further precise knowledge of the carbon signals in the 96-0 ppm region, the isolated pseudo-lignin samples were investigated by DEPT (θ = 135 C°) edited ^{13}C NMR spectroscopy, and Figure 4.3 represents the DEPT-135 NMR spectrum of pseudo-lignin extracted from pretreated holocellulose B. According to DEPT NMR analysis, the two peaks centered at ~72 ppm and ~63 ppm can be attributed to hydroxylated methylene groups. Signals at 61-59 ppm and ~56 ppm correspond to the methoxy groups connected to aromatic rings. Furthermore, their intensities are stronger for pseudo-lignin extracted from pretreated holocellulose than those from pretreated α-cellulose, which may be due to the presence of 4-*O*-methyl-D-glucuronic acid in the hemicellulose of poplar [188]. Pseudo-lignin also possesses aliphatic structures, as can be deduced from the signals in the 50-20 ppm region, where the peaks centered at ~30 ppm and ~26 ppm correspond to CH groups while the signals at ~29 ppm represent CH_2 groups according to the DEPT-135 NMR spectra. In addition, there are two CH_2 groups centered at ~38 ppm and ~28 ppm for pseudo-lignin extracted from holocellulose B. Furthermore, the ^{13}C NMR spectra of pseudo-lignin extracted from pretreated holocellulose are similar, in addition to the similar FT-IR spectra and molecular weights, suggesting they have similar structural features. This is probably due to pseudo-lignin was formed from the same substrate and/or the difference in these two pretreatment severities was not distinct enough to significantly change the pseudo-lignin structure.

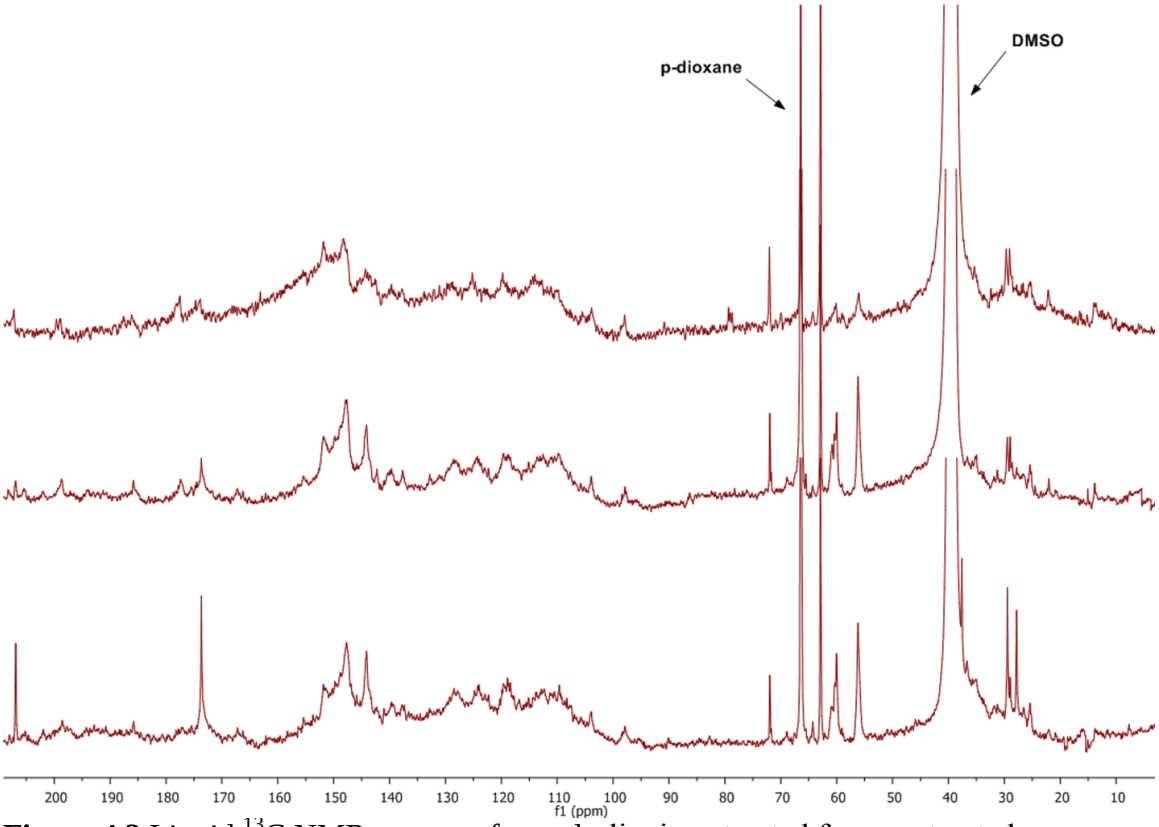

Figure 4.2 Liquid ^{13}C NMR spectra of pseudo-lignin extracted from pretreated α-cellulose (top), holocellulose (0.1M) (middle) and holocellulose (0.2M) (bottom)

Table 4.5 Peak assignments for ^{13}C NMR spectra of pseudo-lignin [187]

Chemical shift (ppm)	Assignment
208-205	C=O in ketones
203-185	C=O in aldehydes
178-172	C=O in carboxylic acids
155-142	Aromatic C-O
142-125	Aromatic C-C
125-96	Aromatic C-H
72, 63	Hydroxylated methylene
61-59, 56	Methoxy groups connected to aromatic rings
50-20	Aliphatic carbons

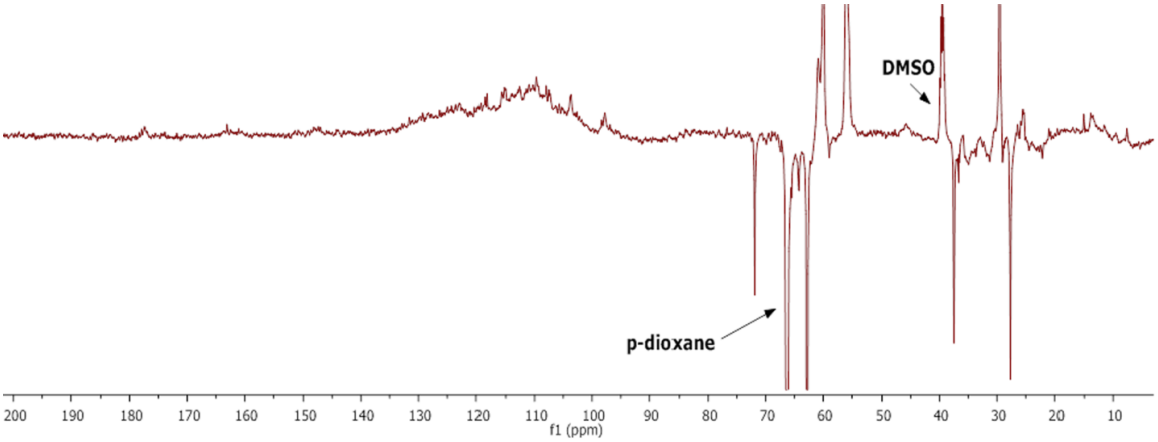

Figure 4.3 DEPT-135 NMR spectrum of pseudo-lignin extracted from pretreated holocellulose (0.2M)

4.3.4 Mechanistic Consideration

Although the concept of pseudo-lignin has been applied for several decades, there has been a lack of detailed mechanistic studies of pseudo-lignin formation during pretreatment, probably owing to the complexity of pseudo-lignin structure and the heterogeneity of reaction media. The data from lignin and carbohydrate analysis indicates the proportion of pseudo-lignin increases as the amount of carbohydrates retained decreases. The previous study [109] showed that a large fraction of the carbohydrates was detected in the form of furans after dilute acid pretreatment. In addition to the presence of high proportions of unsaturated carbons in the pseudo-lignin structure, it can conclude that the hydrolysis of polysaccharides to the corresponding monosaccharides, and the subsequent dehydration and fragmentation of sugars take place during dilute acid pretreatment. It is generally accepted that 5-hydromethylfurfural (HMF) and furfural are the first and main dehydration products of hexoses and pentoses respectively [15]. Further rearrangements of HMF and/or furfural to yield other aromatic compounds have been suggested in the literature. For instance, 1,2,4-benzenetriol (BTO) was reported to

be generated from the hydrolytic ring-opening reaction of HMF in yields of up to 46% at 50% HMF conversion [189]. Additionally, 3,8-dihydroxy-2-methylchromone (DMC) was found to be the major aromatic component in the slightly acidic degradation of D-xylose [190]. These results suggest BTO and DMC are the key intermediates for peudo-lignin formation during dilute acid pretreatment. The subsequent reaction stages involve polycondensation and/or polymerization reactions. BTO can rapidly react with HMF and/or furfural via aromatic electronphilic substitution and polycondensation reaction to produce a three-dimensional polymer under acid catalysis. In the presence of oxygen, oxidative polymerization of BTO to form a poly(phenylene)-like structure is also possible [191]. The above reaction pathways are summarized in Figure 4.4, which suggest high temperature and the presence of acid and oxygen are the crucial conditions for pseudo-lignin formation during dilute acid pretreatment. This indicates lower temperature, lower acid concentration and/or anaerobic condition may suppress pseudo-lignin generation during pretreatment.

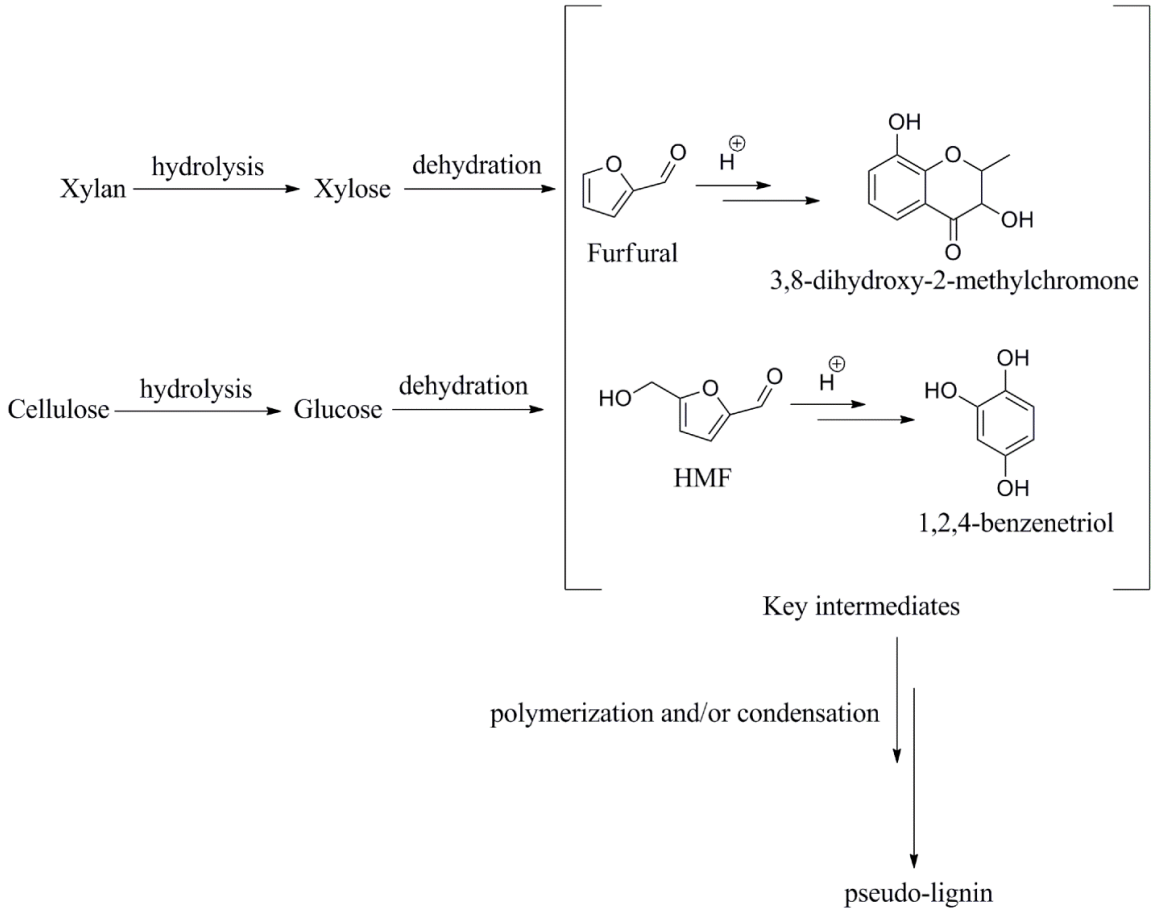

Figure 4.4 Hypothesized reaction pathways for pseudo-lignin formation

4.3.5 Pseudo-lignin/Enzyme Interaction

Donohoe *et al.* [158] observed that lignin droplets appear on the cell wall of biomass after dilute acid pretreatment, which act as a physical barrier to prevent enzyme access to the carbohydrate fraction of biomass during enzymatic hydrolysis. The previous study revealed the presence of pseudo-lignin droplets on the surface of pretreated holocellulose [109]. To investigate if there are interactions between pseudo-lignin droplets and enzymes, several pseudo-lignin on holocellulose lignocellulosic samples were prepared, and the glucose yields of enzymatic hydrolysis of these samples were compared with dilute acid pretreated poplar and holocellulose. The physical structure of the pseudo-lignin on holocellulose sample and pretreated holocellulose was studied by SEM

imaging. Compared to the surface of pretreated holocellulose (Figure 4.5 top), discrete spherical droplets representing pseudo-lignin balls were presented on the surface of pretreated holocellulose of the pseudo-lignin on holocellulose sample (Figure 4.5 bottom). These pseudo-lignin droplets hypothesized could be detrimental to enzymatic hydrolysis of pretreated biomass. Indeed, the enzymatic hydrolysis results (Figure 4.6) clearly indicate the presence of pseudo-lignin/enzymes interaction, since the glucose yield declines as the lignin and/or pseudo-lignin content increases. Pseudo-lignin on holocellulose samples at 10% addition level have the highest glucose yields (~74% after 48 h) among all pseudo-lignin on holocellulose samples, whereas samples at 40% addition level have the lowest (~46% after 48 h). In general, pseudo-lignin on holocellulose samples with the same pseudo-lignin content have the similar glucose yield, which is probably caused by the similar structure of pseudo-lignin extracted from pretreated holocellulose. Pretreated holocellulose has the highest glucose yield (~ 80% after 48 hr) among all samples while pretreated poplar gave the lowest (~40% after 48 h), which may be due to the lignin content of pretreated poplar under the conditions studied.

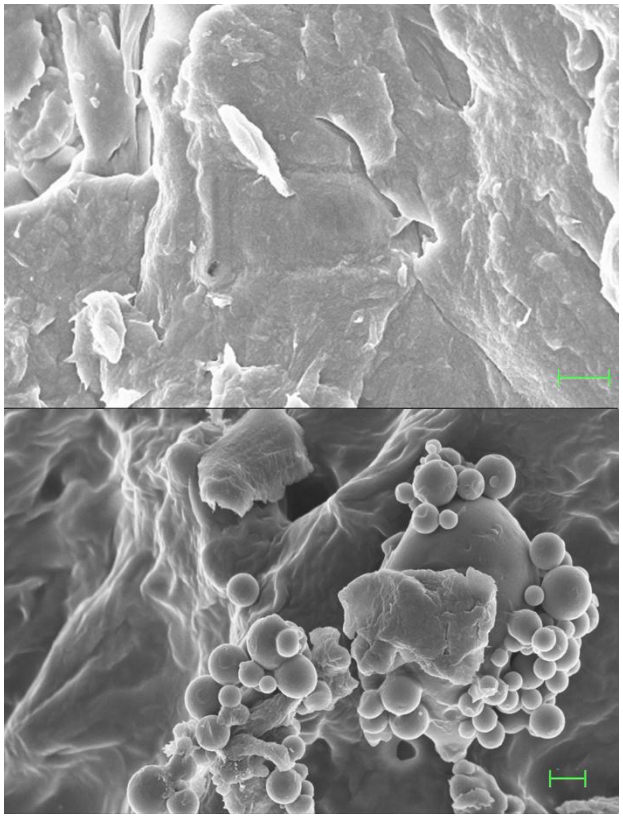

Figure 4.5 SEM images of pretreated holocellulose (top) and the pseudo-lignin on holocelluose lignocellulosic sample (bottom). All scale bars are equivalent to 1 µm

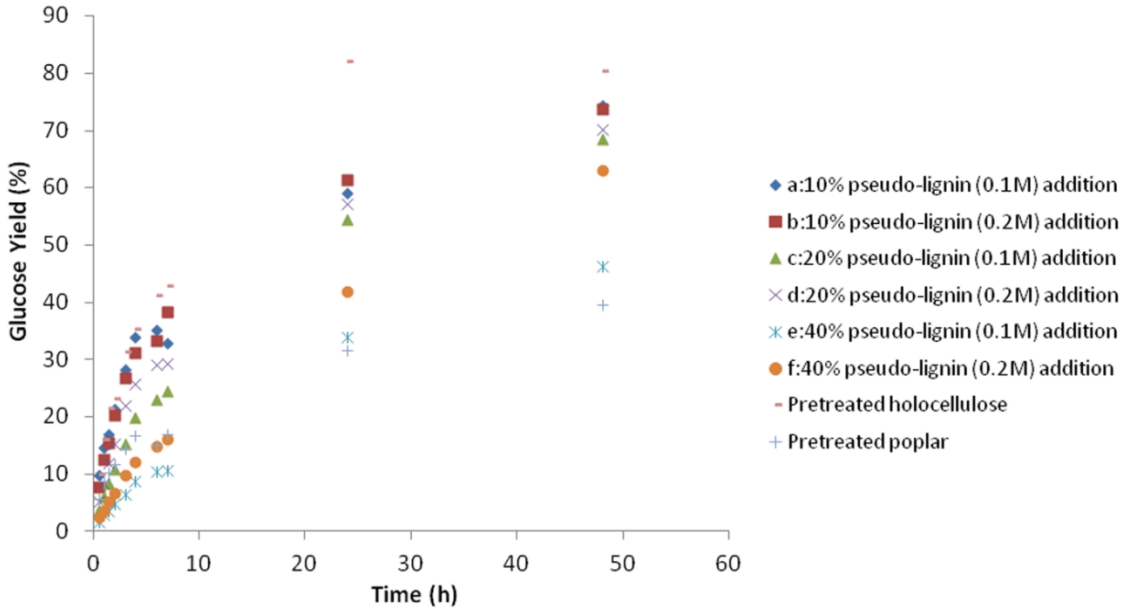

Figure 4.6 Time course of glucose yield of various samples after 48 h of enzymatic hydrolysis

4.4 Conclusion

Results from chemical and spectroscopic analysis indicated that during dilute acid pretreatment, cellulose and hemicellulose in hybrid poplar biomass underwent acid-catalyzed dehydration, fragmentation, rearrangement and polycondensation and/or polymerization reactions to produce an acid-insoluble material termed pseudo-lignin, which consists of carbonyl, carboxylic, aromatic and aliphatic structures. Pseudo-lignin not only yields a positive Klason lignin value, but also significantly inhibits enzymatic hydrolysis of cellulose. This suggests that dilute acid pretreatment should be performed at lower severity and/or anaerobic conditions in order to avoid the formation of pseudo-lignin.

CHAPTER 5

CARBOHYDRATE DERIVED-PSEUDO-LIGNIN CAN RETARD CELLULOSE BIOLOGICAL CONVERSION[2]

5.1 Introduction

Abundant and renewable lignocellulosic biomass containing large amounts of structural polymeric sugars, can play a significant role in the development of energy independent and secure societies provided that this resource can be tapped efficiently and economically [192]. To derive fuels and chemicals from cellulosic biomass, a number of process steps must be applied, with pretreatment being essential to overcome the natural resistance of most lignocellulosics to sugar release [64]. Unfortunately, pretreatment is also one of the most expensive steps in the overall process. Pretreatment enhances cellulase accessibility to cellulose, and its efficacy is associated with altering the biomass structure through lignin/hemicellulose and other components dislocation/physical removal [63,64]. Several leading thermochemical pretreatment technologies employing acids, bases, or just water have been reported to enhance cellulosic biomass digestibility significantly [10]. Dilute acid and water-only (hydrothermal) pretreatments are often employed to enhance biomass digestibility, and steam explosion (catalyzed or uncatalyzed), liquid hot water, and flowthrough approaches have been most commonly used to pretreat biomass [62,129]. However, although both hydrothermal and dilute acid

[2] This manuscript was accepted for publication in Biotechnology & Bioengineering, 2012. It is entitled as – Carbohydrate Derived-Pseudo-Lignin Can Retard Cellulose Biological Conversion. The other authors are Rajeev Kumar and Charles Wyman from Department of Chemical and Environmental Engineering at Bourns College of Engineering; Poulomi Sannigrahi, Seokwon Jung and Art Ragauskas from School of Chemistry and Biochemistry at Georgia Institute of Technology

pretreatments achieve physical removal/dislocation of hemicellulose and lignin and enhance cellulose accessibility several fold, recoveries of sugars from hemicellulose and cellulose in most cases are less than 80% and 95%, respectively [183]. Monomeric forms of carbohydrates released into the aqueous phase during pretreatment can degrade into soluble compounds, for example, furans (furfural (FF) and hydroxymethyl furfural (5-HMF)) and acids (levulinic acid (LA) and formic acid (FA)). These can further degrade to form insoluble carbon enriched compounds often termed as chars and/or pseudo-lignin [11,193,194,195]. It has been postulated [16,184] and confirmed [109] that carbohydrates released during thermochemical pretreatments degrade to lignin-like (pseudo-lignin) compounds. However, it has never been determined whether these carbohydrate degradation products adversely affect cellulose digestion. In addition, it has been hypothesized and recently confirmed that lignin melts at temperatures above its glass transition temperature, which varies with solvent type and other conditions [196,197], moves to outer cell walls, and redeposits back on the cellulose surface, where it greatly hampers cellulose digestibility by blocking cellulase access to the substrate and/or unproductively binding cellulase [62,158]. Selig *et al.* [198] indicated that during dilute acid pretreatment, lignin derived from corn stem rind, added exogenously with filter paper, deposited on the cellulose surface in the form of globules that hampered hydrolysis rates and yields. However, it was not possible to distinguish whether these globules were from lignin or pseudo-lignin resulting from degradation of carbohydrates fraction of biomass or some combination of both.

In this study the effects of carbohydrate-derived pseudo-lignin on cellulose saccharification were investigated, and mechanisms were hypothesized to explain the

results. Due to the complex structure of cellulosic biomass, the wet chemistry method for compositional analysis defined by National Renewable Energy Laboratory (NREL, Golden, CO) does not distinguish between acid-insoluble lignin naturally found in plants and pseudo-lignin resulting from sugars degradation during pretreatment. Therefore, to avoid the complexity often encountered with interpretation of results for real biomass, pure Avicel cellulose alone and mixed with pure xylan or monomeric xylose sugar was pretreated with dilute sulfuric acid over the range of pretreatment severities often found to give best conversion results[3]. Following pretreatment, the solids were subjected to enzymatic hydrolysis and physical and chemical characterizations to elucidate the effects of xylan degradation products on enzymatic hydrolysis and support identification of possible mechanisms to explain the results.

5.2 Experimental Section

5.2.1 Materials

Materials, reagents and enzymes were prepared as described in Chapter 3 (Chapter 3.1.1 Chemicals and Materials).

5.2.2 Pretreatment

Dilute acid pretreatment of Avicel PH 101 cellulose alone and mixed with xylan or with xylose was performed in a 1 L (working volume 800 mL) Hastelloy C Parr reactor (Parr Instruments, Moline, IL). The Avicel cellulose loading was 5 wt% (40 g dry basis), and xylan or xylose was added to cellulose at a 0.5:1 weight ratio, representative of the typical ratio for natural lignocellulosic biomass. Pure xylose mixed with Avicel cellulose

[3]The cellulose and xylan described in this chapter are from Avicel cellulose and beechwood xylan, respectively, which means they are from difference source as compared to other chapters in this thesis study. The cellulose and xylan described in other chapters are exclusively from hybrid poplar.

was also pretreated as a control to evaluate any effects on cellulose reactivity that might be due to factors other than pseudo-lignin. The reactor cover was equipped with a K-type thermocouple (Model KQSS-316G-18; Omega Engineering Inc., Stamford, CT) positioned at the center of the reactor to monitor inside temperature, and a 3.5 in diameter helical shaped impeller on a two-piece shaft driven by a variable speed DC motor assembly provided mixing and heat transfer (A1750HC, Parr Instruments). A temperature controlled 4 kW fluidized sand bath was used to more rapidly heat the reactor (model SBL-2D, Techne Inc., Burlington, NJ), and the heating time to reach the desired reaction temperature of between 4 and 5 min was not included in the stated reaction time.

The DAP conditions were as reported in the literature for variety of biomass types (Wyman et al., 2009, 2011) and are summarized along with the corresponding combined severity factors (CSF) in Table 5.1. Following pretreatment, the reactor was cooled to below 508C in a RT water bath, and then the slurry was immediately transferred to 500mL centrifuge bottles (Catalog No.14-375-359, Fisher Scientific) that were centrifuged for 10 min at 10,000 rpm to separate solids from the liquid in a Beckman centrifuge (Model No. J2-21, Beckman Coulter, Inc., Brea, CA). After the first centrifugation, liquid samples were collected from the supernatant for further analysis, with the rest of the supernatant discarded. Some of the unwashed solids were collected for imaging and hydrolysis experiments, and the rest was washed at least five to seven times with RT deionized (DI) water until the supernatant pH was close to neutral. Then, the solids were scraped off from the centrifuge bottles and stored in Ziplock1 bags at 4 ºC for further experiments. Solids were analyzed for moisture content and composition according to NREL standard laboratory analytical procedures.

Table 5.1 Pretreatment conditions, resulting solids composition, and xylan/xylose recovery for dilute acid pretreatment of Avicel alone and mixed with xylan or xylose

Pretreatment Conditions	CSF[a]	Substrate	Solids composition (%; dry mass basis)				Xylan/xylose accounted for[c] (%)
					Lignin		
			C	Xyn	Acid soluble	K/ Pseudo[b]	
NA		Cellulose	98.5	0.0	0.25	0.0	NA
		Xyn	2.2[d]	69.6	1.38	1.08	
		Pseudo-lignin[e]	0.0	0.0	0.46	97.9	
140-1wt%- 30 min[f]	1.94	Cellulose	99.0	< 2	0.27	0.0	
		C+ Xyn	99.5		0.28	0.0	98
		C+ Xys	102.6		0.29	0.0	99
160-0.5wt%- 40 min	2.38	Cellulose	100.5		0.28	0.40	ND
		C+ Xyn	100.3		0.29	0.53	
		C+ Xys	99.2		0.30	1.50	
160-1wt%- 40 min	2.66	Cellulose	101.2	0.0	0.31	0.51	NA
		C+ Xyn	95.6		0.41	3.45	93
		C+ Xys	97.8		0.45	3.16	85
170-1wt%- 40 min	2.95	Cellulose	93.2		0.46	3.07	NA
		C+ Xyn	89.8		0.51	8.1	79
		C+ Xys	89.1		0.55	10.6	64
180-2wt%- 40 min	3.56	Cellulose	11.5		0.93	85.7	NA
		C+ Xyn	9.25		0.80	88.2	17
		C+ Xys	5.06		0.82	94.4	12

C, cellulose; Xyn, xylan; Xys, xylose; NA, not applicable; ND, not determined.
[a]CSF, combined severity factor that includes pretreatment time, temperature, and pH; pH values used for CSF calculations were based on H^+ concentration in the solution.
[b]Carbohydrate derived pseudo-lignin.
[c]Recovery of xylose/xylan = 100*(A-B)/A, where A is the initial amount of xylose/xylan (g) and B is the amount of xylose/xylan + xylose/xylan equivalent of furfural in the pretreatment solution (g).
[d]Glucan, collectively referred to anhydrous glucose regardless of source.
[e]Xylose derived pseudo-lignin.
[f]Pretreatment conditions represent: reaction temperature in ^oC-wt% acid solution and reaction time.

5.2.3 Pseudo-lignin from Pure Xylose

Pseudo-lignin solids were formed from pure xylose in the 1 L Parr reactor with a xylose loading of 15wt% (120 g) in a 5 wt% dilute sulfuric acid solution at 180 ºC for 150 min.

In order to maximize the yield of pseudo-lignin, the reaction conditions were deliberately chosen to be harsher than those typically applied in dilute acid pretreatments of biomass. After 150 min of reaction at 180 ºC, the reactor was cooled to RT in a water bath. The pseudo-lignin formed in the reactor mostly settled in a cake to the bottom but also formed a sticky layer on the impeller and thermocouple probe. Pseudo-lignin samples were scraped off and washed repeatedly by vacuum filtration until the filtrate pH was neutral. The washed pseudo-lignin solids were homogenized in a coffee grinder (Model No. BCG 1000B1; KitchenAid Appliances), and analyzed for moisture content with a halogen moisture analyzer (HB43-S; Mettler Toledo, Columbus, OH).

5.2.4 Enzymatic Hydrolysis

Enzymatic hydrolysis of untreated Avicel cellulose and washed dilute acid pretreated (DAPt) solids were performed at 50^{o}C and 150 rpm in Multitron shakers (Model AJ125; Infors-HT, Laurel, MD, USA) following a modified NREL standard protocol [198]. In this case, 50 ml was used as the total reaction volume instead of the 10 ml volume specified in the NREL protocol. A solids concentration corresponding to a cellulose content of 1% (w/v) was added to 125 ml Erlenmeyer glass flasks (Catalog No. 10-041-20, Fisher Scientific, Pittsburg, PA, USA) that contained 50 mM sodium citrate buffer mixed with Accellerase®1500 cellulase at protein loadings of 5 and 15 mg /g cellulose (equivalent to app. 2.5 and 7.5 FPU/g cellulose) and 0.1% sodium azide to prevent microbial growth. The mixture was hydrolyzed in duplicates for up to 120 hours, with substrate blanks without enzymes and enzyme blanks without substrate also run in parallel.

To determine the effect of pure xylose derived pseudo-lignin on Avicel cellulose conversion, enzymatic hydrolysis was conducted at solids loadings equal to 1% (w/v) cellulose, with pseudo-lignin added to cellulose at pseudo-lignin-to-cellulose mass ratios of 0.0, 0.05, 0.15, 0.45, and 0.65. Hydrolysis was conducted for up to 120 hours at 50^{o}C with Accellerase®1500 cellulase at protein loadings of either 5 or 15 mg/g cellulose. Other conditions were the same as above.

To follow sugar release during enzymatic hydrolysis, about 1 ml of a thoroughly mixed sample was withdrawn periodically into a 2 ml microcentrifuge tube (Eppendorf PCR clean microcentrifuge tubes, Catalog No. 05-402-95, Fisher Scientific, Pittsburgh, PA) using an Eppendorf pipette and mixed with about 15µl of 10wt% sulfuric acid to bring the samples pH to 1-3, Aminex HPX-87H column operating pH range. Adding acid to the samples, the sulfuric acid negative peak on the HPLC chromatogram is avoided allowing smoother integration. To remove solids from the liquid, samples were centrifuged using Eppendorf microcentrifuge (Model No. 5424, Fisher Scientific, Pittsburgh, PA) at 14600 rpm for 5 minutes. Then about 450 µl of clarified supernatant was transferred into a 500 µl polypropylene snap ring vial (Vendor No. 98842; Grace Davision, Deerfield, IL) and run in an HPLC along with sugars standards. Cellulose conversion for enzymatic reactions was calculated as:

$$\text{Cellulose conversion (\%)} = 100*[0.90*(\text{Glucose (g)} + 1.053*\text{Cellobiose (g)})]/ \text{Initial cellulose (g)}$$

For pretreated solids, cellulose loading was based on the amount of cellulose in pretreated solids. The change (or drop) in cellulose conversion was calculated as:

$$\text{\% Change in conversion} = 100*(X-Y)/X$$

where X is the cellulose conversion for the untreated or pretreated control and Y is the cellulose conversion for untreated or pretreated cellulose mixed with xylan or xylose.

5.2.5 Cellulose Solubilization and Xylan/Xylose Recovery Calculations for Pretreatment

The amount of cellulose solubilized during pretreatment was calculated based on the amounts of cellobiose, glucose, hydroxymethyl furfural (HMF), and levulinic acid (LA) identified in the pretreatment liquid:

$$\text{Cellulose solubilized during pretreatment (\%)} = 100 * [0.9*(\text{Cellobiose (g)} *1.053+\text{Glucose (g)}) + (\text{HMF (g)}/0.7784) + (\text{LA (g)}/0.716)]/ \text{Initial amount of cellulose (g)}$$

where, 0.9477,1.11, 0.9, 0.7784, and 0.716 are the mass conversion factors based on the stoichiometry for conversion of cellobiose to cellulose, cellulose to glucose, glucose to cellulose, cellulose to HMF, and cellulose to LA, respectively.

The amount of xylan/xylose recovered after pretreatment was calculated based on the amounts of xylose and furfural (FF) identified in the pretreatment liquid as follows:

$$\text{Xylan recovery (\%)} = 100 * [0.88*\text{Xylose (g)} + (\text{FF (g)}/0.727)]/ \text{Initial amount of xylan (g)}$$

$$\text{Xylose recovery (\%)} = 100*[\text{Xylose (g)} + (\text{FF (g)}/0.640)]/ \text{Initial amount of xylose (g)}$$

The amount of xylan/xylose lost to pseudo-lignin can be calculated as:

$$\text{Xylan/ xylose lost to pseudo-lignin} = 100 - \text{Xylan/ xylose recovery (\%)}$$

where, 1.136, 0.727, 0.640, and 0.88 are the mass conversion factors based on the stoichiometry for conversion of xylan to xylose, xylan to furfural, xylose to furfural, and

xylose to xylan, respectively. Formic acid was not included due to the low concentration detected in the liquid for pretreatment of Avicel alone and for pretreatment of Avicel mixed with xylan or xylose.

5.2.6 Samples Analysis

Liquid samples collected from supernatants after pretreatments and periodically collected over the course of enzymatic hydrolysis were analyzed on a Waters Alliance HPLC (Model 2695; Waters Co., Milford, MA) equipped with an auto sampler (Waters 2695) and a 2414 refractive index (RI) detector. To separate sugars and their degradation compounds (for pretreatment liquor) via HPLC, a Bio-Rad Aminex® HPX-87H (Polystyrene-divinylbenzene sulfonic acid resin packing; 300 x 7.8 mm; Catalog No.125-0140) column along with a micro-guard cation cartridge (Catalog No.125-0129; 30 x 4.6 mm; Bio-Rad Laboratories, Hercules, CA) were used. The column was heated to 65^{o}C, with 5mM sulfuric acid at a flow rate of 0.6 ml/ min as the carrier solvent. The chromatograms were integrated, and data was imported to Microsoft Excel files using Empower® 2 software (Waters Co., Milford, MA).

5.2.7 BSA/Purified CBHI Protein Adsorption on Pseudo-lignin

Albumin from bovine serum (BSA, 98% purity, Batch No. 078K0730, Sigma-Aldrich, St. Louis, MO) and purified CBHI (Cel7A) adsorption was performed at RT in a 50 mM sodium citrate buffer (pH~ 5.0). A 10 mg/ml BSA protein stock was prepared in 50 mM citrate buffer for adsorption experiments. Pure xylose derived pseudo-lignin solids with BSA protein or CBHI were incubated overnight in 2 ml microcentrifuge vials on an end-over-end rugged rotator (Glass-Col, LLC, Terre Haute, IN) equipped with a variable speed DC motor turning at about 20 rpm. Following overnight incubation, the tubes were

centrifuged in a bench top Eppendorf microcentrifuge (Model No.5424, Fisher Scientific, Pittsburgh, PA) at 14,600 rpm for 5 minutes, and the amount of free protein in the supernatant was determined by the standard BCA method [199]. A fixed loading of 10 g/L pseudo-lignin was used for adsorption kinetics, with BSA/ CBHI protein added at 0-2 mg/ml (0-200 mg protein/g solids). To determine the effect of pseudo-lignin loadings on the relative free protein in solution, a fixed 2 mg/ml BSA protein concentration was used, while the pseudo-lignin solids loading was varied from 0 to 100 g/L. Substrate blanks without protein and protein blanks without solids were run for both sets of experiments.

5.2.8 Solid-State ^{13}C CP/MAS NMR and FT-IR

The solid-state ^{13}C CP/MAS NMR and FT-IR experiments were performed according to the procedure described in Chapter 3 (Chapter 3.3.4.4 and Chapter 3.3.3).

5.2.9 Scanning Electron Microscopy

SEM characterization was performed according to the procedures described in Chapter 3 (3.3.5 Scanning Electron Microscopy (SEM)).

5.3 Results and Discussion

5.3.1 Solids Composition, Pseudo-lignin Formation, and Recovery of the Components

Dilute sulfuric acid pretreatment was performed on Avicel cellulose alone and mixed with beechwood xylan or xylose over a range of severities corresponding to CSF 1.94 (140^{o}C- 1wt% acid solution- 30 min) to 3.56 (180^{o}C- 2wt% acid solution- 40 min). Figure 5.1 shows the physical images of untreated Avicel cellulose, xylose derived pseudo-lignin, and washed pretreated solids of Avicel cellulose alone and mixed with

xylan or xylose. Avicel cellulose solids turned from white for untreated to brownish and then dark black as pretreatment severity was increased. The change in color from white to brownish was observed at lower severities for pretreated solids of Avicel cellulose mixed with xylan or xylose than for cellulose alone, with the sample that had been mixed with xylose being darker. However, at the most severe pretreatment conditions (CSF~ 3.56), pretreated solids for all three were dark black, resembling xylose derived pseudo-lignin. The starting substrates (Avicel cellulose, beechwod xylan, and xylose) had almost no K-lignin. Beechwood xylan contained about 70% xylan, 2.2% glucan, 6.0% ash, <1% arabinan on a dry wt. basis, with the rest being uronic acids and protein, as shown elsewhere [200,201]. Solids from pretreatment of Avicel mixed with xylan or with xylose had higher amounts of pseudo-lignin than Avicel alone at all conditions (Figure 5.2a). Consistent with findings by Sannigrahi et al. [109], the amount of ash free acid-insoluble lignin in the pretreated solids increased with pretreatment severity, with a negligible amount at CSF 1.94 and the highest amount at CSF 3.56 (95wt%) for cellulose mixed with xylose, as shown in Figure 5.2a and Table 5.1. This increase in K-lignin content resulted from carbohydrate degradation to lignin-like compounds called pseudo-lignin [109,202]. At similar conditions, however, working with delignified poplar (holocellulose with 67.2% glucan and 21.8% xylan), Sannigrahi *et al.* [109] observed a somewhat different trend in pseudo-lignin formation. For example, in our study at CSF 2.95, the amount of pseudo-lignin was about 8% (dry weight basis) for pretreatment of Avicel mixed with xylan, while Sannigrahi *et al.* [109] reported about 30wt% pseudo-lignin at CSF 2.97 for poplar holocellulose. The differences could be attributed to the substrates used and their initial compositions. For instance, the substrates for this study contained a

small amount of acid-soluble and acid-insoluble lignin, whereas their study employed poplar holocellulose with about 6.6% acid soluble lignin. In addition, cellulose in Avicel PH101 is more crystalline than in poplar and other biomass feedstocks [75,119], with the result that it is less prone to breakdown during dilute acid pretreatment than amorphous cellulose [203]. Therefore, it is anticipated that biomass that is less crystalline or with more free sugars, starch, pectin, more acid labile hemicelluloses, or acid soluble lignin is more likely to form higher amounts of pseudo-lignin when pretreated at high severities [185,204]. Acid-soluble lignin and its degradation products released during dilute acid pretreatment may also interact with sugar degradation products to increase pseudo-lignin formation [205].

As shown in Table 5.1, solids resulting from pretreatment of cellulose mixed with xylan contained almost no residual xylan except at the least severe conditions of 140^{o}C in 1wt% acid for 30 min (CSF 1.94, xylan content <2wt%). The xylan/xylose accounted for shown in Table 5.1 includes xylose left in the solids plus xylose monomers, xylose oligomers, and xylose equivalents of furfural in solution decreased drastically with pretreatment severity (from ~98% at CSF 1.94 to < 15% at CSF 3.56), consistent with the well-known fragility of xylan/xylose compared to cellulose [206].

Pretreatment conditions	Avicel cellulose	Avicel cellulose mixed with xylan	Avicel cellulose mixed with xylose
None			
140°C-1wt% acid- 30 min (CSF~1.94)			
160°C -0.5wt% acid - 40 min (CSF~2.38)			
160°C -1wt% acid - 40 min (CSF~2.66)			
170°C -1wt% acid- 40 min (CSF~2.95)			
180°C -2wt% acid - 40 min (CSF~3.56)			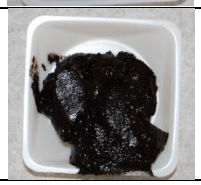
Xylose derived pseudo-lignin (180-5wt%-150 min)			

Figure 5.1 Pictures of untreated Avicel cellulose, xylose derived-pseudo-lignin, and dilute acid pretreated Avicel cellulose alone and mixed with xylan or xylose at the pretreatment conditions applied. CSF-combined severity factor

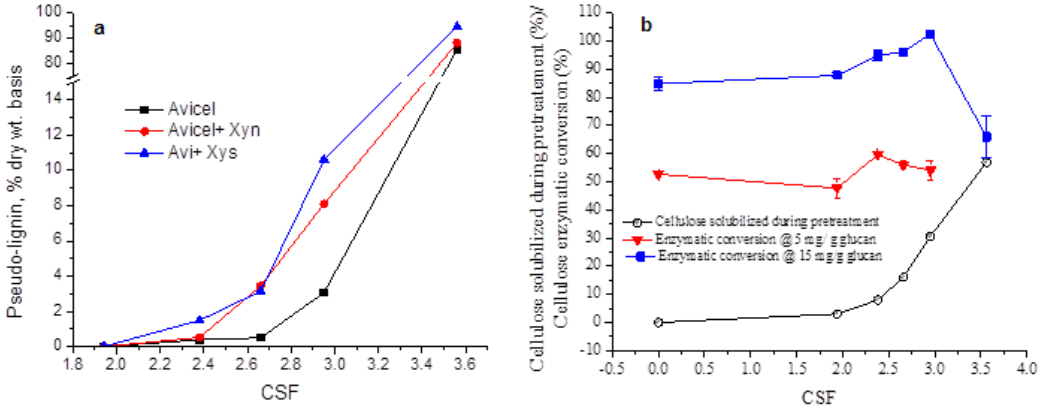

Figure 5.2 a: Pseudo-lignin (% K-lignin, dry wt. basis) in pretreated solids versus combined severity factor (CSF) for dilute acid pretreatment of Avicel cellulose alone and mixed with xylan (Xyn) or xylose (Xys). **b:** The amount of cellulose solubilized during pretreatment and cellulose digested by Accellearse11500 cellulase at loadings of 5 and 15 mg protein/g cellulose in the residual solids resulting from dilute acid pretreatment of Avicel cellulose versus combined severity factor

5.3.2 Effect of Dilute Sulfuric Acid Pretreatment on Avicel Cellulose Digestibility

The amount of cellulose solubilized during pretreatment increased with pretreatment severity and was about 60% at the most severe conditions used here (CSF~3.56). Because cellulose solubilization was defined to only account for the amounts of cellobiose, glucose, HMF, and LA in the pretreatment liquid, the actual loss of cellulose must be higher than shown in Figure 5.2b due to degradation of these compounds into pseudo-lignin and other unidentified compounds [193,203]. It is often speculated that the amorphous portion of cellulose is preferably solubilized by chemical and biological catalysts compared to the crystalline part, with the result that cellulose becomes more recalcitrant with prolonged pretreatment time or enzymatic hydrolysis [118]. However, Figure 5.2b shows that the enzymatic digestion of dilute acid pretreated Avicel cellulose compared to its digestibility without pretreatment followed a different trend with increasing severities at the two cellulase protein loadings of 5 and 15 mg/g cellulose in

the pretreated solids tested. In particular, except for the result for CSF 3.56, the 4 hours initial rate and 72 hours cellulose conversion either increased by ~13-20% (depending on cellulase loading) or were unchanged over the range of pretreatment severities covered, as shown in Figure 2b and Table 5.2. Although pretreating Avicel at CSF 2.95 generated about 3wt% pseudo-lignin, they did not appear to have a negative impact on the final cellulose conversion compared to results for untreated cellulose. However, digestion of cellulose with a 5 mg cellulase loading was lower than for Avicel pretreated at lower severity conditions that produced less pseudo-lignin. At 3.56 CSF, cellulose conversion with a 15 mg protein/ g cellulose cellulase loading dropped to 66% from ~95% for untreated Avicel cellulose, a decrease of about 30%. This drop could be attributed to reduced cellulose accessibility as a result of increased crystallinity, pseudo-lignin deposition (95% by weight) on cellulose, and/or reduced cellulase effectiveness due to non-specific binding of cellulase to pseudo-lignin.

Table 5.2 Effect of dilute acid pretreatment on cellulose digestibility for cellulase loadings of 5 and 15 mg protein/g cellulose in pretreated solids for Avicel alone and mixed with birchwood xylan or pure xylose

Pretreatment conditions	Substrate	5 mg/g cellulose		15 mg/g cellulose	
		4h	120h	4h	120h
		% Conv.[a] ± SD (% change[b])	% Conv. ± SD (% change)	% Conv. ± SD (% change)	% Conv.± SD (% change)
Untreated	C	15.2 ± 0.28	58.9 ± 0.83	26.3 ± 0.28	94.5 ± 3.1
None	C+Xyn	ND		11.0 ± 0.28 (55) [c]	75 ± 2.2 (22)
140-1wt%- 30 min[d]	C	14.5 ± 0.2	56.5 ± 1.5	29.7± 0.1	94.3± 0.4
	C+ Xyn	13.1 ± 0.8 (9.6)	41 ± 1.0 (27.4)	25.7 ± 0.2 (13.4)	65.1 ± 0.7 (30.9)
	C+ Xys	14.1 ± 0.7 (2.7)	49.2 ± 0.3 (12.9)	28 ± 0.2 (5.7)	88 ± 0.6 (7.0)
160-0.5wt%- 40 min	C	17.8 ± 0.1	65.2 ± 1.5	32.8 ± 0.5	98.0 ± 1.5
	C+ Xyn	17.0 ± 1.1	54.2 ± 1.4	29.1 ± 1.2	83.0 ± 1.3

		(4.4)	(16.8)	(11.5)	(15.3)
	C+ Xys	17.0 ± 0.7 (4.4)	47.6 ± 0.8 (27.0)	33.3 ± 0.4 (NS)	81.1 ± 0.6 (17.2)
Table 5.2 continued					
160-1wt%- 40 min	C	18.2 ± 0.1	61.9 ± 2.3	32.3 ± 0.6	100.4 ± 0.4
	C+ Xyn	12.4 ± 0.3 (31.8)	48.6 ± 0.6 (21.5)	29.0 ± 0.9 (10.2)	85.6 ± 1.7 (14.7)
	C+ Xys	16.6 ± 0.4 (8.8)	52.6 ± 0.6 (15.0)	29.8 ± 0.3 (7.7)	87.2 ± 0.1 (13.1)
170-1wt%- 40 min	C	12.3 ± 1.0	60.5 ± 4.1	32.0 ± 0.3	100.5 ± 0.8
	C+ Xyn	12.2 ± 0.8 (NS)	53.5 ± 0.5 (11.5)	27.8 ± 0.7 (13.1)	94.0 ± 0.8 (6.5)
	C+ Xys	13.2 ± 0.1 (NS)	64.8 ± 0.8 (NS)	30.1 ± 0.5 (6.0)	92.0 ± 1.1 (8.5)
180-2wt%- 40 min	C	ND		NA	66.0 ± 7.5
	C+ Xyn				NA
	C+ Xys				36.9 ± 7.1 (44)

C, Avicel cellulose; Xyn, xylan; Xys, xylose; NA, not available; NS, not significant; ND, not determined.
[a]Cellulose conversion = 100 × (glucose [g] + 1.053 × cellobiose [g])/(1.11_initial cellulose [g]).
[b]% change in conversion over control = 100 × (% conv. for control - % conv. for solids)/% conv. for control.
[c]For this set of experiments, xylan and Avicel cellulose were physically mixed together at a ratio of 0.5, and enzymatic hydrolysis was performed.
[d]Pretreatment conditions represent: reaction temperature in ºC—wt% acid solution and reaction time.

5.3.3 Enzymatic Hydrolysis of Pretreated Solids

Pretreated solids were extensively washed to remove soluble compounds inhibitory to cellulase such as xylose, xylooligomers, glucose, and furfural [195,207,208]. Washed solids from dilute acid pretreatment of Avicel cellulose alone and mixed with xylan or xylose were subjected to enzymatic hydrolysis at cellulase protein loadings of 5 and 15 mg protein/g cellulose in the pretreated solids. For comparison, untreated Avicel cellulose physically mixed with beechwood xylan (cellulose to xylan weight ratio 2:1) was also enzymatically hydrolyzed at a cellulase loading of 15 mg/g cellulose at similar conditions (50 mM citrate buffer, pH 5.0, 50 ºC, and 150 rpm). The cellulose conversions and their standard deviations following 4 and 120 hours of enzymatic hydrolysis are

summarized in Table 5.2 for application of both cellulase loadings to solids prepared over a range of pretreatment severities. Also summarized in parenthesis in the Table 5.2 are the percent changes in cellulose digestion of solids resulting from pretreatment of Avicel cellulose mixed with xylan or xylose compared to results for digestion of Avicel cellulose that had been pretreated by itself at the same severity.

Digestibility of Solids Prepared At Low Severity (Negligible Pseudo-lignin)

The liquid fraction from pretreatment at CSF 1.94 contained very small amounts of carbohydrate degradation products (LA, HMF, FA, and FF), and greater than 98% of the original xylan/xylose could be accounted for, as shown in Table 5.1. The resulting washed solids had a small amount of xylan (<2%) and little pseudo-lignin. However, surprisingly, the 4 and 120 hour enzymatic digestibilities of solids resulting from pretreatment of cellulose mixed with xylan or xylose were still considerably lower than digestion of cellulose that was pretreated alone at the same severities (Table 5.2). In particular, cellulose conversion after 120 hours of hydrolysis of solids prepared by pretreatment of cellulose mixed with xylan dropped to 41% from 56.5% for hydrolysis of cellulose alone (27.4% drop) at a cellulase protein loading of 5 mg/g cellulose and to 65% from 94.3% (31% drop) at a loading of 15 mg/g cellulose. These results were quite unexpected. Although the 6-7wt% ash content makes it a significant constituent in commercial beechwood xylan, little was left after pretreatment so that it would be highly unlikely to impact hydrolysis. However, it can be hypothesized that possible cellulose acetylation due to the presence of acetyl groups and methylation from 4-D-methyl glucuronic acid on the xylan backbone during pretreatment and/or residual xylan (

<2wt%) could result in less reactive cellulose, as it is well known that cellulose methylation and acetylation retards cellulase activity [209].

Causes for cellulose reduced digestibility at low severity: cellulose acetylation. To evaluate further whether acetylation was the cause for reduced cellulose conversion for solids prepared at CSF 1.94 that had negligible pseudo-lignin, Avicel cellulose at 5wt% solids loading together with different acetic acid concentrations (acetic acid to Avicel weight ratios of 0.10, 0.25, 0.50, or 1.0) was pretreated at 140 ºC in 1wt% dilute sulfuric acid for 30 min (CSF~1.94). The resulting solids along with control were enzymatically hydrolyzed at cellulase protein loading of 15 mg/g glucan. The digestibility data showed that there was no remarkable reduction in cellulose reactivity, and, thus, acetylation can be ruled out to be the cause for drop in cellulose conversion.

Causes for cellulose reduced digestibility at low severity: cellulose methylation. To obtain the representative (methyl) glucuronic acid-free xylan used in this study, the same batch of xylan at 10 wt% solid loading was acid-hydrolyzed at similar conditions used for pretreatment, i.e., in 1wt% dilute sulfuric acid at 140 ºC for 30 minutes. The remaining unhydrolyzed xylan solids were separated from the liquid by vacuum filtration. The xylose solution obtained from xylan acid hydrolysis that presumably contained free (methyl) glucuronic acids was used as a (methyl) glucuronic acid source, and Avicel at 5wt% solid loading was pretreated with this xylose solution (Avicel to xylose weight ratio ~ 2) at similar pretreatment conditions that were used for pretreatment of Avicel mixed with untreated xylan. The resulting solids were enzymatically hydrolyzed at cellulase protein loading of 15 mg/ g glucan in pretreated solids with other conditions being similar as described in the experimental section. The enzymatic digestion showed

that methyl glucuronic acids released from the xylan backbone in pretreatment had no apparent impact on Avicel cellulose reactivity.

Causes for cellulose reduced digestibility at low severity: residual xylan. The washed solids resulting from pretreatment of Avicel mixed with xylan at CSF 1.94 had about 2wt% unhydrolyzed residual xylan. Thus, to identify whether small amounts of residual xylan had a role in cellulose reduced conversion, pretreated solids for Avicel control and Avicel mixed with xylan were hydrolyzed with cellulase (15 mg protein/g glucan) alone, and cellulase supplemented with Multifect® xylanase at protein loading of 7.5 mg/g glucan (total protein loading- 22.5 mg/g glucan in pretreated solids). As shown in Figure 5.3, adding xylanase increased the reactivity of cellulose from dilute acid pretreated Avicel mixed with xylan. It was quite surprising that such a small amount of residual, non-structural xylan had such a significant impact on cellulose digestibility, and the drop in final conversion was greater than could be accounted for by cellulase inhibition (~22%) by xylooligomers when xylan was physically mixed with Avicel (xylan to Avicel wt. ratio of 0.5, corresponding to 33% xylan) before enzymatic hydrolysis (Table 5.2). Although still unclear, this significant finding led us hypothesize that hemicelluloses solubilize during low severity dilute acid and hydrothermal pretreatments, but may precipitate onto the cellulose surface upon cooling by forming strong bonds. Although evidence supports such precipitations and bond formation in pulping [210,211], it has never been reported for pretreatment, and the impacts of such precipitations on cellulose enzymatic hydrolysis are not reported. This hypothesis needs further research and is beyond the scope of this study.

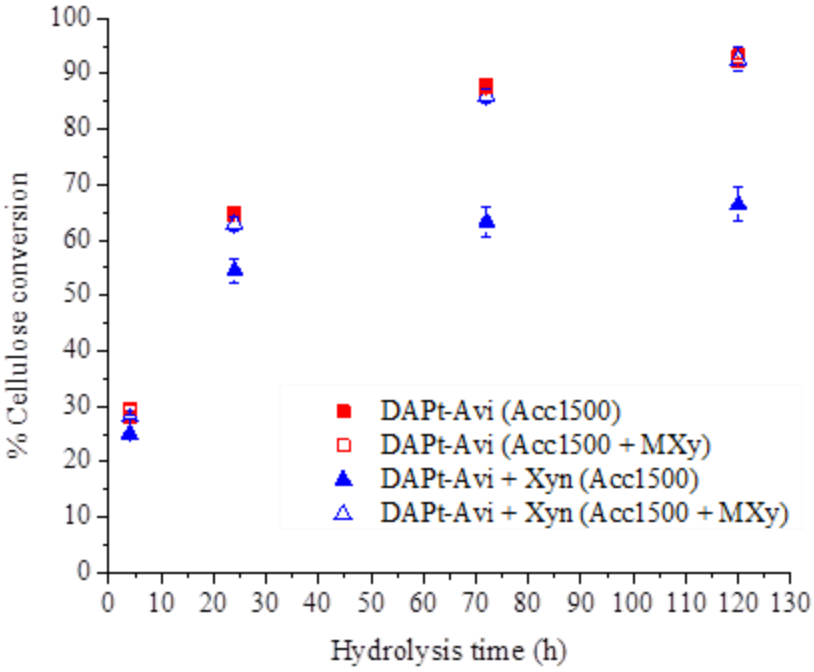

Figure 5.3 Effect of *Multifect* xylanase (MXy) supplementation (7.5 mg protein/g glucan) to *Accellearse 1500* (Acc1500) cellulase (15 mg protein/g glucan) on cellulose conversion for washed solids from dilute acid pretreatment (140^{o}C in 1wt% sulfuric acid for 30 minutes) of Avicel by itself and mixed with xylan. DAPt- Avi – dilute acid pretreated Avicel cellulose; DAPt- Avi + Xyn- dilute acid pretreated Avicel mixed with xylan

Digestibility of Solids Prepared At Other Severities

Although increasing pretreatment severity from 1.94 to 2.38 increased the amount of pseudo-lignin (wt% dry basis) from 0% to 0.53% for pretreatment of cellulose mixed with xylan, the conversion loss shown in Table 5.2 for CSF OF 2.38 was less than for CSF 1.94: 16.8% vs. 27% and 15.3% vs. 31% at cellulase loading of 5 and 15 mg protein/g cellulose, respectively. However, conversion of cellulose in solids resulting from pretreatment of cellulose mixed with xylose that had more pseudo-lignin (1.5wt %) dropped more for a CSF of 2.38 than for a CSF of 1.94 (from 65.2% to 47.6% and from

98% to 81.1% for cellulase loadings of 5 and 15 mg protein/g cellulose, respectively). For cellulose mixed with xylan, the drop in conversion for CSF 2.38 (160 ºC-0.5wt%, 40 min) could be due to both pseudo-lignin and the negligible amount of residual xylan, if any, as shown earlier. However, for cellulose mixed with xylose, it appeared that the drop in conversion was exclusively due to pseudo-lignin that comprised about 1.5wt% of solids by dry weight. For a CSF of 2.66 (160 ºC-1.0wt%, 40 min), solids from pretreatment of Avicel cellulose mixed with xylan or with xylose had similar amounts of pseudo-lignin by dry weight (~ 3.5%). Furthermore, as shown in Table 5.2, cellulose in both solids showed almost the same loss in conversion compared to the cellulose control prepared at the same severity (from 100% to 85.6% for cellulose plus xylan and 87.2% for cellulose and xylose at 15 mg protein/g cellulose cellulase mg/g cellulose). Although solids from pretreatment of cellulose mixed with xylan or xylose at a CSF of 2.95 (170 ºC-1.0wt%, 40 min) increased the amount of carbohydrate derived-pseudo-lignin (8-10% by dry wt.) from that at lower severities, cellulose digestibility dropped less than it did at lower severity conditions that produced less pseudo-lignin from xylose or xylan, as shown in Table 5.2. The cause for this observation is not entirely clear but could be physiological/ structural changes in pseudo-lignin formation at or beyond certain conditions/concentrations that affect cellulose hydrolysis. However, more work is needed to validate a mechanism. As shown earlier in Figure 5.2b, digestion of Avicel cellulose in solids pretreated at the most severe conditions of CSF 3.56 dropped from 94.5% for untreated material to 66%, a 30% loss. Despite the fact that solids from pretreatment of Avicel cellulose mixed with xylan or xylose had similar amounts of pseudo-lignin as for Avicel cellulose alone, Table 5.2 shows that cellulose conversion for

the former was only about 50% of the latter at a 15 mg/g cellulose cellulase loading. Thus, it appears that xylose derived pseudo-lignin and their deposition on and/or co-existence with cellulose are more inhibitory to cellulase action than pseudo-lignin derived from six carbon sugars and/or their dehydration products (HMF and levulinic acid).

5.3.4 Pretreated Solids Characterizations

To determine changes in solids characteristics, pretreated solids prepared at various severities for Avicel cellulose alone and mixed with xylan or xylose were characterized by solid-state ^{13}C CP/MAS NMR, FT-IR, and SEM imaging. For comparison, untreated Avicel cellulose alone and physically mixed with xylan, xylose, and xylose-derived pseudo-lignin were also imaged.

Solid-state ^{13}C CP/MAS NMR

The ^{13}C NMR spectra for xylose derived pseudo-lignin and untreated and pretreated solids prepared at various severities are shown in Figure 5.4, with Table 5.3 showing the peak assignments for these spectra. The NMR spectra for untreated Avicel alone, Avicel mixed with xylan or xylose, and pretreated solids at most conditions were predominantly comprised of signals from the six carbons in cellulose. The NMR spectrum from xylose derived pseudo-lignin showed broad peaks (due to spectral overlap) corresponding to aliphatic C, unsaturated C, and carbonyl (C=O) functionalities. These signals were also observed in dilute acid pretreated poplar holocellulose after pretreatment at CSF > 3.27 [109]. Figure 5.4a shows the spectra for untreated Avicel cellulose and cellulose pretreated at various severities, and the spectra for dilute acid pretreated Avicel cellulose alone and mixed with xylan or xylose prepared at CSF 2.38, CSF 2.95, and CSF 3.56 are shown in Figure 5.4b, c, and d, respectively. Figure 5.4a also shows the cellulose

crystallinity determined from NMR data for untreated and pretreated solids for Avicel cellulose. For pretreated solids prepared at CSF 3.56, the % crystallinity (%CrI) could not be determined due to weak signals for cellulose carbons. Figure 5.4a shows that there was no apparent change in the cellulose structure, except at that the most severe condition (CSF 3.56) showed strong carbonyl, aromatic, and aliphatic signals. Cellulose crystallinity increased with pretreatment severity by few points (from 71.9% for untreated to about 75.8% for Avicel pretreated at CSF 2.95) and did not seem to have a negative impact on cellulose digestibility, as shown earlier in Figure 5.2b. Although wet chemistry compositional analysis (Table 5.1) revealed that all pretreated solids prepared at CSF ≥ 2.38 had noticeable amounts of pseudo-lignin, NMR spectra only had strong signals attributed to pseudo-lignin for solids prepared at CSF 3.56 that had more than 80 wt% pseudo-lignin. The spectra of samples prepared at CSF 3.56 were significantly different from those from other samples, with strong signals from carbonyl, aromatic, and aliphatic structures (Figure 5.4d and Table 5.3). In addition, these spectra were different from each other, probably due to differences in substrates. For instance, the methoxy signals (56 ppm) were stronger for pretreated solids of cellulose mixed with xylan or xylose than for the sample cellulose alone, possibly due to large proportions of 4-O-methyl glucuronic acid in xylan.

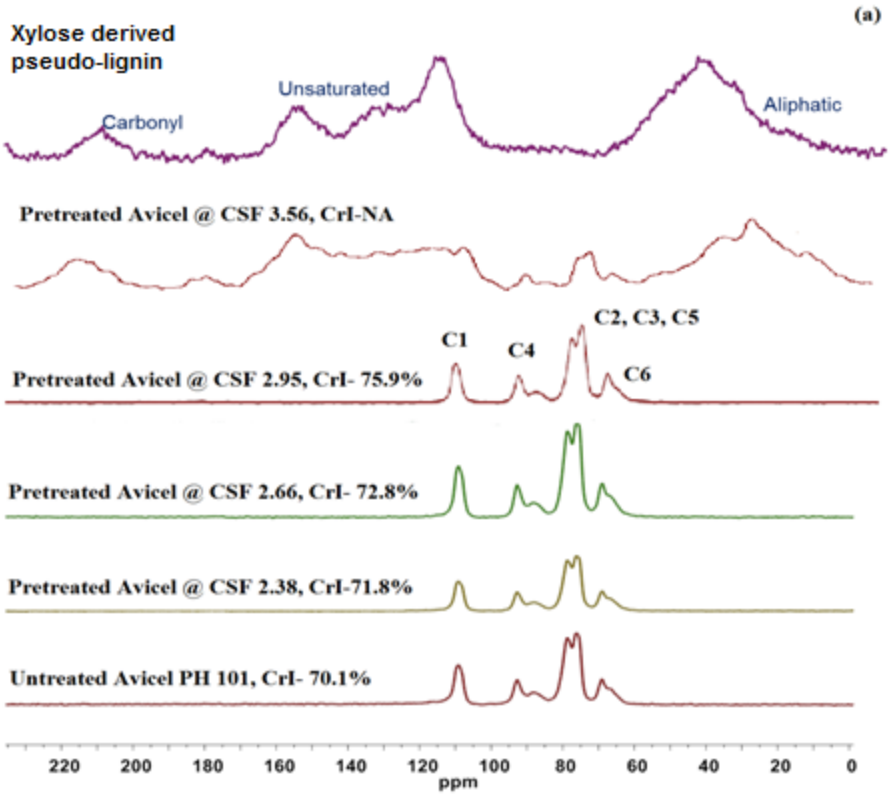
(a)
Xylose derived pseudo-lignin
Carbonyl
Unsaturated
Aliphatic
Pretreated Avicel @ CSF 3.56, CrI-NA
C1
C4
C2, C3, C5
C6
Pretreated Avicel @ CSF 2.95, CrI- 75.9%
Pretreated Avicel @ CSF 2.66, CrI- 72.8%
Pretreated Avicel @ CSF 2.38, CrI-71.8%
Untreated Avicel PH 101, CrI- 70.1%
220 200 180 160 140 120 100 80 60 40 20 0
ppm

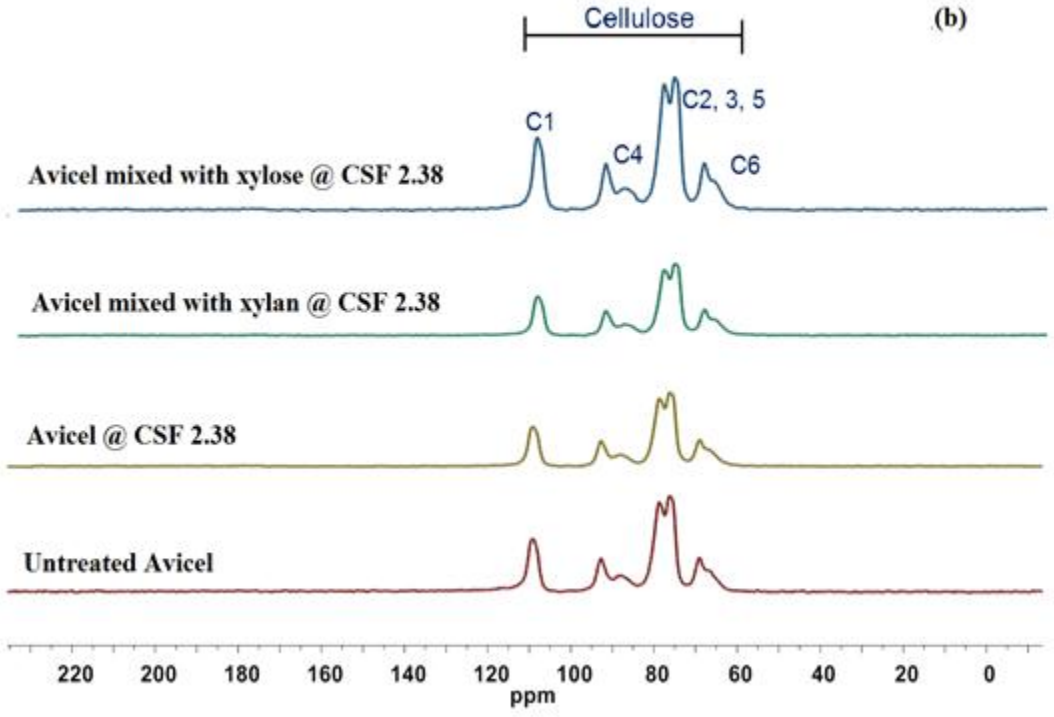
(b)
Cellulose
C1
C4
C2, 3, 5
C6
Avicel mixed with xylose @ CSF 2.38
Avicel mixed with xylan @ CSF 2.38
Avicel @ CSF 2.38
Untreated Avicel
220 200 180 160 140 120 100 80 60 40 20 0
ppm

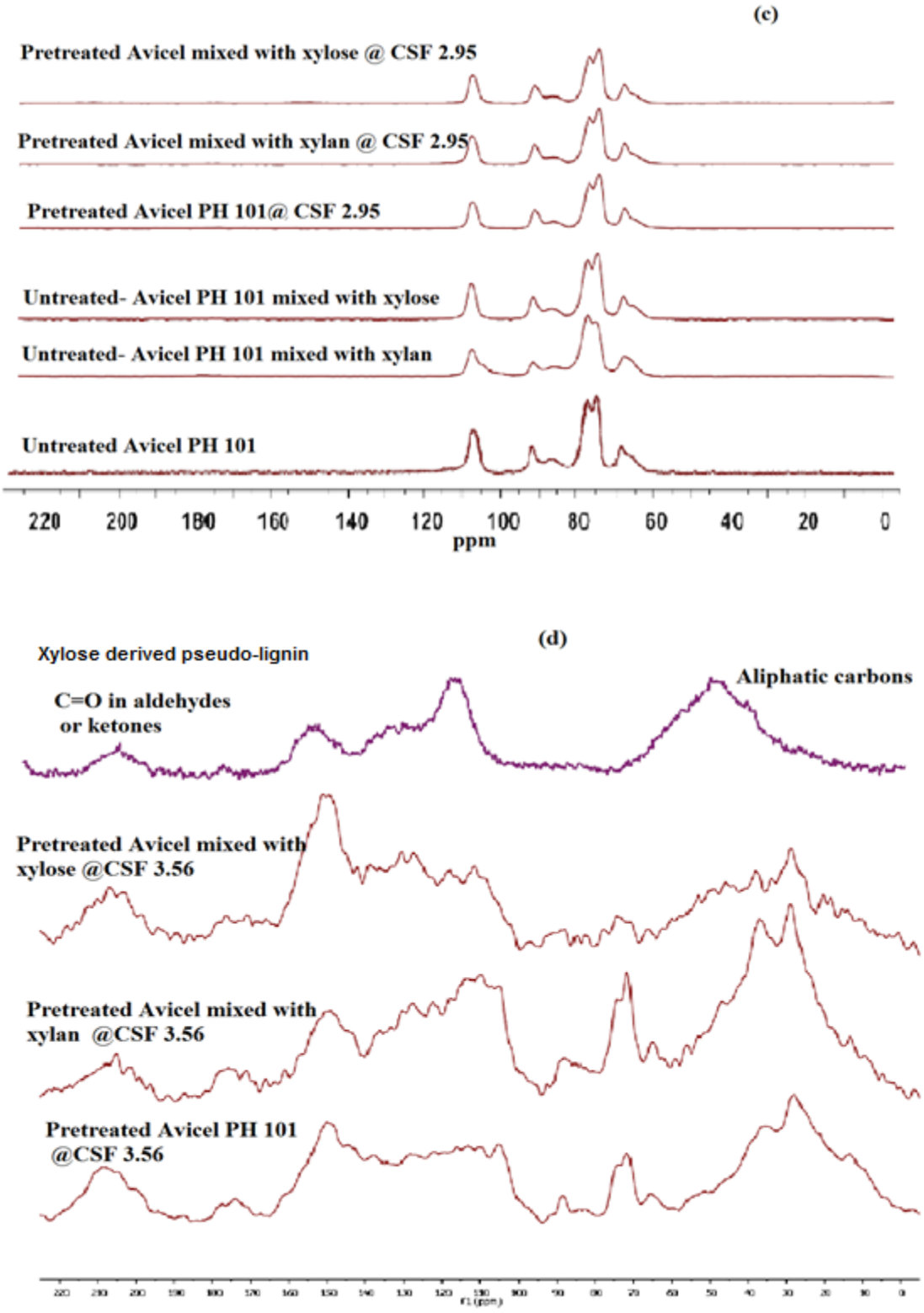

Figure 5.4 Solid-state 13C CP/MAS NMR spectra of (**a**) untreated and dilute acid pretreated Avicel cellulose PH 101, along with crystallinity index (CrI) values calculated

from NMR data, prepared at various severities, and comparison with xylose derived-pseudo-lignin; (**b**) dilute acid pretreated Avicel cellulose alone and mixed with xylan or xylose prepared at CSF 2.38; (**c**) untreated Avicel cellulose alone and physically mixed with xylan or xylose and pretreated solids prepared for these at CSF 2.95; and (**d**) dilute acid pretreated (CSF 3.56) Avicel cellulose alone and mixed with xylan or xylose. NA, not available

Table 5.3 Peak assignments in the NMR spectra [187]

Chemical shift (ppm)	Assignment
220-196	C=O in aldehydes or ketones
178-168	C=O in carboxylic acids or esters
155-142	Aromatic C-O
142-125	Aromatic C-C
125-102	Aromatic C-H
109-100	C1 of cellulose and/or C1 of xylan/xylose
92-86	The crystalline C4 of cellulose
86-79	The amorphous C4 of cellulose and/or C4 of xylan/xylose
79-68	C2, C3 and C5 of cellulose and/or C2, C3 of xylan/xylose
68-58	C6 of cellulose and/or C5 of xylan/xylose
60-55	Methoxy related to aromatic rings
50-10	Aliphatic carbons

FT-IR Analysis of Solids Recovered from Pretreatment

FT-IR spectra of various solids used in this study are shown in Figure 5.5, with peak assignments presented in Table 5.4. Figure 5.5a shows FT-IR spectra for untreated Avicel cellulose alone and pretreated at various severities, and Figures 5.5b-d present FT-IR spectra from pretreated solids prepared at various severities for cellulose mixed with xylan/xylose and their comparison with untreated cellulose and xylose derived pseudo-lignin. Consistent with the NMR data, the Avicel cellulose structure remained intact at all conditions until a CSF of 3.56 and showed signals from cellulose. Pseudo-lignin sample showed a peak at 1594.7 cm-1 due to aromatic ring stretching that correlates to the unsaturated C signal seen in the NMR spectra and a peak at 1695.6 cm-1 arising from C=O stretching in ketones. However, these peaks were non-existent for pretreated samples prepared at severities below CSF 3.56. The strong peaks from cellulose and

xylan, and the weak peaks from the carbonyl and aromatic stretching regions in the spectra of these samples suggest that the carbohydrates in these samples remained almost intact during pretreatment. However, compositional data suggested otherwise, as pretreated solids for cellulose mixed with xylan or xylose prepared at CSF 2.95 contained more than 8wt% pseudo-lignin. Therefore, it can be hypothesized that insoluble compounds other than those listed/identified here contribute to the positive K-lignin values in Table 5.1. The FT-IR spectra from solids prepared at CSF 3.56 had strong peaks associated with the carbonyl and aromatic stretching regions. These FT-IR and ^{13}C CP/MAS NMR analyses of pseudo-lignin in samples for CSF 3.56 are consistent with literature results [109].

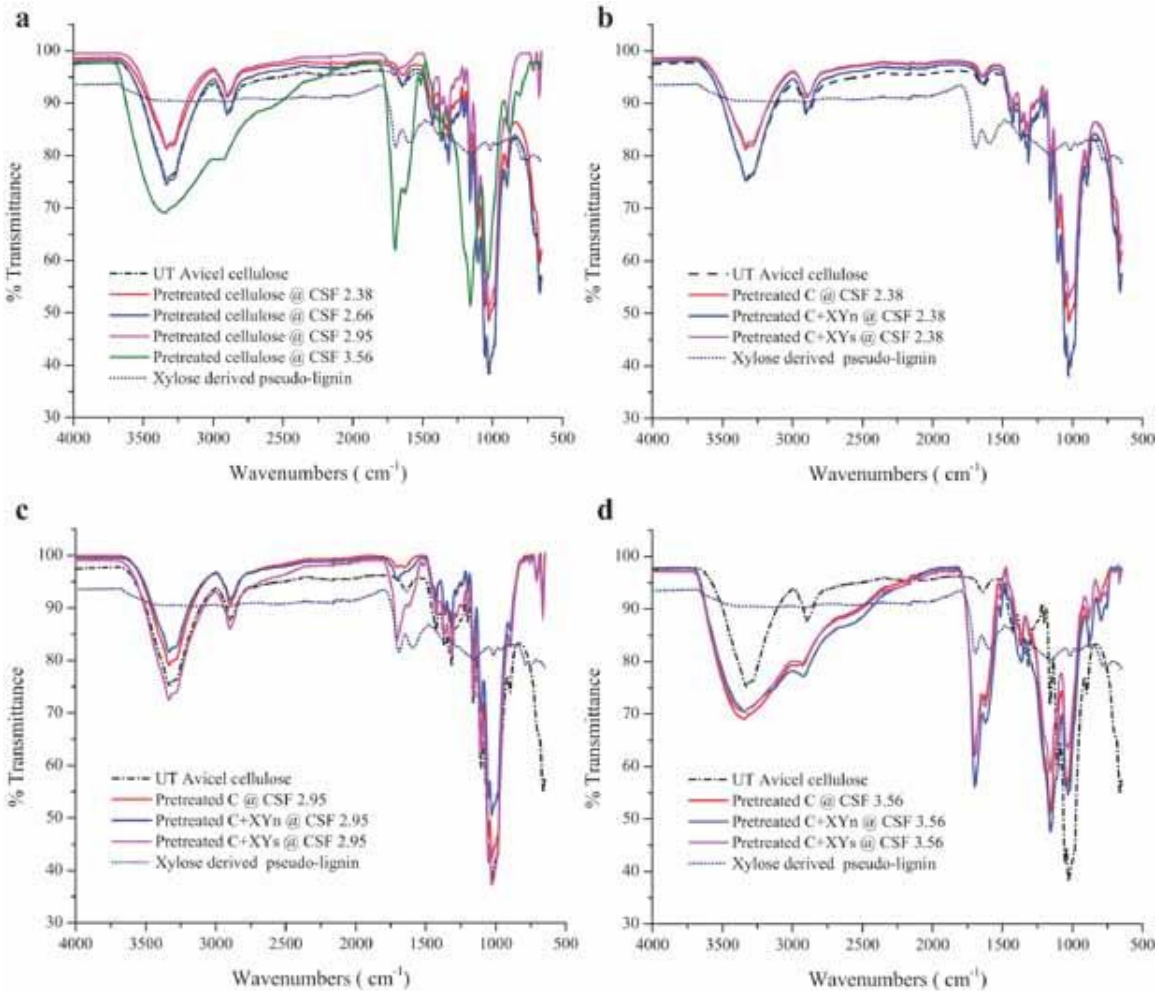

Figure 5.5 FT-IR spectra of untreated and dilute acid pretreated Avicel PH 101 cellulose prepared at various severities, and comparison with spectra for xylose derived-pseudo-lignin and dilute acid pretreated Avicel cellulose alone and when mixed with xylan or xylose: (**a**) untreated, (**b**) CSF 2.38, (**c**) CSF 2.95, and (**d**) CSF 3.56

Table 5.4 Peak assignments for the FT-IR spectra of recovered solids [187]

Wavenumber (cm^{-1})	Assignment
890.2	β-glycosidic linkages between sugar units
1054.5	C-O stretching at cellulose C-3, C-6 and C-C stretching
1162.1	Asymmetric bridge stretching of C-O-C in cellulose and hemicellulose
1314.3	-CH_2 wagging vibrations in cellulose and hemicellulose
1431.0	Symmetric –CH_2 bending in cellulose and hemicellulose
1594.7	Aromatic ring stretching (lignin)
1696.0	C=O stretching in unconjugated ketones
3342.91	O-H stretching in alcohols or phenols

SEM Characterization of Solids Recovered from Pretreatment

The untreated Avicel cellulose, xylose derived pseudo-lignin, and pretreated solids were characterized using SEM. Several images were taken for each sample, with a few representative examples shown in Figure 5.6. Spherical droplets, which have been previously reported to be formed during pseudo-lignin formation [109] were seen in some of the samples. While the NMR and FT-IR data did not show evidence of the formation of lignin-like materials for solids prepared at CSF less than 3.56, a few spherical droplets can be seen in the SEM images for solids pretreated even at CSF 2.66 (Figure 5.6b) and even more for solids from pretreatment at CSF 2.95. More of these droplets were evident on the surface of the pretreated solids of cellulose mixed with xylan or xylose compared to cellulose pretreated alone at the same severities. However, unlike solids pretreated at high severities, where droplets seemed plentiful, as noted by arrows in Figures 5.6c and d (CSF 2.95 and 3.56, respectively), the occurrence of such drops were not widespread for severities less than 2.95, suggesting that these conditions were not severe enough to form significant amounts of solid degradation products, in agreement with the compositional data in Table 5.1. The xylose-derived pseudo-lignin sample shown in Figures 5.6e and e'was entirely made up of pseudo-lignin spheres as were the solids prepared at higher severity shown in Figure 6c and 6d. These results add evidence that pseudo-lignin is formed from acid catalyzed degradation of carbohydrates that deposit on the surface and may cause the observed drop in cellulose conversion.

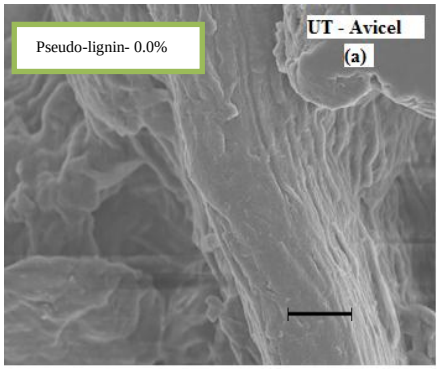

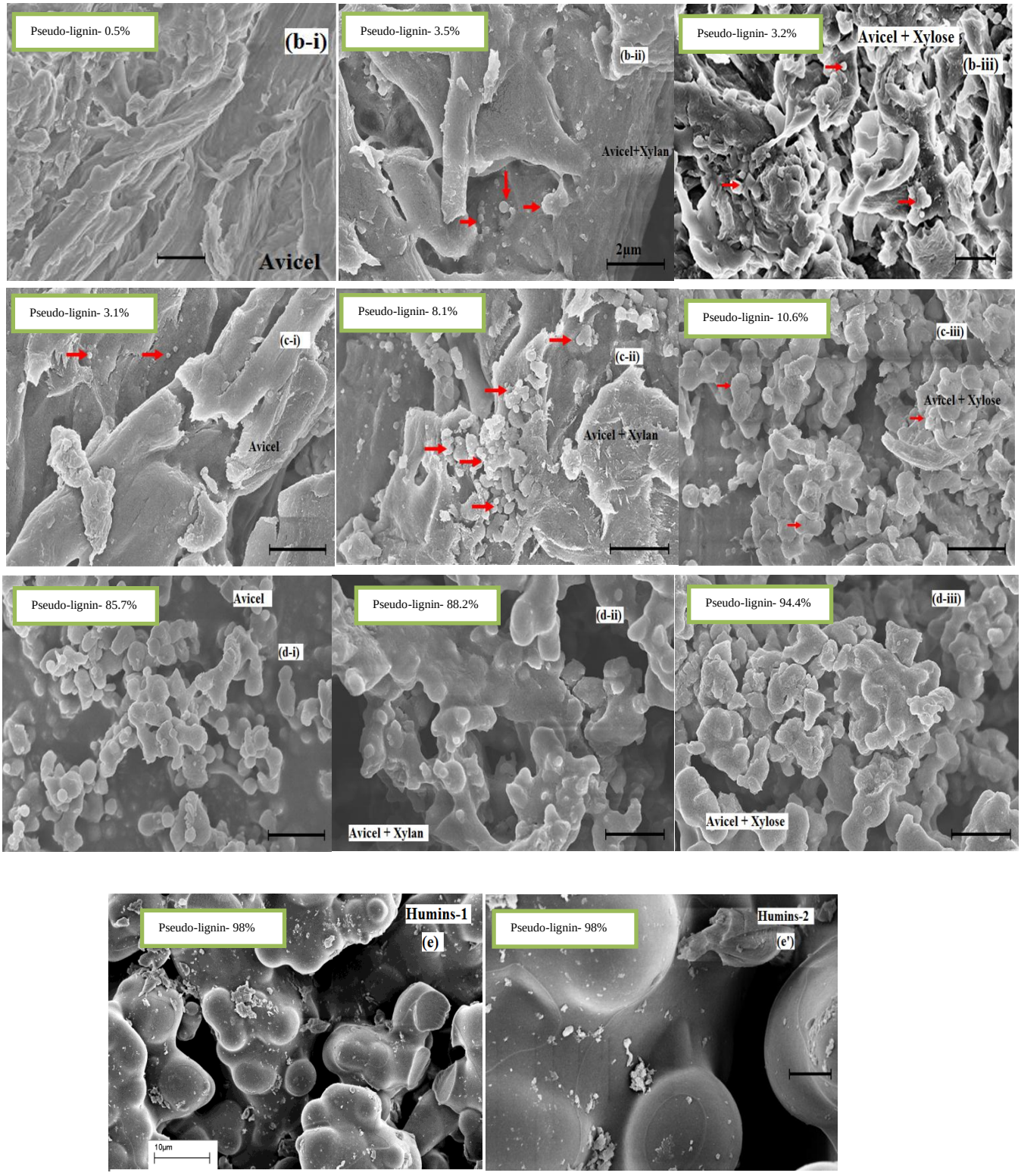
Pseudo-lignin- 0.5%
(b-i)
Avicel
Pseudo-lignin- 3.5%
(b-ii)
Avicel+Xylan
2µm
Pseudo-lignin- 3.2%
Avicel + Xylose
(b-iii)
Pseudo-lignin- 3.1%
(c-i)
Avicel
Pseudo-lignin- 8.1%
(c-ii)
Avicel + Xylan
Pseudo-lignin- 10.6%
(c-iii)
Avicel + Xylose
Pseudo-lignin- 85.7%
Avicel
(d-i)
Pseudo-lignin- 88.2%
(d-ii)
Avicel + Xylan
Pseudo-lignin- 94.4%
(d-iii)
Avicel + Xylose
Pseudo-lignin- 98%
Humins-1
(e)
10µm
Pseudo-lignin- 98%
Humins-2
(e')

Figure 5.6 SEM images of (**a**) untreated Avicel cellulose (magnification 20k×) and of pretreated solids at (**b**) CSF 2.66 (magnification 20k×), (**c**) 2.95 (magnification 20k×), and (**d**) 3.56 (magnification 20k×). (**e**) and (**e'**) xylose derived-pseudo-lignin at 5k× and 20k× magnifications. Marker (**i**) designates solids from pretreatment of Avicel cellulose alone, (**ii**) from pretreatment of cellulose mixed with xylan, and (**iii**) cellulose mixed with xylose. For example, figure notation c-iii is for pretreated solids prepared at CSF 2.95 of cellulose mixed with xylose. Scale bar length = 2 mm, unless otherwise noted

5.3.5 Plausible Mechanisms of Hydrolysis Retardation by Pseudo-lignin

Reduced Cellulase Effectiveness through Inhibition/Unproductive Binding

Lignin is known to unproductively bind cellulase and inhibit cellulase action [62]. Similar to lignin, pseudo-lignin derived from carbohydrates may also inhibit and/or bind cellulase unproductively and limit enzyme effectiveness. To evaluate whether pseudo-lignin affects cellulase effectiveness and binds cellulase unproductively, Avicel cellulose was hydrolyzed in the presence of pseudo-lignin. The 120 hour digestibility data in Figures 5.7a and b for cellulase loadings of 5 and 15 mg protein/g cellulose, respectively, show that the presence of xylose derived pseudo-lignin did not have a major impact on the initial cellulose conversion. However, the effect became more pronounced as hydrolysis time was extended, with the extent depending on cellulase and pseudo-lignin loadings and the final cellulose digestibility, as indicated by the 120 h yields reported in Table 5.5. It is interesting to note that even a small amount of pseudo-lignin (5wt% of cellulose) had a noticeable negative impact on cellulose conversion at both cellulase loadings (21% and 9% reductions in 120 hours conversion at 5 and 15 mg/g cellulose enzyme loadings, respectively). Furthermore, Table 5.5 shows that conversion seemed to decrease with pseudo-lignin loading but reached an asymptote. The cause for such behavior is not clear at this point. Another interesting point was that at the highest pseudo-lignin loading (pseudo-lignin to cellulose ratio of 0.65) and for cellulase loading

of 15 mg/g glucan; the decrease in cellulose conversion was almost comparable to decrease for cellulose conversion with xylan (~22%, Table 5.5). For the latter, however, the decrease in initial rate was much higher than for pseudo-lignin (55% vs. 5%), and was due to strong cellulase inhibition by xylooligomers [208]. Adsorption of BSA and purified CBHI on pseudo-lignin in Figure 5.8a revealed that pseudo-lignin binds protein unproductively, while Figure 5.8b shows the relative amount of free protein in solution decreased as the pseudo-lignin loading was increased. Thus, it can be concluded that pseudo-lignin bind protein unproductively and can make less cellulase available for action on cellulose.

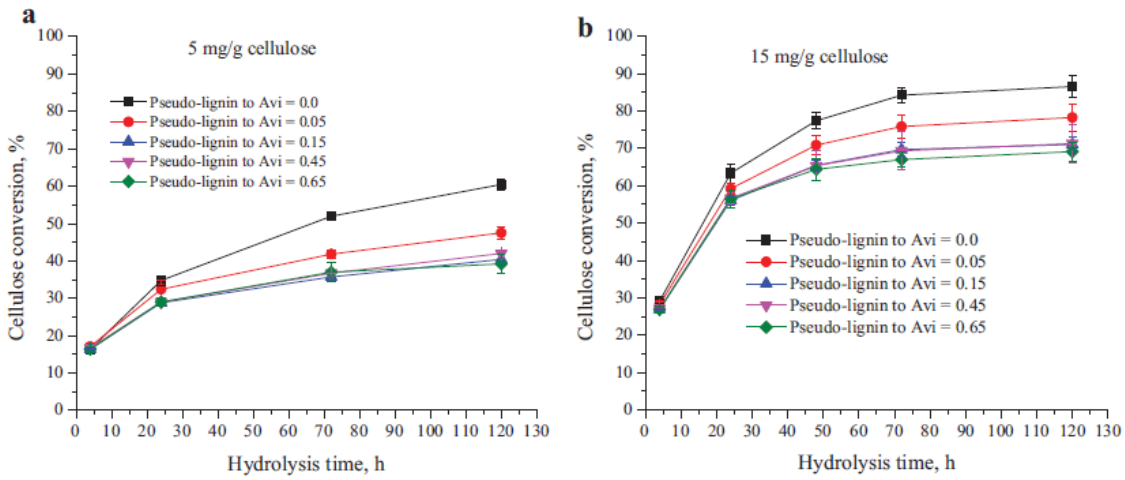

Figure 5.7 Effects of various levels of exogenously added pseudo-lignin on cellulose conversion at cellulase protein loadings of (**a**) 5 mg/g cellulose and (**b**) 15 mg/g cellulose

Table 5.5 Percentage decrease[a] in cellulose conversion, over Avicel cellulose control, with hydrolysis time for various loadings of pseudo-lignin, and a loading of xylan for 5 and 15 mg cellulase/ g cellulose loadings

Substrate	5 mg cellulase/g cellulose				15 mg cellulase/g cellulose			
	4 h	24 h	72 h	120 h	4 h	24 h	72 h	120 h
C + Pseudo-lignin-1	-4.4	6.8	19.6	21.4	3.2	6.6	10.0	9.6
C + Pseudo-lignin-2	0.1	17.1	31.2	33.2	7.6	11.5	17.3	17.9
C + Pseudo-lignin-3	-1.8	16.7	29.4	30.6	7.2	10.6	17.7	17.6
C + Pseudo-lignin-4	0.1	16.7	28.7	35.1	7.5	10.9	20.4	20.1
C + Xylan[b]	Not determined				55.0	33.4	24.0	22.0

C, Avicel cellulose; Pseudo-lignin-1, pseudo-lignin to cellulose weight ratio = 0.05; Pseudo-lignin 2, pseudo-lignin to cellulose weight ratio = 0.15; Pseudo-lignin-3, pseudo-lignin to cellulose weight ratio = 0.45; Pseudo-lignin-4, pseudo-lignin to cellulose weight ratio = 0.65.
[a]% decrease = 100 × [1 - (Reference sample yield (%)/Control yield (%))].
[b]Xylan to cellulose weight ratio was 0.5.

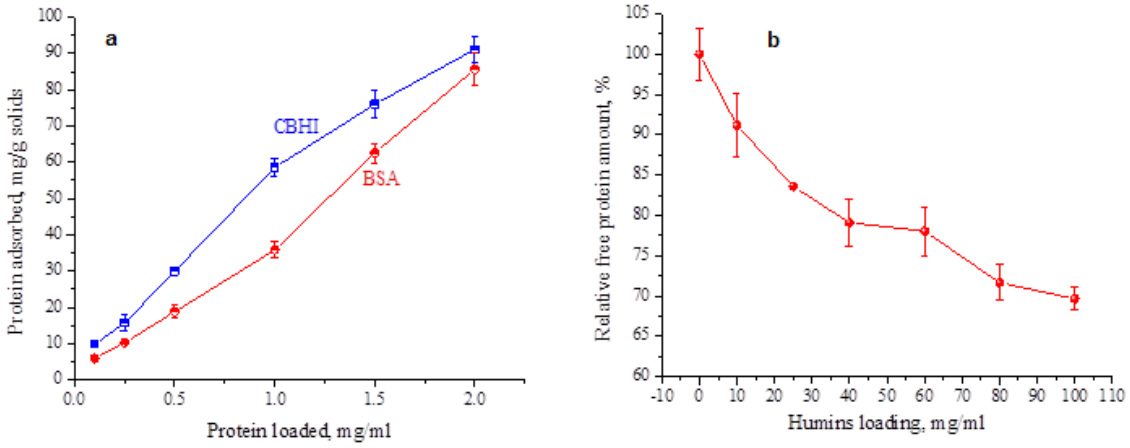

Figure 5.8 a: BSA and purified CBHI protein adsorption on xylose derived pseudo-lignin (mg/g solids) at a pseudo-lignin solids loading of 10 g/L. **b**: Effect of pseudo-lignin loading on relative amount of free BSA protein in solution for a BSA loading of 2 mg/mL

Reduced Cellulose Accessibility

Chemical and physical characterizations and enzymatic hydrolysis data showed that xylan degrades into insoluble compound which can significantly impede cellulose digestibility. Although NMR and FT-IR characterizations did not show strong evidences of pseudo-lignin formation at low severities, SEM imaging and compositional analysis revealed that pseudo-lignin formed even at low severities and deposited on the surface in spheres and/or co-existed with cellulose. Deposition of pseudo-lignin on the cellulose surface would directly affect its accessibility by blocking surface binding sites, and may be another possible cause for decrease in cellulose digestion.

5.4 Conclusion

Avicel cellulose alone and mixed with xylan or xylose was pretreated in dilute sulfuric acid over a range of conditions typically applied to cellulosic biomass to understand what effects xylan derived pseudo-lignin might have on cellulose digestibility. For Avicel cellulose alone, dilute acid pretreatment solubilized a significant amount of cellulose and increased crystallinity by few points (from 70.1% to 75.9%) but did not affect cellulose digestibility negatively until the combined severity factor CSF was increased to 3.56, at which point a large fraction of pseudo-lignin appeared to be formed from cellulose and xylan/xylose degradation. However, pseudo-lignin was formed from xylan/xylose degradation even at severities lower than often applied in dilute acid pretreatment and affected cellulose hydrolysis through reduced cellulase effectiveness and/or cellulose accessibility. The impact of pseudo-lignin was magnified at lower enzyme loadings that would be commercially appropriate. Therefore, pretreatment effectiveness would be improved by avoiding sugar degradation that can lead to pseudo-lignin formation,

particularly for subsequent application of lower enzyme loadings. Furthermore, it was noted that even a small amount of residual (non-structural) xylan, possibly precipitated on cellulose surface, significantly retard cellulose digestibility. However, this finding needs further research to understand hemicellulose (xylan) precipitation, its mechanisms, and its effects on cellulose conversion.

CHAPTER 6

IMPACT OF PSEUDO-LIGNIN VERSUS DILUTE ACID-TREATED LIGNIN ON ENZYMATIC HYDROLYSIS OF CELLULOSE[4]

6.1 Introduction

Increasing global energy demand, unstable and expensive petroleum resources, and concern over global climate changes lead to the development of biofuels from lignocellulosics, which are relatively inexpensive, abundant, and based on sustainable feedstocks [1,2]. To convert lignocellulosics to ethanol, plant polysaccharides need to be deconstructed into their corresponding monosaccharides, which subsequently are biologically fermented to ethanol. Utilization of enzymes to produce fermentable sugars is regarded as the most viable strategy, because enzymatic hydrolysis of lignocellulosics offers several advantages including higher yield, lower byproduct formation and energy requirement, mild operation conditions, and environmentally benign processing compared to conventional chemical hydrolysis [62]. However, native lignocellulosics are recalcitrant to decomposition from enzymes because of their physical features and chemical compositions/structures [1]. Furthermore, lignin has been viewed as one of the major factors contributing to this recalcitrance. During enzymatic hydrolysis, lignin acts as a physical barrier to prevent enzyme access to the carbohydrate fraction of biomass and tends to irreversibly bind to enzymes through hydrophobic interactions that cause a loss in their activities [58,62].

[4] This manuscript was accepted for publication in ACS Sustainable Chemistry & Engineering, 2013. It is entitled as – Impact of Pseudolignin versus Dilute Acid-Pretreated Lignin on Enzymatic Hydrolysis of Cellulose. The other authors are Seokwon Jung and Art Ragauskas from School of Chemistry and Biochemistry at Georgia Institute of Technology.

Pretreatment of lignocellulosic biomass is thus an essential step to overcome recalcitrance and increase overall fermentable sugar yield. Dilute acid pretreatment has been proven to successfully hydrolyze hemicelluloses and disrupt the lignocellulosic structure for a wide range of feedstocks. Generally, DAP leads to an insignificant delignification, thus the lignin content in the pretreated biomass can be comparable to or even higher than that in the starting material [11,42,173]. This phenomenon has been hypothesized to be due, in part, to the formation of a lignin-like material termed pseudo-lignin [15,16].

The formation of pseudo-lignin was only confirmed by Sannigrahi *et al* [109]. Their work demonstrated that pseudo-lignin can be generated from carbohydrates without significant contribution from lignin during DAP, particularly under high-severity pretreatment conditions. Additionally, Hu *et al.* [172] isolated and characterized pseudolignin produced from dilute acid-pretreated poplar holocellulose and α-cellulose. They showed that pseudolignin was polymeric with a Mw ≈ 5000 g/mol and contained carbonyl, carboxylic, aromatic, and aliphatic structures, which were produced from both dilute acid-pretreated cellulose and hemicellulose. Equally important, these studies indicated that the presence of pseudo-lignin on the surface of pretreated biomass can significantly inhibit enzymatic hydrolysis of cellulose. In the present study, pseudo-lignin and dilute acid-pretreated lignin were isolated, and their inhibition properties on enzymatic deconstruction of poplar holocellulose were evaluated and compared.

6.2 Experimental Section

6.2.1 Materials

Samples were prepared as described in Chapter 3 (3.1.2 Biomass Substrate). Hybrid poplar (*Populus trichocarpa x deltoides*) was obtained from Oakridge National Laboratory, TN and Wiley milled to pass a 2-mm screen. The sample was air-dried and stored at -20 ºC.

6.2.2 Pseudo-lignin Preparation

Extractives from hybrid poplar were removed by Soxhlet extraction with ethanol/toluene (1/2, v/v) for 24 h as described in Chapter 3 (3.2.1 Soxhlet Extraction). Holocellulose was isolated from the extractive-free poplar by sodium chlorite bleaching as described in Chapter 3 (3.2.2 Holocellulose Pulping). A two-step dilute acid pretreatment with the first step soaking in 1.0 wt% sulfuric acid (5% solids) while stirring at RT for 4 h was performed on poplar holocellulose. The presoaked slurry was filtered and the solids were washed with excess DI water. The solids were then added to 1.0 wt% sulfuric acid (5% solids) and transferred to a Parr 4560 mini pressure reactor (600 mL) for the second step of the pretreatment (180 °C, 40 min). The reactor was heated to the desired temperature with constant stirring at a heating rate of ~6 °C/min. After pretreatment, the slurry was filtered and the pretreated solids were washed with excess DI water.

Pseudo-lignin was extracted from dilute acid pretreated poplar holocellulose according to the procedures described in Chapter 3 (3.2.5 Pseudo-lignin Preparation).

6.2.3 EMAL Preparation

EMAL was prepared as described in Chapter 3 (3.2.6 Enzymatic Mild Acidolysis Lignin (EMAL) Preparation).

6.2.4 Lignocellulosic Samples Preparation

Pseudo-lignin (Pseudo-L) or dilute acid pretreated lignin (EMAL DAP) was added to poplar holocellulose to produce various lignocellulosic samples. In brief, 12%, 22% and 36% of Pseudo-L or EMAL DAP (Table 6.1) was dissolved in *p*-dioxane/water (10/1, v/v). A sample of poplar holocellulose (dry weight: 0.50 g) was added to the solution, and the mixture was allowed to stir in dark at RT under N_2 protection for 2 h. The slurry was then transferred to an aluminum weigh dish and allowed to air-dry in a fumehood.

Table 6.1 The amount of pseudo-lignin and dilute acid pretreated lignin addition

Sample	Lignin from	Lignin addition (g)	Holocellulose addition (g)	Lignin content (lignin addition/total mass × 100%)
g	Pseudo-lignin	0.07	0.50	12.28
h	Pseudo-lignin	0.14	0.50	21.88
i	Pseudo-lignin	0.28	0.50	35.90
j	EMAL DAP lignin	0.07	0.50	12.28
k	EMAL DAP lignin	0.14	0.50	21.88
l	EMAL DAP lignin	0.28	0.50	35.90
m	Pseudo-L/EMAL DAP (50:50,w/w)	0.07	0.50	12.28
n	Pseudo-L/EMAL DAP (50:50,w/w)	0.14	0.50	21.88
o	Pseudo-L/EMAL DAP (50:50,w/w)	0.28	0.50	35.90
p	NA	NA	0.50	NA

6.2.5 FT-IR Spectroscopic Analysis

Samples were characterized by FT-IR according to the procedures described in Chapter 3 (Chapter 3.3.3 Fourier Transform Infrared (FT-IR) Spectroscopy).

6.2.6 NMR Spectroscopic Analysis

Samples were characterized by ^{13}C NMR and ^{13}C-^{1}H 2D HSQC NMR according to the procedures described in Chapter 3.3.4.1 and 3.3.4.2, respectively.

6.2.7 Scanning Electron Microscopy

Samples were characterized by SEM according to the procedures described in Chapter 3 (Chapter 3.3.5 Scanning Electron Microscopy (SEM)).

6.2.8 Enzymatic Hydrolysis

Enzymatic hydrolysis experiments were performed as described in Chapter 3 (3.2.8 Enzymatic Hydrolysis). A sample of hydrolysis liquid (1.00 mL) at time intervals of 1, 2, 4, 7, 10, 24, 48, and 72 h was withdrawn and the hydrolysis was quenched by submersion for 10 min in a vigorously boiling water bath. The liquid samples were then stored and analyzed as described in Chapter 3 (3.2.8 Enzymatic Hydrolysis). All experiments were performed in duplicate and the results represented the mean values of two independent experiments. The standard deviation associated with the glucose yield at each time interval was in the range of ± 0~10%.

6.3 Results and Discussion

6.3.1 Structural Comparison

The FT-IR spectra of pseudo-lignin and dilute acid pretreated lignin are presented in Figure 6.1. Both samples had a hydroxyl stretching peak centered at ~3300 cm^{-1} but the hydroxyl stretching peak of pseudo-lignin is broader than that of dilute acid pretreated lignin. Furthermore, pseudo-lignin and dilute acid pretreated lignin exhibited aromatic absorptions. Different intensities of the absorption bands at ~1600 cm^{-1} and 1500 cm^{-1} suggest different aromatic structures and differing aromatic substitution patterns between pseudo-lignin and dilute acid pretreated lignin. Pseudo-lignin also possesses carbonyl and carboxylic groups, which can be observed from the strong band at ~1697 cm^{-1} in its FT-IR spectrum.

To further compare the structures of pseudo-lignin and dilute acid pretreated lignin, ^{13}C NMR spectra of these two samples were obtained and this data is summarized in Figure 6.2. A primary qualitative assignment based on literature is proposed in Table 6.2. The peaks centered at 208-205 ppm, 203-185 ppm, and 178-172 ppm from pseudo-lignin can be attributed to C=O in ketones, aldehydes and carboxylic acids, respectively [172]. Whereas the small peak centered at ~166 ppm corresponding to conjugated carboxylic ester group is shown in the ^{13}C NMR spectrum of dilute acid pretreated lignin [212]. This indicates pseudo-lignin contains more carbonyl and carboxylic acid groups than dilute acid pretreated lignin, consistent with the FT-IR characterization. Both the pseudo-lignin and dilute acid pretreated lignin possess aromatic structures. The peaks in the 162-142 ppm region are characteristic of aromatic C-O bonds. Whereas the peaks in the 142-125 ppm and 125-102 ppm regions represent aromatic C-C bonds and aromatic C-H bonds, respectively [212]. Additionally, the characterization of guaiacyl (G) and syringyl (S) units in dilute acid pretreated poplar lignin was identified by the peaks in the regions 125-110 ppm and 109-103 ppm, respectively [42]. Among the aromatic signals, aromatic C-O bonds are the most predominant, and the signal at ~66 ppm which was due to *p*-dioxane which could not be fully removed after extended time in a vacuum oven. With respect to aliphatic structures, pseudo-lignin consists of more oxygenated aliphatic structures that can be observed by the additional peaks at ~72 ppm, ~63 ppm and aliphatics in the region 50-20 ppm. The 13C NMR spectra of these two samples also present common peaks at ~60 ppm and ~56 ppm.

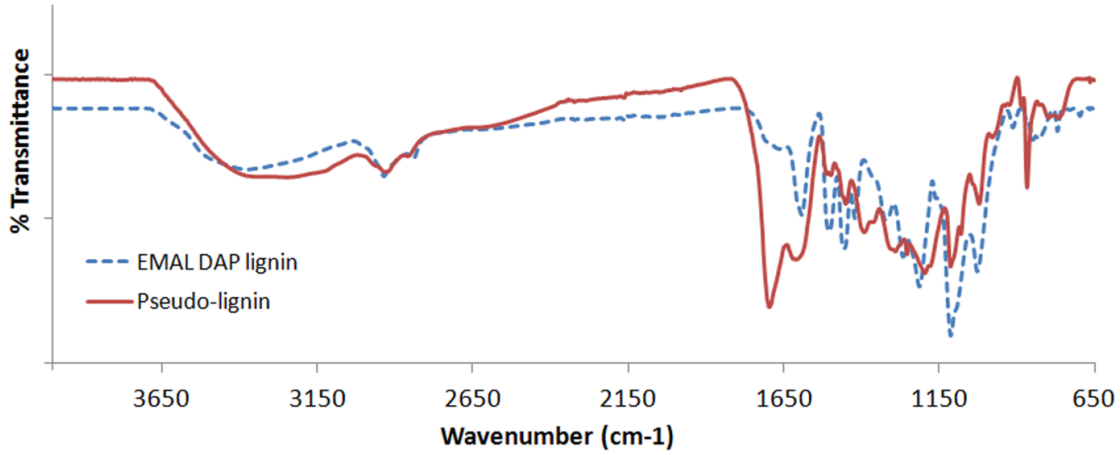

Figure 6.1 FT-IR spectra of pseudo-lignin and dilute acid pretreated lignin

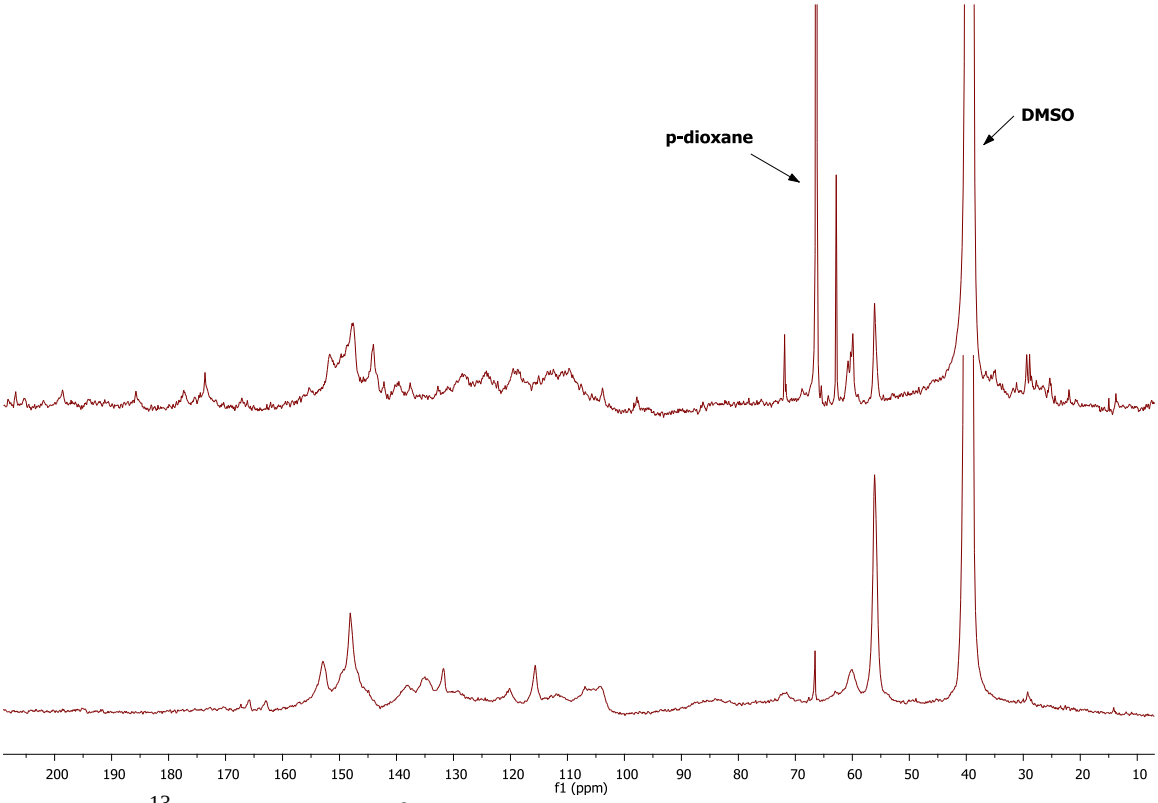

Figure 6.2 ^{13}C NMR spectra of pseudo-lignin (top) and dilute acid pretreated lignin (bottom)

Table 6.2 Peak assignments for ^{13}C NMR spectra of pseudo-lignin and dilute acid pretreated lignin [187]

Chemical shift (ppm)	Assignment
208-205	C=O in ketones
203-185	C=O in aldehydes
178-172	C=O in carboxylic acids
166	Conjugated carboxylic ester group
162-142	Aromatic C-O
142-125	Aromatic C-C
125-102	Aromatic C-H
72, 63	Hydroxylated methylene
60	Methoxy groups connected to aromatic rings for pseudo-lignin; C_γ in β-*O*-4 substructure for dilute acid pretreated lignin
56	Methoxy group connected to aromatic ring
50-20	Aliphatic carbons

To obtain further knowledge of pseudo-lignin and dilute acid pretreated lignin structures, their HSQC spectra are presented in Figure 6.3. The S units in dilute acid pretreated lignin show a major cross peak for the $C_{2,6}/H_{2,6}$ correlation at δ_C/δ_H 103.5/6.7 ppm, and the G units show correlations at δ_C/δ_H 110.6/7.0 ppm and 115.1/6.8 ppm [213]. A considerable amount of *p*-hydroxybenzoate can be observed from $C_{2,6}/H_{2,6}$ correlation at δ_C/δ_H 131.3/7.7 ppm [214]. Compared to dilute acid pretreated lignin, pseudo-lignin shows much weaker C/H correlation signals at different chemical shifts in the aromatic region. The common peak at ~56 ppm can be attributed to the methoxy groups according to the C/H correlation signals at δ_C/δ_H 56.0/3.8 ppm [213]. The C/H correlation in β-*O*-4 substructure of dilute acid pretreated lignin was observed for γ-C position at δ_C/δH

60.0/3.7 ppm [213], whereas this signal from pseudo-lignin was assigned to methoxy group according to the DEPT NMR analysis [172]. The HSQC NMR assignment was summarized in Table 6.3 [213]. The structural characterization shows that the poplar lignin was partially degraded during DAP at 170 °C, 0.5% H_2SO_4, 8 min (CSF: 1.97), and it did not contain a significant proportion of pseudo-lignin after the pretreatment. This is consistent with literature indicating insignificant pseudo-lignin formation during DAP at combined severity lower than 1.77 [109]. On the other hand, pseudo-lignin is a lignin-like aromatic material but is not derived from native lignin which appears to be generated at higher acidic severity conditions. During DAP, the hydrolysis of polysaccharides which leads to some release of monosaccharides, and their subsequent dehydration reactions to form furfural and 5-hydromethylfurfural (HMF) takes place. Further rearrangements of furfural and/or HMF may produce aromatic compounds, which undergo further polymerization and/or polycondensation reactions to form pseudo-lignin [172].

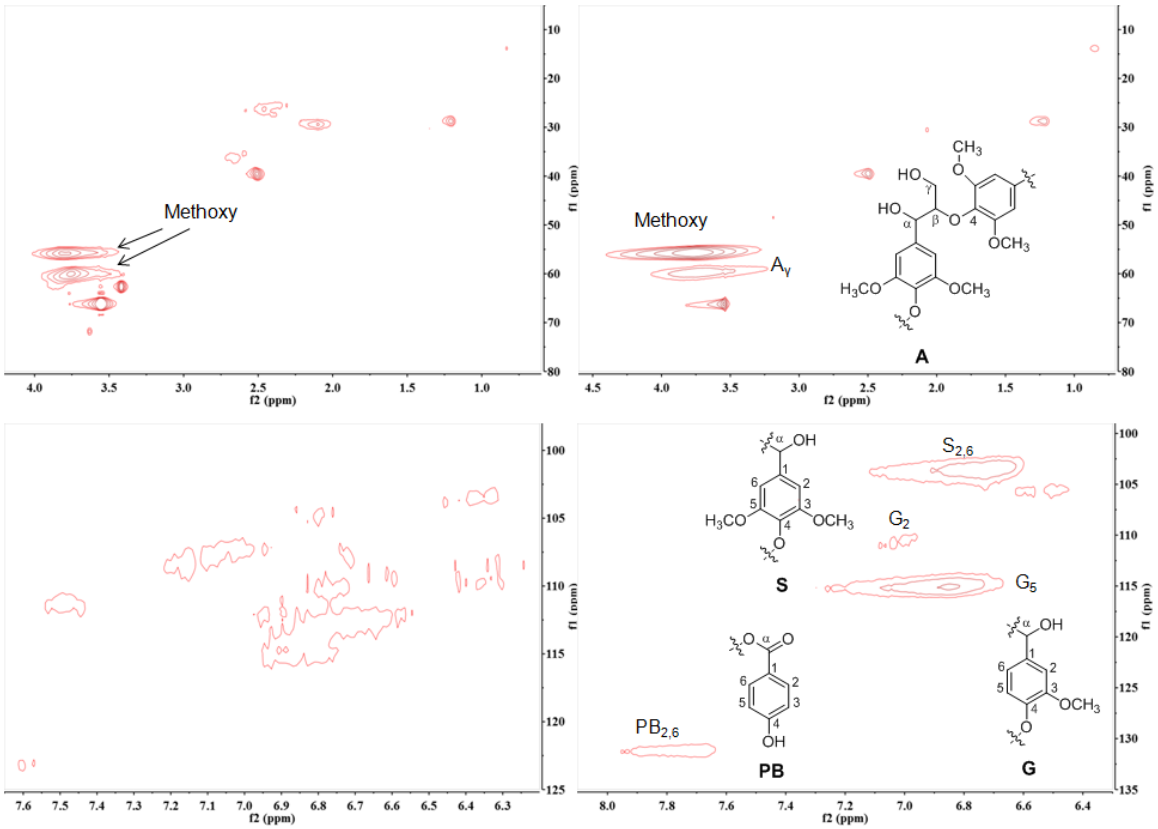

Figure 6.3 2D HSQC NMR spectra of pseudo-lignin (left) and dilute acid pretreated lignin (right).

Table 6.3 Peak assignments for 2D HSQC NMR spectra of pseudo-lignin and dilute acid pretreated lignin [213]

C/H correlation (δ_C/δ_H; ppm)	Assignment
56.0/3.8	Methoxy group connected to aromatic ring
60.0/3.7	Methoxy group connected to aromatic ring for pseudo-lignin; γ-C position in β-*O*-4 substructure of dilute acid pretreated lignin
103.5/6.7	$C_{2,6}/H_{2,6}$ correlation in S lignin units
110.6/7.0	C_2/H_2 correlation in G lignin units
115.1/6.8	C_5/H_5 correlation in G lignin units
131.3/7.7	$C_{2,6}/H_{2,6}$ correlation in *p*-hydroxybenzoate

6.3.2 Enzymatic Hydrolysis Results

When preparing the lignocellulosic samples, pseudo-lignin or dilute acid pretreated lignin was solubilized in *p*-dioxane before the holocellulose sample was added to form a slurry. The purpose of this effort is to incorporate pseudo-lignin or dilute acid pretreated lignin

into the cellulose and hemicellulose structures, rather than creating a dry physical mixture. Compared to the poplar holocellulose, it was visually evident that pseudo-lignin or dilute acid pretreated lignin had coated the cellulose fibers, as the resulting samples became darker with increasing amounts of pseudo-lignin or EMAL. Upon examination of the lignocellulosic samples by SEM (Figure 6.4), pseudo-lignin or dilute acid pretreated lignin droplets were successfully deposited on the holocellulose surface. These droplets have different diameters and were postulated to inhibit enzymatic hydrolysis of cellulose. The enzymatic conversion yields of cellulose for various lignocellulosic samples are summarized in Figure 6.5. The data in Table 6.4 indicated that both pseudo-lignin and dilute acid pretreated lignin inhibited enzymatic hydrolysis of holocellulose in the initial stage (before 24 h of hydrolysis), and hydrolysis inhibition generally increased with pseudo-lignin or dilute acid pretreated lignin content. However, the inhibition effect of dilute acid pretreated lignin was much less significant than pseudo-lignin. In addition, dilute acid pretreated lignin alone had a negligible inhibition after 48 h of hydrolysis, which is consistent with literature reports of a limited effect of dilute acid pretreated lignin on enzymatic hydrolysis of cellulose. In contrast, pseudo-lignin alone had a strong inhibition of 9.5 to 25.1% on the overall enzymatic conversion yield of cellulose, whereas this inhibition was modest (1.9 to 6.7%) for the samples with a 50/50 mixture of pseudo-lignin and dilute acid pretreated lignin. It is well known that lignin has non-productive association with cellulases due to its hydrophobic structural features including hydrogen-bonding, methoxy groups and polyaromatic structures. The structural functionality of methoxy and polyaromaticity of pseudo-lignin revealed by the FT-IR and ^{13}C NMR analysis suggests its hydrophobicity. Indeed, pseudo-lignin is insoluble in water. We

speculate that the hydrophobic structural functionality of pseudo-lignin accounts for its non-productive association with cellulases, resulting in the inhibition effects to enzymatic hydrolysis of cellulose. These results suggest that although pseudo-lignin that is not derived from native lignin is even more detrimental to enzymatic hydrolysis of cellulose than dilute acid pretreated lignin, thus its formation should be avoided.

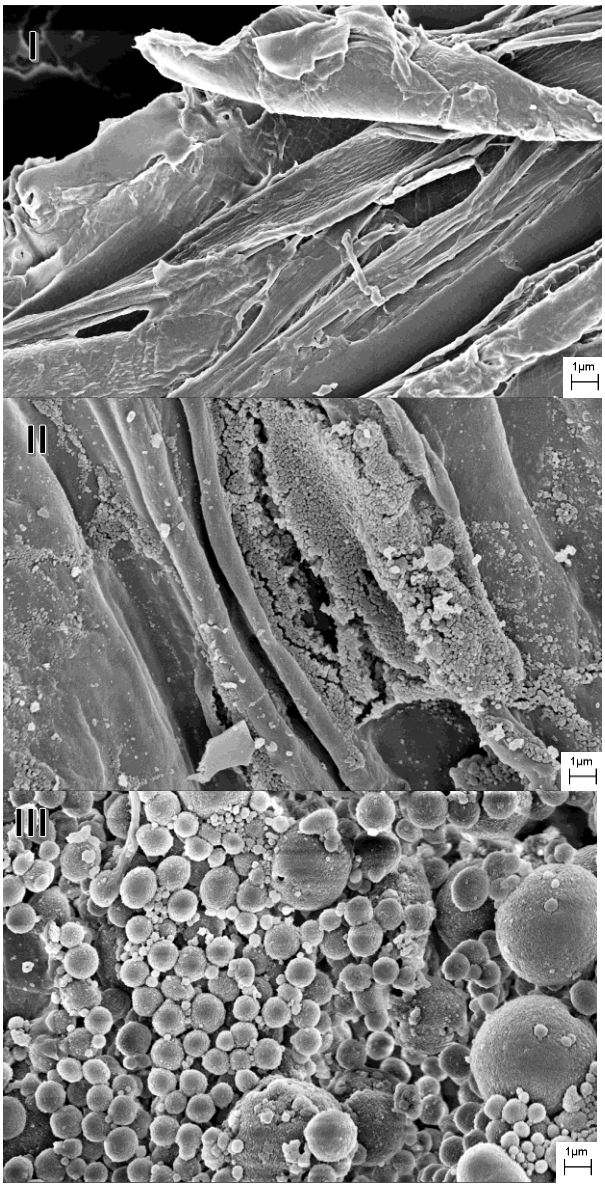

Figure 6.4 SEM images of (I) holocellulose, (II) the lignocellulosic sample with pseudo-lignin, and (III) the lignocellulosic sample with dilute acid pretreated lignin

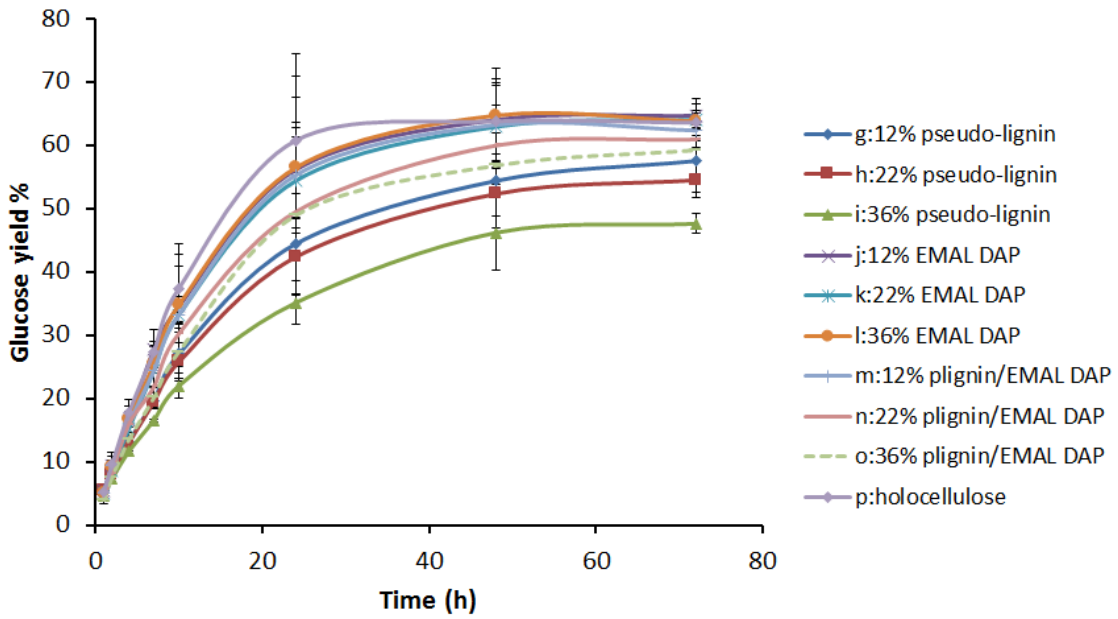

Figure 6.5 Time course of glucose yield of various samples after 72 h of enzymatic hydrolysis

Table 6.4 Average percentage inhibition of enzymatic hydrolysis of holocellulose by pseudo-lignin and dilute acid pretreated lignin

	Enzymatic hydrolysis time (h)							
Samples	1	2	4	7	10	24	48	72
g: 12% pseudo-lignin	0	14.5	26.0	27.9	27.7	26.9	14.7	9.5
h: 22% pseudo-lignin	0	17.2	27.1	28.8	31.1	30.3	18.0	14.2
i: 36% pseudo-lignin	11.2	23.5	34.5	39.4	41.2	42.2	27.6	25.1
j: 12% EMAL DAP	0	1.9	6.4	0	7.6	7.6	0	0
k: 22% EMAL DAP	3.6	10.4	14.3	10.9	11.1	10.5	1.3	0
l: 36% EMAL DAP	2.8	4.2	6.3	6.9	7.0	7.1	0	0
m: 12% Pseudo-L/EMAL DAP*	1.3	1.3	10.1	10.7	11.2	9.0	0.9	1.9
n: 22% Pseudo-L/EMAL DAP*	16.9	14.1	10.0	20.1	19.1	18.6	6.0	4.1
o: 36% Pseudo-L/EMAL DAP*	22.2	20.3	23.9	26.2	26.7	19.4	10.9	6.7
p: holocellulose (control)	0	0	0	0	0	0	0	0

*Pseudo-lignin and dilute acid pretreated lignin were mixed 50/50 by weight.

6.4 Conclusion

Results from the spectroscopic analysis indicated that although pseudo-lignin and dilute acid pretreated lignin have some common structural features, the poplar lignin pretreated at 170 °C, 0.5% H_2SO_4, 8 min did not contain detectable amounts pseudo-lignin; on the other hand, pseudo-lignin is not derived from native lignin but is a lignin-like aromatic

material. The enzymatic hydrolysis studies revealed that the impact of pseudo-lignin on enzymatic deconstruction of cellulose was much more detrimental than that of dilute acid pretreated lignin. This study suggests that dilute acid pretreatment should be performed at lower severe conditions thereby avoiding the formation of pseudo-lignin.

CHAPTER 7

SUPPRESSION OF PSEUDO-LIGNIN FORMATION UNDER DILUTE ACID PRETREATMENT CONDITIONS[5]

7.1 Introduction

As global energy consumption is continuing to rise, the world is pursuing the development of renewable energy sources such as lignocellulosic ethanol to address vital strategic, economic and environmental issues with the depleting fossil fuels [1,2]. Lignocellulosic biomass such as wood, grass, and agricultural and forest residues are an inexpensive and abundant feedstock for sustainable production of fuels and chemicals [2]. To convert biomass to ethanol, plant polysaccharides must be deconstructed into their corresponding monosaccharides, which subsequently are biologically fermented to ethanol. Utilization of enzymes to produce fermentable sugars is viewed as the most viable strategy, because enzymatic hydrolysis of biomass offers several advantages such as higher yield, lower byproduct formation and energy requirement, mild operation conditions, and environmentally benign processing compared to conventional acid hydrolysis [62]. Unfortunately, the yield of ethanol production from native lignocellulosic biomass is relatively low due to the natural resistance of plant cell walls to decomposition from microbes and enzymes [1].

Pretreatment of lignocellulosic biomass is an essential step to overcome recalcitrance and increase overall fermentable sugar yield. It utilizes various technologies such as chemical

[5]This manuscript was accepted for publication in RSC Advances, 2014. It is entitled as – Suppression of pseudo-lignin formation under dilute acid pretreatment conditions. The other author is Art Ragauskas from School of Chemistry and Biochemistry at Georgia Institute of Technology.

treatment to alter plant cell wall structural features so that the polysaccharide fractions become more accessible and amenable to enzymatic hydrolysis. Dilute acid pretreatment (DAP) has been considered to be among the leading and most promising pretreatment technologies that can enhance fermentable sugar release performance [5,9]. DAP involves the treatment of biomass with a combination of an acidic solution, heat and pressure with residence times ranging from less than a minute to 1 h, which is generally carried out using 0.4 – 2.0 wt% H_2SO_4 at a temperature of 140 – 200 °C [12]. Generally, DAP does not lead to significant delignification. This phenomenon has been hypothesized to be due, in part, to the formation of a lignin-like material termed pseudo-lignin [15,16], and its formation was confirmed by Sannigrahi *et al* [109]. Their work demonstrated that pseudo-lignin can be generated from carbohydrates without significant contribution from lignin during DAP, particularly at high-severity pretreatment conditions. In addition, Hu *et al.* [172] isolated and characterized pseudo-lignin produced from dilute acid-treated poplar holocellulose and α-cellulose. They showed that pseudo-lignin was polymeric and contained carbonyl, carboxylic, aromatic, and aliphatic structures, which were produced from both dilute acid-treated cellulose and hemicellulose. In a continued study, Hu *et al.* [215] reported that pseudo-lignin is not derived from native lignin but is a lignin-like aromatic material, which is even more detrimental to enzymatic deconstruction of cellulose when compared to dilute acid-treated lignin. This latter study clearly indicated that the formation of pseudo-lignin during DAP should be avoided. During DAP, the hydrolysis of polysaccharides leads to the release of some monosaccharides, and subsequent dehydration reactions lead to the formation of furfural and 5-hydromethylfurfural (HMF). Further rearrangements of

furfural and/or HMF may produce aromatic compounds, which undergo further oxidative polymerization and/or polycondensation reactions to form pseudo-lignin [215]. Oxygen thus may play a role in pseudo-lignin formation. In addition, using a surfactant such as Tween-80 during DAP has been shown to significantly increase lignin removal [216] and thus could potentially assist in the solubilization of pseudo-lignin. It has also been reported that addition of dimethyl sulfoxide (DMSO) to the reaction medium containing dilute HCl solution can suppress undesired HMF side reactions during the process of HMF production [217]. With these issues in mind, we modified the DAP process with different methods including performing DAP under O_2 or N_2; adding surfactant (Tween-80) to the reaction mixture; and using water/DMSO mixture as reaction medium, with the intention of exploring new methods of suppressing pseudo-lignin formation. These studies demonstrated that using a water/DMSO mixture in the DAP process can significantly reduce pseudo-lignin formation at high-severity pretreatment conditions. To the best of our knowledge, this is the first report demonstrating that the amount of pseudo-lignin generated during DAP can be reduced, and this study contributes to further understanding of fundamental principles behind DAP technology, in order to develop a more effective, economic and environmentally benign DAP technology.

7.2 Experimental Section

7.2.1 Materials

Samples were prepared as described in Chapter 3 (3.1.2 Biomass Substrate). Hybrid poplar (*Populus trichocarpa x deltoides*) was obtained from Oakridge National

Laboratory, TN and Wiley milled to pass a 2-mm screen. The sample was air-dried and stored at -20 ºC.

7.2.2 Dilute Acid Pretreatment

Extractives from hybrid poplar were removed by Soxhlet extraction with ethanol/toluene (1/2, v/v) for 24 h as described in Chapter 3 (3.2.1 Soxhlet Extraction). Holocellulose was isolated from the extractive-free poplar by sodium chlorite bleaching as described in Chapter 3 (3.2.2 Holocellulose Pulping). A two-step dilute acid pretreatment with the first step soaking in 1.0 wt% sulfuric acid (5% solids) while stirring at RT for 4 h was performed on poplar holocellulose. The presoaked slurry was filtered and the solids were washed with excess DI water. The solids were then added to 1.0 wt% sulfuric acid (5% solids) and transferred to a Parr 4560 mini pressure reactor (600 mL) for the second step of the pretreatment (Table 7.1). Experiments conducted with O_2 or N_2 were 1) 4 min gas bubbling through the reactor (inlet tube releases gas at the very bottom of the reactor, and mixing distributes gas for better saturation); 2) 5 min gas bubbling; and 3) 10 min gas bubbling plus 100 psi gas pressure over atmospheric pressure. The other parameters were the same as in control DAP. In the DAP study with surfactant, 5% (w/w) of Tween-80 was added based on dry biomass weight. The reactor was heated to the desired temperature from RT with constant stirring at a heating rate of ~6 °C/min. After pretreatment, the reactor was cooled to RT in an ice-water bath. The slurry was filtered and the pretreated solids were washed with excess DI water.

Table 7.1 The conditions for the second step in two-step DAP of poplar holocellulose

Sample	Second step pretreatment conditions
Control DAP	180 ºC, 1.0 wt% H_2SO_4, 40 min
R (O_2)	180 ºC, 1.0 wt% H_2SO_4 at 100 psi O_2, 40 min
S (N_2)	180 ºC, 1.0 wt% H_2SO_4 at 100 psi N_2, 40 min
T (DMSO)	180 ºC, 1.0 wt% H_2SO_4 (H_2O/DMSO : 4/1; v/v), 40 min
U (Tween)	180 ºC, 1.0 wt% H_2SO_4 with 5% (w/w) Tween-80, 40 min

7.2.3 Pseudo-lignin Preparation

Pseudo-lignin was extracted from holocellulose samples recovered from various DAP conditions according to the procedures described in Chapter 3 (3.2.5 Pseudo-lignin Preparation).

7.2.4 Lignocellulosic Samples Preparation

Pseudo-lignin generated from DAP in water/DMSO mixture (Pseudo-lignin (DMSO)) or produced from control DAP conditions (Pseudo-lignin (Control)) was added to poplar holocellulose to produce various lignocellulosic samples. In brief, a sample of pseudo-lignin (dry weight: 0.10 g) was dissolved in p-dioxane/water (10/1, v/v). A sample of poplar holocellulose (dry weight: 0.50 g) was added to the solution, and the mixture was stirred in dark at RT under N_2 protection for 2 h. The slurry was then transferred to an aluminum weigh dish and allowed to air-dry in a fumehood.

7.2.5 Acid-Insoluble Lignin (K-Lignin) and Carbohydrate Analysis

Carbohydrate profiles and acid-insoluble lignin content in various samples were determined as described in Chapter 3 (Chapter 3.3.1 Carbohydrate and Acid-insoluble Lignin Analysis).

7.2.6 Molecular Weight Analysis of Isolated Pseudo-lignin

The molecular weights of pseudo-lignin samples were determined as described in Chapter 3 (Chapter 3.3.2 Molecular Weight Analysis).

7.2.7 FT-IR Spectroscopic Analysis

Samples were characterized by FT-IR according to the procedures described in Chapter 3 (Chapter 3.3.3 Fourier Transform Infrared (FT-IR) Spectroscopy).

7.2.8 NMR Spectroscopic Analysis

Samples were characterized by ^{13}C NMR, ^{13}C-^{1}H 2D HSQC NMR and DEPT-135 ^{13}C NMR according to the procedures described in Chapter 3.3.4.1, 3.3.4.2 and 3.3.4.3, respectively.

7.2.9 Enzymatic Hydrolysis

Enzymatic hydrolysis experiments were performed as described in Chapter 3 (3.2.8 Enzymatic Hydrolysis). A sample of hydrolysis liquid (1.00 mL) at time intervals of 1, 2, 4, 10, 24, and 48 h was withdrawn and the hydrolysis was quenched by submersion for 10 min in a vigorously boiling water bath. The liquid samples were then stored and analyzed as described in Chapter 3 (3.2.8 Enzymatic Hydrolysis). All experiments were performed in duplicate and the results represented the mean values of two independent experiments. The standard deviation associated with the glucose yield at each time interval was in the range of ± 0~4%.

7.3 Results and Discussion

7.3.1 Screen of Modified Dilute Acid Pretreatment Conditions

The detailed mechanism of how pseudo-lignin is formed during DAP is still unclear. Previous studies strongly suggested that during DAP, the hydrolysis of polysaccharides (e.g. xylan and cellulose) leads to some release of monosaccharides (e.g. xylose and glucose), which are then converted to furfural and HMF. Further rearrangements of

furfural and/or HMF are responsible for the formation of pseudo-lignin [172,215]. One can thus conclude that furfural and especially HMF are the key intermediates for pseudo-lignin formation, and their stabilization from further reactions may effectively suppress pseudo-lignin formation. DMSO has recently been shown to prevent undesired side reactions of HMF in HMF production [217], which is due to the preferential arrangement of DMSO in the vicinity of the C1 carbon of HMF molecules. This strongly indicates that DMSO protects the C1 carbon of the HMF molecule from further reactions, thus we hypothesized that DMSO could suppress pseudo-lignin formation during DAP. Furthermore, the fragmentation and rearrangement reactions of HMF at severe DAP conditions can produce phenolic compounds such as 1,2,4-benzenetriol [172]. In the presence of oxidants such as oxygen, oxidative polymerization of phenolic compounds is one of the potential reactions to form pseudo-lignin [172], thus DAP performed under O_2 or N_2 may facilitate or curb pseudo-lignin formation. In addition, surfactants are well-known pretreatment additives, and Qing *et al.* [216] reported that dilute acid pretreating corn stover with Tween-80 could remove more lignin from the solids, probably by forming emulsions that reduce lignin redeposition back on the biomass surface through interaction of Tween-80 with hydrophobic lignin during pretreatment. Pseudo-lignin is also hydrophobic [215], and thus it is possible to reduce pseudo-lignin deposition by pretreating with surfactant.

To test our hypotheses, a series of DAP conditions using O_2/N_2; Tween-80 or DMSO were conducted, and pseudo-lignin and carbohydrate analysis of solids recovered from various DAP conditions was performed. This data was summarized in Table 7.2. The starting material (i.e. untreated poplar holocellulose) had very low acid-insoluble lignin

content, thus the dramatic increase in acid-insoluble lignin content of pretreated samples strongly suggests the generation of pseudo-lignin during DAP. As expected, solids recovered from DAP performed under O_2 consisted mainly of pseudo-lignin (~89%). However, DAP conducted under N_2 did not diminish pseudo-lignin formation, in contrast, it resulted in moderately higher (~6%) pseudo-lignin content when compared to the control DAP. These results suggest that oxidative reaction is one but not the only one reaction that leads to produce pseudo-lignin during DAP. As a result, DAP with O_2 could facilitate pseudo-lignin formation very likely through promoting oxidative reactions, while N_2 could suppress oxidative reactions but cannot curb other reactions to produce pseudo-lignin from furfural and/or HMF, or prevent carbohydrates from forming furfural and HMF. In the DAP study with Tween-80, this resulted in the lowest solids recovery yield (~13%), and (~10%) higher pseudo-lignin content than the control DAP. This indicates that pseudo-lignin is hydrophobic just like lignin, but its formation cannot be curbed by dilute acid pretreating with surfactants. In contrast to N_2 and Tween-80, addition of DMSO to DAP reaction medium effectively reduced pseudo-lignin content by approximately 30% and increased solids recovery yield by around 20%. The effectiveness of DMSO was further supported by the FT-IR analysis of recovered solids (Figure 7.1). For instance, the FT-IR spectrum of sample T (DMSO) resembles that of holocellulose, implying a minor proportion of pseudo-lignin in recovered solids. On the other hand, all the remaining spectra of control DAP, sample R (O_2), S (N_2) and U (Tween) showed C=O stretching and aromatic C=C stretching peaks at ~1705 cm^{-1} and ~1615 cm^{-1}, respectively, which are the characteristic structural features of pseudo-lignin [172,215].

In the presence of DMSO, it has been suggested that the coordination of HMF with water can be reduced due to the competition between water oxygen and DMSO oxygen to be in the first solvation shell of HMF, with DMSO having a stronger interaction [218,219]. According to the molecular dynamics simulation of HMF in DMSO/H_2O mixture (Figure 7.2 a), the angular distribution of water molecules around carbonyl oxygen atom do not compete for the same space with the DMSO molecule interacting with the C1 carbon atom, showing that the water molecules hydrogen-bonded to the C1 carbonyl oxygen would not hamper the coordination of DMSO around the C1 carbon. High patches of DMSO can be seen near the hydrogen atom of the HMF hydroxyl group due to stronger hydrogen bond than water molecules (Figure 7.2 b). Furthermore, the highest density region of DMSO around HMF is around the C1 atom and for water molecules, it is around the only hydroxyl group of HMF (Figure 7.2 c) [218]. As the cleavage of C1 atom of HMF eventually leads to form pseudo-lignin, the reduction of HMF-water coordination and the preferential solvation of the C1 carbon by DMSO can protect the HMF molecule from further reactions to form pseudo-lignin in the aqueous medium.

Table 7.2 Acid-insoluble lignin (K-lignin) and carbohydrate contents of various samples (based on dried samples)

Sample	Solids recovery %	K-lignin %	Xylan %	Glucan %	Total %
Holocellulose	NA	4.3	2.9	93.4	100.6
Control DAP	18.9	42.0	0	54.4	96.4
R (O_2)	18.1	89.2	0	4.3	93.5
S (N_2)	19.1	48.7	0	47.1	95.8
T (DMSO)	37.8	14.7	0	86.2	100.9
U (Tween)	13.3	52.1	0	45.0	97.1

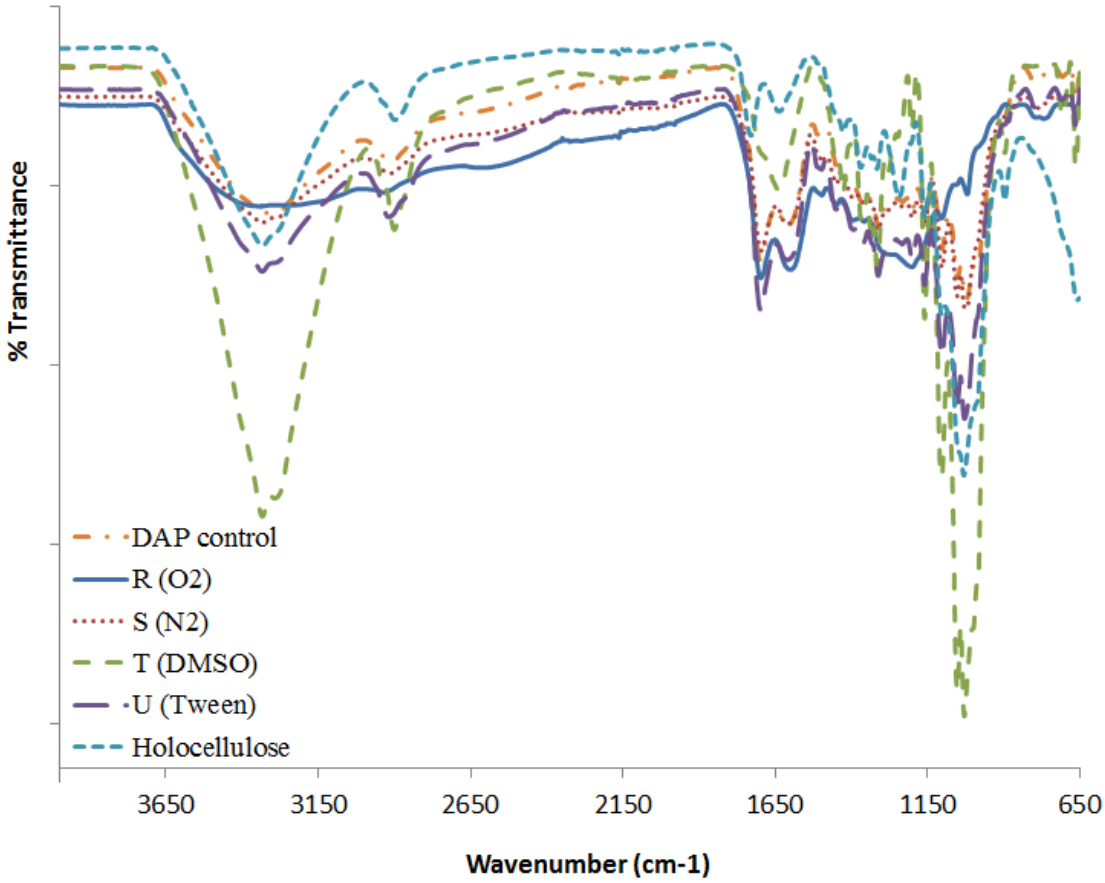

Figure 7.1 FT-IR spectra of solids recovered from various DAP conditions

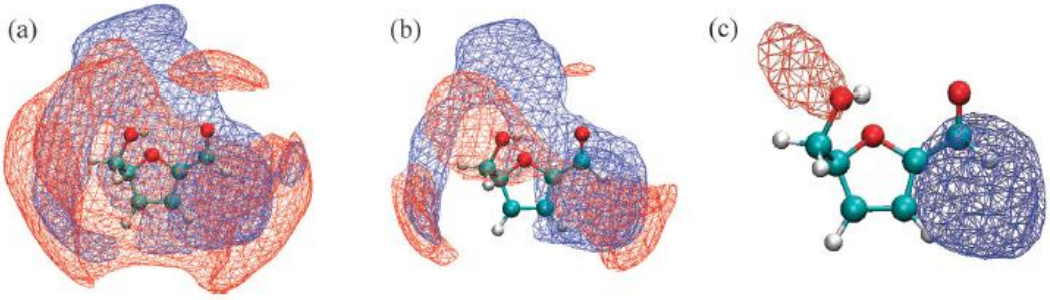

Figure 7.2 Volumetric map of the time averaged distribution of oxygen atoms in water and DMSO around an HMF molecule in the simulation. Red colored surfaces indicate water oxygen atoms and blue colored surfaces indicate DMSO oxygen atoms. The maps are depicted in order of increasing isovalue

7.3.2 Further Optimization of the Amount of DMSO in Dilute Acid Pretreatment

The pseudo-lignin content of solids recovered from DAP in water/DMSO mixture (4/1; v/v) was the lowest among all DAP examined conditions. However, it is difficult to

extract any pseudo-lignin from pretreated solids at such low proportion, and the volume of DMSO used was relatively high. Therefore, in order to isolate sufficient pseudo-lignin for structural characterization, the amount of DMSO used in DAP was further optimized with the intention of lowering DMSO volume while still maintaining moderate pseudo-lignin content. We screened water/DMSO volume ratio ranging from 4 to 1 to 20 to 1, while maintaining all other experimental parameters (i.e. 180 ºC, 1.0 wt% H_2SO_4 and 40 min), and analyzed pseudo-lignin contents of recovered solids. These results were summarized in Table 7.3. In general, increasing the volume ratio of DMSO led to a reduction in pseudo-lignin proportion and an increase in solids recovery yield. At water/DMSO: 20/1 ratio, both the pseudo-lignin content and the solids recovery yield were comparable to the control DAP, suggesting the amount of DMSO was too low to suppress pseudo-lignin formation. At low DMSO concentration condition, the solvent coordination around HMF is dominated by the interaction between the oxygen atoms of water and the carbon atoms of HMF. In addition, water can form hydrogen bonds with the oxygen atom attached to C1 atom of HMF [219]. The acidic aqueous condition thus leads to further rearrangements of HMF and/or furfural to yield other aromatic compounds which in turn can be converted to pseudo-lignin. Reducing the DMSO ratio from water/DMSO: 12/1 to 15/1 resulted in only a slightly increase in pseudo-lignin content and even higher solids recovery yield. As a result, water/DMSO: 15/1 ratio was chosen as the pretreatment condition to isolate pseudo-lignin and investigate if DMSO could change any structural features of pseudo-lignin.

Table 7.3 Acid-insoluble lignin (K-lignin) and carbohydrate contents of solids recovered from DAP in water/DMSO mixture (based on dried samples)

Sample	Solids recovery %	K-lignin %	Glucan %	Total %
Control DAP (no DMSO)	18.9	42.0	54.4	96.4
H_2O/DMSO (4/1; v/v)	37.8	14.7	86.2	100.9
H_2O/DMSO (10/1; v/v)	24.2	34.8	62.0	96.8
H_2O/DMSO (12/1; v/v)	24.6	30.6	65.1	95.7
H_2O/DMSO (15/1; v/v)	27.2	31.2	66.7	97.9
H_2O/DMSO (20/1; v/v)	19.1	37.4	59.1	96.5

7.3.3 Structural Characterization of Isolated Pseudo-lignin

Pseudo-lignin samples generated from DAP in water/DMSO (15/1; v/v) mixture (Pseudo-lignin (DMSO)) and from control DAP conditions (Pseudo-lignin (Control)) were isolated following a literature protocol [172]. Their FT-IR spectra were presented in Figure 7.3. The spectra suggest that pseudo-lignin produced from the two conditions had similar functionalities, particularly in the case of hydroxyl, aliphatic C-H, C=O (carbonyl and/or carboxylic) and aromatic functional groups. The hydroxyl stretching peaks at ~3333 cm^{-1} are strong and broad, indicating the presence of hydrogen-bonding in pseudo-lignin samples. The strong bands at ~1705 cm^{-1} conjugated with ~1615 and ~1516 cm^{-1} can be attributed to C=O conjugated with aromatic ring. Perhaps the biggest difference between these two samples was the presence of strong stretching peak at ~1665 cm^{-1} corresponding to α, β-unsaturated aldehyde or ketone in pseudo-lignin (DMSO) sample, whereas this peak was absent in pseudo-lignin (control) sample. These observations indicate dehydration and aromatization reactions of carbohydrates took place during the formation of pseudo-lignin.

To further characterize and compare the functional groups in isolated pseudo-lignin samples, their ^{13}C NMR spectra were obtained and the spectra were presented in Figure 7.4. The ^{13}C NMR spectra are predominantly comprised of signals from carbonyl,

carboxylic, aromatic and aliphatic structures. The peaks in the 153-142 ppm region are characteristic of aromatic C-O bonds, whereas the peaks in the 142-102 ppm regions represent aromatic C-C bonds and aromatic C-H bonds. The signal at δ 66 ppm was due to *p*-dioxane which could not be fully removed after extended time in a vacuum oven. To obtain better knowledge of NMR signals besides aromatic carbons, distortionless enhancement by polarization transfer-135 (DEPT-135) NMR spectra of pseudo-lignin samples were obtained (Figure 7.5). DEPT-135 is a useful tool to determine the presence of primary, secondary and tertiary carbon atoms, which gives positive CH and CH_3 signals while negative CH_2 signals. According to the DEPT-135 NMR analysis, the CH peaks centered at ~177 pm correspond to conjugated aldehyde groups, which is further confirmed by the C/H correlation at δ_C/δ_H 177.2/9.6 ppm (Figure 7.6), while the signal at ~162 ppm is attributed to the tertiary carbon belonging to the carboxylic group of formate, which is confirmed by the C/H correlation at δ_C/δ_H 161.7/8.2 ppm (Figure 7.7). Furthermore, the DEPT NMR analysis revealed that the peaks in the 133-102 ppm region are characteristic of aromatic C-H bonds, thus aromatic C-C bonds belong to the 142-133 ppm region. In the case of aliphatic structures, most secondary carbon atoms are located in the 72-62 ppm region, suggesting these CH_2 groups belong to ethers, alcohols or carboxylic esters. In addition, the methoxy groups of pseudo-lignin are identified by the peaks centered at ~60 ppm and ~56 ppm, which are also observed by the C/H correlations at δ_C/δ_H 60.2/3.8 ppm and δ_C/δ_H 56.0/3.8 ppm, respectively (Figure 7.5). The origin of the methoxy group of pseudo-lignin was postulated to come from 4-*O*-methyl-D-glucuronic acid in the poplar hemicellulose [172], and the low intensity of the methoxy peak could support this postulate because of the low xylan content in untreated poplar holocellulose.

The NMR characterization of pseudo-lignin samples is consistent with the FT-IR analysis, showing pseudo-lignin samples produced from the two conditions had similar structural features. This suggests that although DMSO can suppress the pseudo-lignin formation, it does not involve a change in the mechanism of pseudo-lignin formation during the course of DAP.

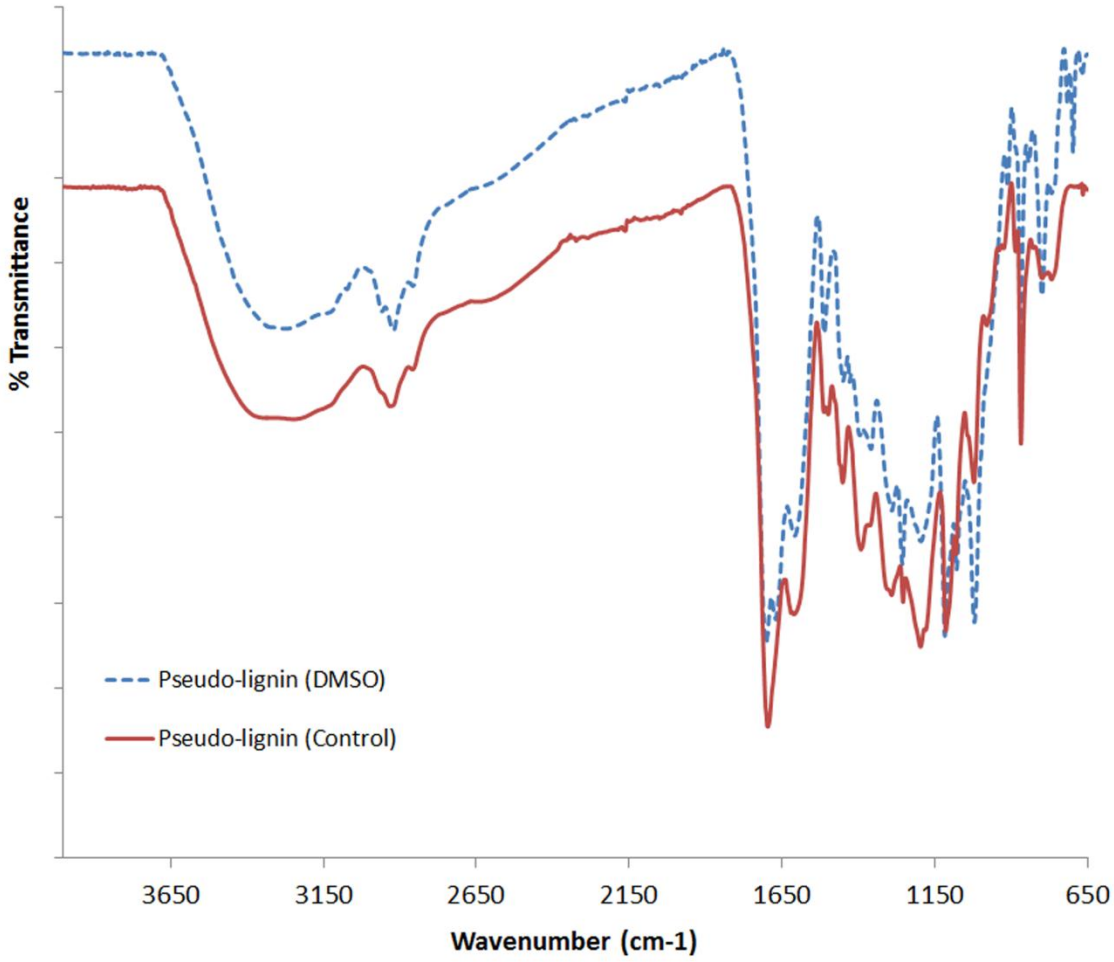

Figure 7.3 FT-IR spectra of pseudo-lignin (DMSO) and pseudo-lignin (control)

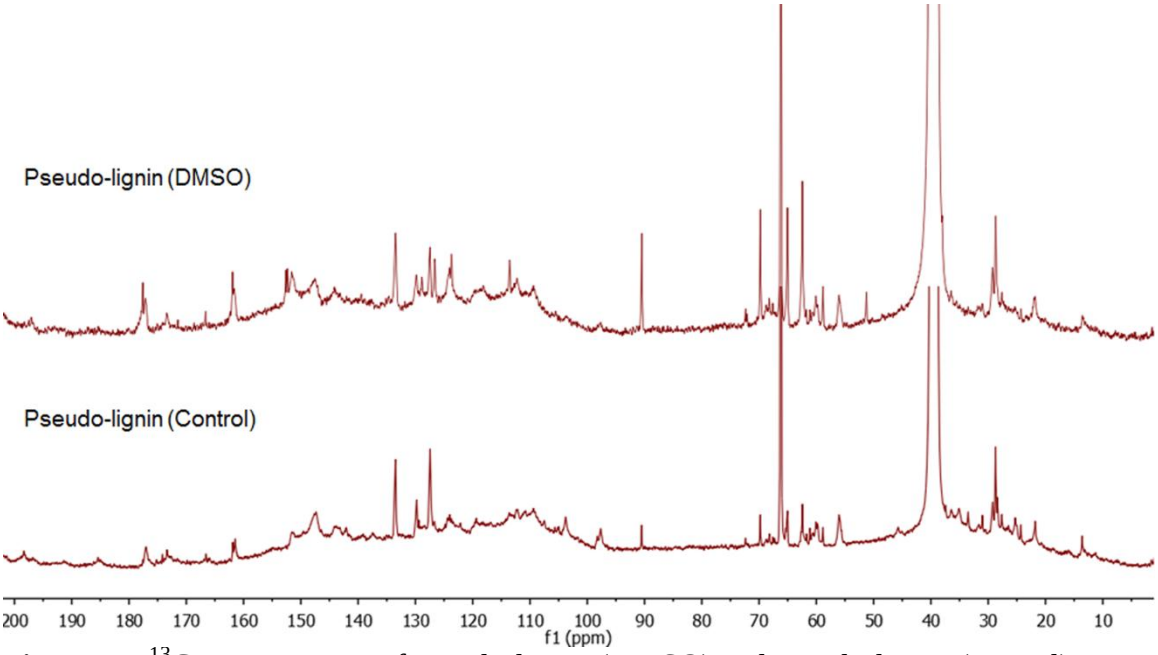

Figure 7.4 ^{13}C NMR spectra of pseudo-lignin (DMSO) and pseudo-lignin (control)

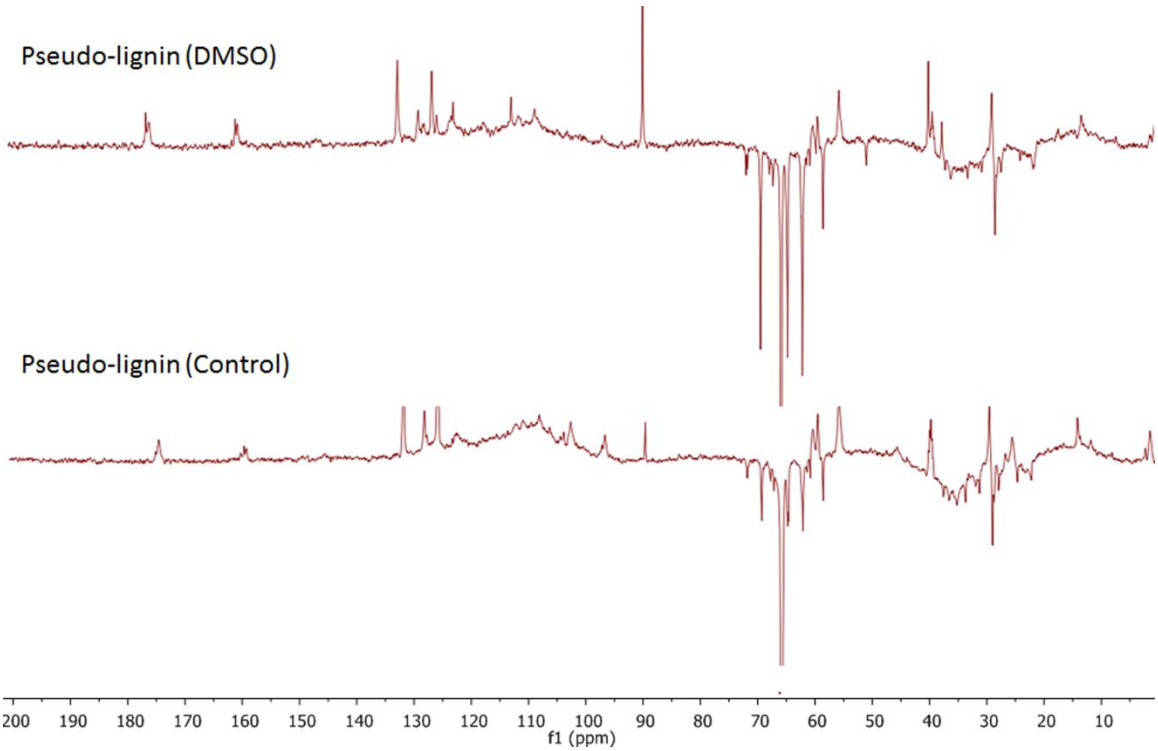

Figure 7.5 DEPT-135 NMR spectra of pseudo-lignin (DMSO) and pseudo-lignin (control)

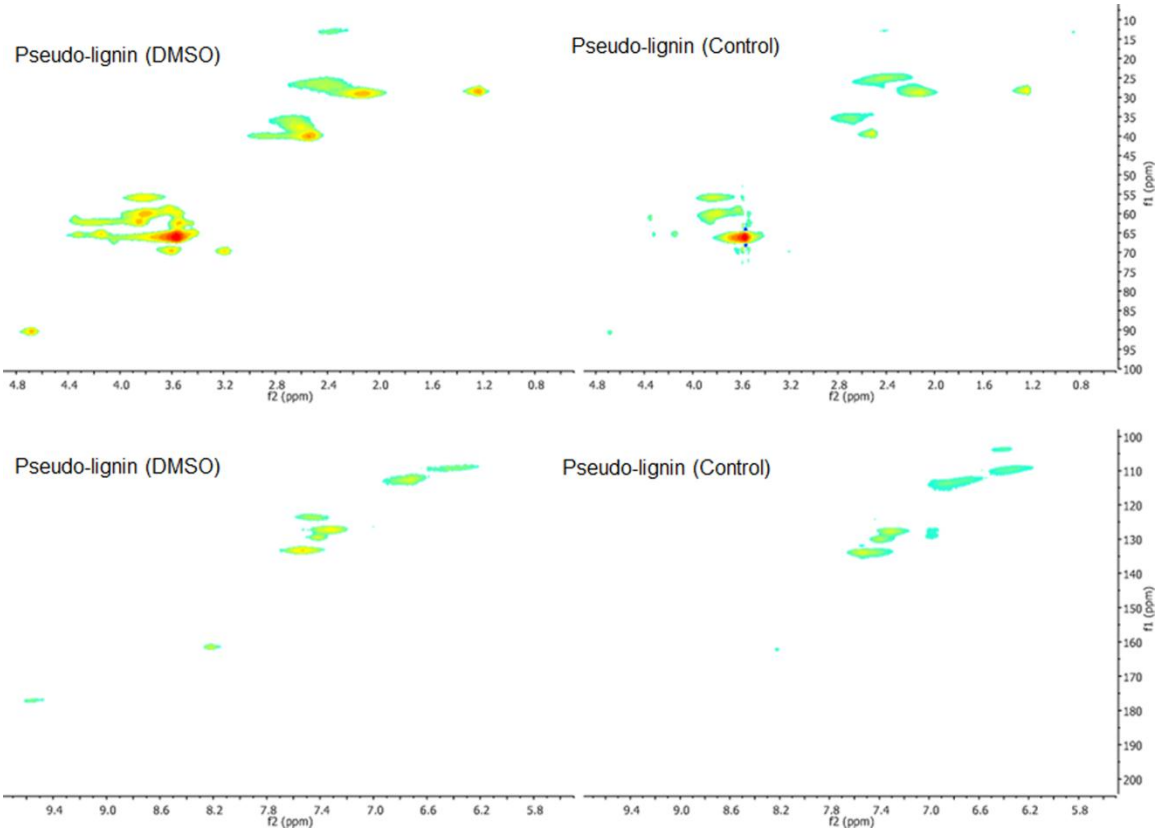

Figure 7.6 2D HSQC NMR spectra of pseudo-lignin (DMSO) and pseudo-lignin (control)

7.3.4 Molecular Weight Analysis of Isolated Pseudo-lignin

The molecular weights of pseudo-lignin (DMSO) and pseudo-lignin (control) were represented in Table 7.4. In general, the molecular weights of isolated pseudo-lignin samples were much lower than those of milled wood lignin (M_n ~4060 g/mol; M_w ~10002 g/mol) from poplar. Furthermore, pseudo-lignin samples produced from two conditions had similar molecular weights, which is very likely attributed to their similar structural features. In addition, polydispersity (PDI) values greater than 1 indicate that pseudo-lignin is not homogeneous.

Table 7.4 Molecular weights of isolated pseudo-lignin samples

Sample	M_n (g/mol)	M_w (g/mol)	PDI (M_w/M_n)
Pseudo-lignin (DMSO)	1.78×10^3	3.36×10^3	1.89
Pseudo-lignin (Control)	1.84×10^3	3.74×10^3	2.03

7.3.5 Enzymatic Hydrolysis Results

When preparing the lignocellulosic samples, pseudo-lignin was incorporated into the cellulose and hemicellulose structures by dissolution and evaporation rather than physically mixing with holocellulose. This protocol has been frequently used in literature, leading to a successful deposition of pseudo-lignin droplets on the holocellulose surface [172,215]. These pseudo-lignin droplets have been shown to inhibit enzymatic hydrolysis of cellulose, probably by blocking cellulases surface binding sites; and through non-productive association with cellulases due to the hydrophobicity of pseudo-lignin [215,220]. The inhibition property of pseudo-lignin generated from aqueous DMSO DAP on enzymatic deconstruction of poplar holocellulose was evaluated and compared with that of pseudo-lignin acquired from routine DAP. The enzymatic conversion yields of cellulose for various lignocellulosic samples were represented in Figure 7.6. The data indicates that neither the presence of pseudo-lignin (DMSO) nor pseudo-lignin (control) had a major impact on the initial cellulose conversion (before 4 h of enzymatic hydrolysis). However, the inhibition effect became more pronounced as the hydrolysis time was extended, which reached the maximum reduction in glucose yield around 20% at 24 h and 48 h of hydrolysis time for pseudo-lignin (DMSO) and pseudo-lignin (control), respectively. Furthermore, the results suggest that these two pseudo-lignin samples had similar inhibition effects, which is very likely due to their similar molecular weights and structural features. The inhibition effects of pseudo-lignin to enzymatic hydrolysis of cellulose is enhanced as its content increases [172,215,220], thus although DMSO did not reduce the inhibition effects of pseudo-lignin, it can significantly suppress

pseudo-lignin formation during DAP, which in turn can increase the enzymatic digestibility of cellulose after the pretreatment.

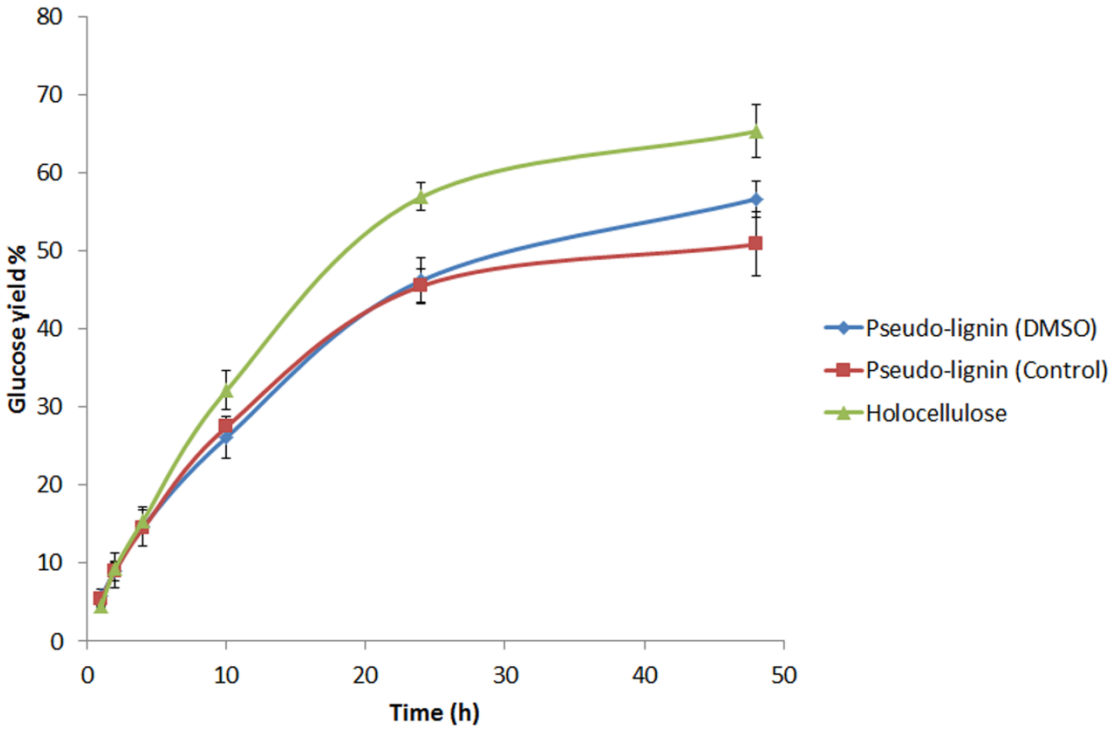

Figure 7.7 Time course of glucose yield of various samples after 48 h of enzymatic hydrolysis

7.4 Conclusion

In summary, we have demonstrated that addition of DMSO to DAP reaction medium can effectively suppress pseudo-lignin formation, even at high-severity pretreatment conditions. Although DMSO has exceptional pseudo-lignin suppression property, it did not change pseudo-lignin molecular weight or any of its structural features significantly. In addition, although DMSO cannot reduce the inhibition effect of pseudo-lignin to enzymatic deconstruction of cellulose, its pseudo-lignin suppression effect can in turn increase the enzymatic digestibility of cellulose after DAP. This study showed that the

amount of pseudo-lignin formed during DAP is controllable, which is a good contribution to development of a more economic and effective DAP technology.

CHAPTER 8

OVERALL CONCLUSIONS

The increasing concerns on reducing dependency on fossil fuels, decreasing greenhouse gas emissions and improving energy security drive to the utilization of renewable and sustainable resources to produce transportation fuels, chemicals and materials. Biofuels derived from non-food based lignocellulosic biomass have taken a leading position as a viable option to supplement depleting fossil fuels. The production of cellulosic ethanol through biological route has garnered extensive interest over the past decade, however, it still faces the major challenges such as the high cost of pretreatment and the low efficiency of enzymatic hydrolysis of plant cell wall polysaccharides to sugars. Further improvement of the cellulosic ethanol production process is thus contingent on deeper understanding of pretreatment chemistry, as well as improved understanding of the inhibitors to enzymatic deconstruction of biomass. In this thesis, various analytical tools were used to study the chemistry of pseudo-lignin generated during dilute acid pretreatment, and its inhibition to enzymatic hydrolysis of cellulose was identified and investigated. Furthermore, this thesis provides a potential solution to optimize dilute acid pretreatment to reduce pseudo-lignin formation and enhance overall sugar recovery, which is a good contribution to the biorefining industry.

The primary goal of this thesis was to study the chemistry of pseudo-lignin, which often causes an increase in acid-insoluble lignin content during dilute acid pretreatment of biomass. The first study (Chapter 4) started with the idea of characterizing pseudo-lignin extracted from poplar holocellulose and α-cellulose after dilute acid pretreatment. The

poplar holocellulose and α-cellulose contained insignificant amount (less than 5%) of acid-insoluble lignin, but this content increased dramatically after pretreatment, indicating the formation of pseudo-lignin. In addition, pseudo-lignin is polymeric with molecular weight ($M_w \approx 5000$ g/mol) much less than that of poplar milled wood lignin ($M_w \approx 10002$ g/mol), which can be produced from both dilute acid pretreated cellulose and hemicellulose, and its proportion increases as the pretreatment severity increases. FT-IR and NMR characterization revealed that pseudo-lignin is comprised of carbonyl, carboxylic, aromatic, methoxy and aliphatic structural features, suggesting that hydrolysis of biomass polysaccharides to the corresponding sugar monomers, and the subsequent dehydration and fragmentation of sugars as well as rearrangement and polycondensation and/or polymerization reactions lead to the formation of pseudo-lignin during DAP. Furthermore, discrete spherical pseudo-lignin droplets were deposit on the surface of biomass after DAP, and the results from enzymatic hydrolysis study strongly indicated that pseudo-lignin interacts with cellulases to significantly reduce cellulose enzymatic digestibility.

Dilute acid as well as hydrothermal pretreatments often lead to a significant hemicellulose loss to soluble furans and insoluble degradation products, collectively termed as pseudo-lignin. The second study (Chapter 5) was conducted in order to understand the factors contributing to sugar yields reduction from pretreated biomass and understand the possible influence of carbohydrate derived pseudo-lignin on cellulose conversion at the moderate to low enzyme loadings necessary for economic bioethanol production. Avicel cellulose and beechwood xylan/xylose were used instead of real biomass with the purpose of avoiding the complexity encountered with interpretation of

results for real biomass. Dilute acid pretreatment of Avicel cellulose alone and mixed with beechwood xylan or xylose was performed at various severities. Consistent with the previous study, the amount of pseudo-lignin in the pretreated solids increased with pretreatment severity, with a negligible amount at CSF 1.94 and the highest amount at CSF 3.56 (95 wt%) for cellulose mixed with xylose. However, there was more pseudo-lignin formed in the pretreated poplar holocellulose compared to that in Avicel cellulose mixed with xylan at similar severity. This difference could be attributed to poplar holocellulose that is less crystalline and with more acid labile hemicellulose or acid-soluble lignin is more likely to produce higher proportions of pseudo-lignin when pretreated at high severities. FT-IR and solid-state ^{13}C CP/MAS NMR analysis of pretreated solids showed that there was no apparent change in cellulose structure at all conditions except at the most severe condition (CSF of 3.56), which showed strong carbonyl, aromatic, and aliphatic signals. Although the NMR and FT-IR data did not show the evidence of pseudo-lignin formation for solids prepared at CSF less than 3.56, pseudo-lignin droplets were observed in the SEM images for these solid samples. More of these droplets were evident on the surface of the pretreated solids of cellulose mixed with xylan or xylose compared to cellulose pretreated alone at the same severities. Enzymatic hydrolysis study revealed that the presence of carbohydrate derived pseudo-lignin did not have a major impact on the initial cellulose conversion, but the effect became more pronounced as hydrolysis time was extended. More importantly, even a small amount of pseudo-lignin (5 wt% of cellulose) had a noticeable negative impact on cellulose-to-glucose conversion. This reduction in cellulose conversion was due to unproductive binding between pseudo-lignin and cellulase protein, which was supported

by the relative amount of free protein in solution decreased as the pseudo-lignin loading increased. In addition, deposition of pseudo-lignin on the cellulose surface can directly affect its accessibility by blocking surface binding sites, and may be another possible reason to reduce cellulose enzymatic digestibility.

Since there are strong evidences supporting that pseudo-lignin is detrimental to enzymatic deconstruction of cellulose, it is essential and important to compare its inhibition effects with native lignin after DAP. In Chapter 6, EMAL was isolated from poplar after an 8 min pretreatment at 170 °C using 0.5 wt% H_2SO_4. FT-IR and ^{13}C NMR characterization revealed that the poplar lignin was partially degraded during the pretreatment and did not contain detectable amounts of pseudo-lignin. Holocellulose was treated with varying amounts of pseudo-lignin and/or EMAL dissolved in *p*-dioxane and then dried. The treated and control holocellulose was then treated to a standard cellulase treatment, and the results from enzymatic hydrolysis of these samples showed that the dilute acid-pretreated lignin inhibited hydrolysis in the initial stage but had a negligible impact on the overall cellulose-to-glucose conversion yield. In contrast, pseudo-lignin significantly reduced the overall enzymatic conversion yield of cellulose to glucose. This study suggests that pseudo-lignin formation needs to be avoided because it is more detrimental to enzymatic hydrolysis of cellulose than dilute acid-pretreated lignin.

In the last chapter (Chapter 7) of this thesis, DAP was modified by performing it under O_2 or N_2; adding surfactant (Tween-80) to the reaction mixture; or using a water-dimethyl sulfoxide (DMSO) mixture as reaction medium, in order to reduce pseudo-lignin formation. Pseudo-lignin analysis showed that only the addition of DMSO to DAP reaction medium can effectively suppress pseudo-lignin formation. This was attributed to

DMSO preferentially solvating and stabilizing 5-hydroxymethyl furfural which is the key intermediate to form pseudo-lignin, thereby reducing the overall yield of pseudo-lignin. Furthermore, the addition of DMSO was shown not to reduce pseudo-lignin molecular weight or change any of its structural features significantly. Therefore, pseudo-lignin generated from aqueous DMSO DAP had similar inhibition properties as compared to that acquired from routine DAP at equal mass dosages. This study is the first demonstration that the amount of pseudo-lignin formed during DAP can be reduced, which contributes to further optimization of DAP technology.

CHAPTER 9

RECOMMENDATIONS FOR FUTURE WORK

The studies in this thesis have provided a firm step forward into a comprehensive understanding of pseudo-lignin chemistry during DAP. It is well known that thermochemical pretreatment enhances biomass digestibility by partial removal or redistribution of lignin, but this strategy results in sugar degradation and loss at high severities. This research further emphasized that the sugar degradation and loss is undesirable due to it can form pseudo-lignin that significantly reduces enzymatic conversion efficiency. Nevertheless, the mechanistic study of pseudo-lignin discovered that the addition of DMSO during DAP effectively increased solid recovery yield and reduced pseudo-lignin formation, which offers a valuable solution to the challenge that how to effectively reduce lignocellulosic recalcitrance at high severities while maintaining the integrity of fermentable sugars. In order to gain an even deeper insight into pseudo-lignin chemistry, several projects might be conducted which are listed as follows:

- To further support the hypothesized reaction pathways leading to carbohydrate-derived pseudo-lignin formation, glucose, xylose, 5-hydroxymethylfurfural (HMF) and furfural will be subjected to pretreatments at 180 °C using 1.0 wt% H_2SO_4 at various durations (e.g. 5, 10, 20, 30 and 40 min), respectively. After cooling to RT, the solution mixtures will be centrifuged and dried under vacuum overnight to isolate the solids. FT-IR and ^{13}C NMR analysis will be performed on these solids to obtain time-wise structural characterization information. By

comparing these characterization data (glucose vs. HMF and xylose vs. furfural), we can obtain valuable information with respect to pseudo-lignin formation reaction pathways. In addition, the liquid products will be identified by liquid chromatography/mass spectroscopy (LC/MS) and high-performance liquid chromatography (HPLC).

- The pseudo-lignin in this thesis study exclusively refers to carbohydrate-derived pseudo-lignin. However, lignin is also one of the major components in biomass, and it may react with carbohydrate degradation products via polycondensation reactions to contribute to the yield of pseudo-lignin. Indeed, the results from Chapter 5 suggest that biomass with more lignin is more likely to produce higher amounts of pseudo-lignin at severe pretreatment conditions. Therefore, it is important to characterize the molecular weight and chemical structure of pseudo-lignin extracted from the mixture of poplar holocellulose and milled wood lignin at different weight ratios after DAP, and compare the results with carbohydrate-derived pseudo-lignin, in order to evaluate the role of lignin in pseudo-lignin formation. In addition, it is also necessary to evaluate the inhibition effects of this pseudo-lignin to enzymatic hydrolysis of cellulose in comparison to carbohydrate-derived lignin.
- Although the addition of DMSO to DAP reaction medium can effectively reduce pseudo-lignin formation, it is difficult to recover DMSO from aqueous medium due to its high boiling point and the miscibility in a wide range of organic solvents as well as water. As a result, future DAP optimization method will rely on the development of a heterogeneous catalyst or surfactant that can coordinate

and protect furfural and HMF during DAP, so that the equilibrium of pseudo-lignin formation would shift toward the carbohydrates. This process can not only reduce pseudo-lignin formation but can also be economical due to the catalyst or surfactant can be recovered and recycled.

- SEM characterization of pseudo-lignin-on-holocellulose samples can examine the successful deposition of pseudo-lignin droplets on the surface of holocellulose. To further ensure the holocellulose surface is covered by the pseudo-lignin droplets in the enzymatic hydrolysis reaction medium, a modified Simons' stain method will be used to measure the cellulose accessibility at various time intervals during enzymatic hydrolysis. Enzymatic hydrolysis experiments will be conducted in 1 wt% pseudo-lignin-on-holocellulose sample suspension in 50 mM citrate buffer (pH 4.8) with cellulase and β-glucosidase loadings of 20 FPU/g and 40 CBU/g, respectively. The mixture will be incubated at 50 °C under continuous agitation at 140 rpm. A sample of 1 mL will be taken after 2, 8, 24, 48 and 72 h, boiled for 10 min (to denature the enzymes) then frozen. At the same time periods larger volume samples will be also taken and not boiled but thoroughly washed then heat treated in boiling water for 10 min. This way the cellulose mixture will be washed off to avoid sticking. Sugar release will be analyzed by a Dionex HPLC equipped with pulsed amperometric detection. To measure the amount of adsorbed dye on the holocellulose, a sample of 30 mg of pseudo-lignin-on-holocellulose will be weighed into three 15 mL Corning polypropylene centrifuge tubes. To each tube 0.3 mL of PBS (phosphate buffered saline solution) (pH 6, 0.3M PO4, 1.4 M NaCl) will be added. The DO solution (10 mg/mL) will be

added in a series of increasing volumes (0.167, 0.333, 0.667 mL) to a series of six tubes, each containing a lignocellulosic sample and PBS. The DB solution (10 mg/mL) will be also added to each tube in a series of increasing volumes (0.167, 0.333, 0.667 mL), thus creating a set of tubes with a 1:1 mixture of DO and DB dyes at increasing concentrations. This will be used to measure the dye adsorption isotherm. Distilled water will be added to make up the final volume in the centrifuge tubes to 3.0 mL. These tubes will be incubated for 48 h at 75 °C with shaking at 200 rpm. After the incubation period, the tubes will be centrifuged at 10,000 rpm for 5 min and a sample of the supernatant will be placed in a cuvette and the absorbance will be read on a Perkin Elmer Lambda-35 UV/Vis spectrophotometer at 455 nm and 624 nm which represents the wavelength of maximum absorbance for DO and DB, respectively. The amount of dye adsorbed onto the holocellulose fiber will be determined using the difference in the concentration of the initial added dye and the concentration of the dye in the supernatant. The reduced cellulose accessibility of pseudo-lignin-on-holocellulose sample compared to holocellulose will indicate the holocellulose surface is covered by the pseudo-lignin droplets in the enzymatic hydrolysis reaction medium.

REFERENCES

1. Himmel, M. E.; Ding, S. Y.; Johnson, D. K.; Adney, W. S.; Nimlos, M. R.; Brady, J. W.; Foust, T. D., Biomass recalcitrance: Engineering plants and enzymes for biofuels production. *Science* **2007,** *315* (5813), 804-807.

2. Ragauskas, A. J.; Williams, C. K.; Davison, B. H.; Britovsek, G.; Cairney, J.; Eckert, C. A.; Frederick, W. J.; Hallett, J. P.; Leak, D. J.; Liotta, C. L.; Mielenz, J. R.; Murphy, R.; Templer, R.; Tschaplinski, T., The path forward for biofuels and biomaterials. *Science* **2006,** *311* (5760), 484-489.

3. Bothast, R. J.; Schlicher, M. A., Biotechnological processes for conversion of corn into ethanol. *Applied microbiology and biotechnology* **2005,** *67* (1), 19-25.

4. Marchetti, J. M.; Miguel, V. U.; Errazu, A. F., Possible methods for biodiesel production. *Renew Sust Energ Rev* **2007,** *11* (6), 1300-1311.

5. Hu, F.; Ragauskas, A., Pretreatment and Lignocellulosic Chemistry. *BioEnergy Research* **2012,** *5* (4), 1043-1066.

6. Zhang, Y. H. P., Reviving the carbohydrate economy via multi-product lignocellulose biorefineries. *J Ind Microbiol Biot* **2008,** *35* (5), 367-375.

7. Sierra, R.; Smith, A.; Granda, C.; Holtzapple, M. T., Producing fuels and chemicals from lignocellulosic biomass. *Chemical Engineering Progress* **2008,** *104* (8), S10-S18.

8. US: Fuels: Renewable Fuel Standard. http://www.epa.gov/otaq/fuels/renewablefuels/regulations.htm Accessed 05/23/2014.

9. Pu, Y.; Hu, F.; Huang, F.; Davison, B. H.; Ragauskas, A. J., Assessing the molecular structure basis for biomass recalcitrance during dilute acid and hydrothermal pretreatments. *Biotechnology for biofuels* **2013,** *6* (1), 15-25.

10. Wyman, C. E.; Dale, B. E.; Elander, R. T.; Holtzapple, M.; Ladisch, M. R.; Lee, Y. Y., Coordinated development of leading biomass pretreatment technologies. *Bioresource Technology* **2005,** *96* (18), 1959-1966.

11. Sannigrahi, P.; Ragauskas, A. J.; Miller, S. J., Effects of Two-Stage Dilute Acid Pretreatment on the Structure and Composition of Lignin and Cellulose in Loblolly Pine. *Bioenergy Research* **2008,** *1* (3-4), 205-214.
12. Jung, S.; Foston, M.; Sullards, M. C.; Ragauskas, A. J., Surface Characterization of Dilute Acid Pretreated Populus deltoides by ToF-SIMS. *Energy & Fuels* **2010,** *24*, 1347-1357.
13. Mao, J. D.; Holtman, K. M.; Franqui-Villanueva, D., Chemical Structures of Corn Stover and Its Residue after Dilute Acid Prehydrolysis and Enzymatic Hydrolysis: Insight into Factors Limiting Enzymatic Hydrolysis. *Journal of Agricultural and Food Chemistry* **2010,** *58* (22), 11680-11687.
14. Pingali, S. V.; Urban, V. S.; Heller, W. T.; McGaughey, J.; O'Neill, H.; Foston, M.; Myles, D. A.; Ragauskas, A.; Evans, B. R., Breakdown of Cell Wall Nanostructure in Dilute Acid Pretreated Biomass. *Biomacromolecules* **2010,** *11* (9), 2329-2335.
15. Li, J. B.; Henriksson, G.; Gellerstedt, G., Carbohydrate reactions during high-temperature steam treatment of aspen wood. *Applied Biochemistry and Biotechnology* **2005,** *125* (3), 175-188.
16. Li, J. B.; Henriksson, G.; Gellerstedt, G., Lignin depolymerization/repolymerization and its critical role for delignification of aspen wood by steam explosion. *Bioresource Technology* **2007,** *98* (16), 3061-3068.
17. Historic U.S. fuel Ethanol Production. http://ethanolrfa.org/pages/statistics#A Accessed 05/23/2014.
18. Cheng, H.; Wang, L., Lignocelluloses Feedstock Biorefinery as Petrorefinery Substitutes. **2013**.
19. Kumar, P.; Barrett, D. M.; Delwiche, M. J.; Stroeve, P., Methods for Pretreatment of Lignocellulosic Biomass for Efficient Hydrolysis and Biofuel Production. *Industrial & Engineering Chemistry Research* **2009,** *48* (8), 3713-3729.
20. Saha, B. C., Hemicellulose bioconversion. *J Ind Microbiol Biot* **2003,** *30* (5), 279-291.
21. Sannigrahi, P.; Ragauskas, A. J.; Tuskan, G. A., Poplar as a feedstock for biofuels: A review of compositional characteristics. *Biofuel Bioprod Bior* **2010,** *4* (2), 209-226.

22. Hodgson, E. M.; Nowakowski, D. J.; Shield, I.; Riche, A.; Bridgwater, A. V.; Clifton-Brown, J. C.; Donnisona, I. S., Variation in Miscanthus chemical composition and implications for conversion by pyrolysis and thermo-chemical bio-refining for fuels and chemicals. *Bioresource Technology* **2011,** *102* (3), 3411-3418.
23. Silva, G. G. D.; Guilbert, S.; Rouau, X., Successive centrifugal grinding and sieving of wheat straw. *Powder Technol* **2011,** *208* (2), 266-270.
24. Sun, J. X.; Mao, F. C.; Sun, X. F.; Sun, R. C., Comparative study of hemicelluloses isolated with alkaline peroxide from lignocellulosic materials. *Journal of Wood Chemistry and Technology* **2004,** *24* (3), 239-262.
25. Silverstein, R. A.; Chen, Y.; Sharma-Shivappa, R. R.; Boyette, M. D.; Osborne, J., A comparison of chemical pretreatment methods for improving saccharification of cotton stalks. *Bioresource Technology* **2007,** *98* (16), 3000-3011.
26. Hallac, B. B.; Ragauskas, A. J., Analyzing cellulose degree of polymerization and its relevancy to cellulosic ethanol. *Biofuel Bioprod Bior* **2011,** *5* (2), 215-225.
27. Pu, Y. Q.; Zhang, D. C.; Singh, P. M.; Ragauskas, A. J., The new forestry biofuels sector. *Biofuel Bioprod Bior* **2008,** *2* (1), 58-73.
28. Nishiyama, Y.; Langan, P.; Chanzy, H., Crystal structure and hydrogen-bonding system in cellulose Ibeta from synchrotron X-ray and neutron fiber diffraction. *J Am Chem Soc* **2002,** *124* (31), 9074-9082.
29. Pu, Y.; Ziemer, C.; Ragauskas, A. J., CP/MAS 13C NMR analysis of cellulase treated bleached softwood kraft pulp. *Carbohydr Res* **2006,** *341* (5), 591-597.
30. Nishiyama, Y.; Sugiyama, J.; Chanzy, H.; Langan, P., Crystal structure and hydrogen bonding system in cellulose I(alpha) from synchrotron X-ray and neutron fiber diffraction. *J Am Chem Soc* **2003,** *125* (47), 14300-14306.
31. Larsson, P. T.; Hult, E. L.; Wickholm, K.; Pettersson, E.; Iversen, T., CP/MAS 13C-NMR spectroscopy applied to structure and interaction studies on cellulose I. *Solid state nuclear magnetic resonance* **1999,** *15* (1), 31-40.
32. Stephens, C. H.; Whitmore, P. M.; Morris, H. R.; Bier, M. E., Hydrolysis of the amorphous cellulose in cotton-based paper. *Biomacromolecules* **2008,** *9* (4), 1093-9.

33. Foston, M.; Hubbell, C. A.; Davis, M.; Ragauskas, A. J., Variations in Cellulosic Ultrastructure of Poplar. *Bioenergy Research* **2009,** *2* (4), 193-197.
34. Samuel, R.; Pu, Y.; Foston, M.; Ragauskas, A. J., Solid-state NMR characterization of switchgrass cellulose after dilute acid pretreatment. *Biofuels* **2009,** *1* (1), 85-90.
35. Nagy M. Biofuels from lignin and novel biodiesel analysis. Georgia Institute of Technology, Ph.D. thesis 2009.
36. Willfor, S.; Sundberg, A.; Hemming, J.; Holmbom, B., Polysaccharides in some industrially important softwood species. *Wood Science and Technology* **2005,** *39* (4), 245-258.
37. Willfor, S.; Sundberg, A.; Pranovich, A.; Holmbom, B., Polysaccharides in some industrially important hardwood species. *Wood Science and Technology* **2005,** *39* (8), 601-617.
38. Jacobs, A.; Dahlman, O., Characterization of the molar masses of hemicelluloses from wood and pulps employing size exclusion chromatography and matrix-assisted laser desorption ionization time-of-flight mass spectrometry. *Biomacromolecules* **2001,** *2* (3), 894-905.
39. Reddy, N. R.; Palmer, J. K.; Pierson, M. D.; Bothast, R. J., Wheat straw hemicelluloses - composition and fermentation by human-colon bacteroides. *Journal of Agricultural and Food Chemistry* **1983,** *31* (6), 1308-1313.
40. Davin, L. B.; Lewis, N. G., Lignin primary structures and dirigent sites. *Current opinion in biotechnology* **2005,** *16* (4), 407-415.
41. Chakar, F. S.; Ragauskas, A. J., Review of current and future softwood kraft lignin process chemistry. *Industrial Crops and Products* **2004,** *20* (2), 131-141.
42. Samuel, R.; Pu, Y.; Raman, B.; Ragauskas, A. J., Structural characterization and comparison of switchgrass ball-milled lignin before and after dilute acid pretreatment. *Appl Biochem Biotechnol* **2010,** *162* (1), 62-74.
43. Robinson, A. R.; Mansfield, S. D., Rapid analysis of poplar lignin monomer composition by a streamlined thioacidolysis procedure and near-infrared reflectance-based prediction modeling. *The Plant journal: for cell and molecular biology* **2009,** *58* (4), 706-714.

44. Cao, S.; Pu, Y.; Studer, M.; Wyman, C.; Ragauskas, A. J., Chemical transformations of Populus trichocarpa during dilute acid pretreatment. *RSC Advances* **2012,** *2* (29), 10925-10936.
45. El Hage, R.; Brosse, N.; Chrusciel, L.; Sanchez, C.; Sannigrahi, P.; Ragauskas, A., Characterization of milled wood lignin and ethanol organosolv lignin from miscanthus. *Polymer Degradation and Stability* **2009,** *94* (10), 1632-1638.
46. Fox, S. C.; McDonald, A. G., Chemical and thermal characterization of three industrial lignins and their corresponding lignin esters. *Bioresources* **2010,** *5* (2), 990-1009.
47. Buranov, A. U.; Mazza, G., Lignin in straw of herbaceous crops. *Industrial Crops and Products* **2008,** *28* (3), 237-259.
48. Ramires, E. C.; Megiatto, J. D., Jr.; Gardrat, C.; Castellan, A.; Frollini, E., Valorization of an industrial organosolv-sugarcane bagasse lignin: Characterization and use as a matrix in biobased composites reinforced with sisal fibers. *Biotechnol Bioeng* **2010,** *107* (4), 612-621.
49. Sjöström, E., Wood Chemistry: Fundamentals and Applications, Second Edition. Gulf Professional Publishing, **1993**.
50. Balakshin, M.; Capanema, E.; Gracz, H.; Chang, H. M.; Jameel, H., Quantification of lignin-carbohydrate linkages with high-resolution NMR spectroscopy. *Planta* **2011,** *233* (6), 1097-1110.
51. Azuma, J.; Takahashi, N.; Koshijima, T., Isolation and characterization of lignin-carbohydrate complexes from the milled-wood lignin fraction of pinus-densiflora sieb et zucc. *Carbohydrate Research* **1981,** *93* (1), 91-104.
52. Mukoyoshi, S. I.; Azuma, J. I.; Koshijima, T., Lignin-carbohydrate complexes from compression wood of pinus-densiflora sieb et zucc. *Holzforschung* **1981,** *35* (5), 233-240.
53. Azuma, J.-I.; Tetsuo, K., Lignin-Carbohydrate Complexes from Various Sources. In *Methods Enzymol.*, Willis A. Wood, S. T. K., Ed.^Eds. Academic Press: **1988**; Vol. Volume 161, pp 12-18.

54. Koshijima, T.; Watanabe, T.; Azuma, J., Existence of benzylated carbohydrate moiety in lignin carbohydrate complex from pine wood. *Chemistry Letters* **1984,** (10), 1737-1740.
55. Lawoko, M.; Henriksson, G.; Gellerstedt, G., Structural differences between the lignin-carbohydrate complexes present in wood and in chemical pulps. *Biomacromolecules* **2005,** *6* (6), 3467-3473.
56. Sticklen, M. B., Plant genetic engineering for biofuel production: towards affordable cellulosic ethanol (Retracted article. See vol 11, pg 308, 2010). *Nature Reviews Genetics* **2008,** *9* (6), 433-443.
57. Laureano-Perez, L.; Teymouri, F.; Alizadeh, H.; Dale, B. E., Understanding factors that limit enzymatic hydrolysis of biomass. *Applied Biochemistry and Biotechnology* **2005,** *121*, 1081-1099.
58. Balan, V.; Sousa Lda, C.; Chundawat, S. P.; Marshall, D.; Sharma, L. N.; Chambliss, C. K.; Dale, B. E., Enzymatic digestibility and pretreatment degradation products of AFEX-treated hardwoods (Populus nigra). *Biotechnol Prog* **2009,** *25* (2), 365-75.
59. Lynd, L. R.; Elander, R. T.; Wyman, C. E., Likely features and costs of mature biomass ethanol technology. *Applied Biochemistry and Biotechnology* **1996,** *57-8*, 741-761.
60. Mooney, C. A.; Mansfield, S. D.; Touhy, M. G.; Saddler, J. N., The effect of initial pore volume and lignin content on the enzymatic hydrolysis of softwoods. *Bioresource Technology* **1998,** *64* (2), 113-119.
61. Kristensen, J. B.; Borjesson, J.; Bruun, M. H.; Tjerneld, F.; Jorgensen, H., Use of surface active additives in enzymatic hydrolysis of wheat straw lignocellulose. *Enzyme and Microbial Technology* **2007,** *40* (4), 888-895.
62. Yang, B.; Wyman, C. E., BSA treatment to enhance enzymatic hydrolysis of cellulose in lignin containing substrates. *Biotechnology and Bioengineering* **2006,** *94* (4), 611-617.
63. Chundawat, S. P.; Beckham, G. T.; Himmel, M. E.; Dale, B. E., Deconstruction of lignocellulosic biomass to fuels and chemicals. *Annual review of chemical and biomolecular engineering* **2011,** *2*, 121-145.

64. Mosier, N.; Wyman, C.; Dale, B.; Elander, R.; Lee, Y. Y.; Holtzapple, M.; Ladisch, M., Features of promising technologies for pretreatment of lignocellulosic biomass. *Bioresour Technol* **2005,** *96* (6), 673-686.
65. Hendriks, A. T.; Zeeman, G., Pretreatments to enhance the digestibility of lignocellulosic biomass. *Bioresour Technol* **2009,** *100* (1), 10-18.
66. Meng, X.; Foston, M.; Leisen, J.; DeMartini, J.; Wyman, C. E.; Ragauskas, A. J., Determination of porosity of lignocellulosic biomass before and after pretreatment by using Simons' stain and NMR techniques. *Bioresour Technol* **2013,** *144*, 467-476.
67. Zeng, M.; Mosier, N. S.; Huang, C. P.; Sherman, D. M.; Ladisch, M. R., Microscopic examination of changes of plant cell structure in corn stover due to hot water pretreatment and enzymatic hydrolysis. *Biotechnol Bioeng* **2007,** *97* (2), 265-278.
68. Park, S.; Baker, J. O.; Himmel, M. E.; Parilla, P. A.; Johnson, D. K., Cellulose crystallinity index: measurement techniques and their impact on interpreting cellulase performance. *Biotechnology for biofuels* **2010,** *3*, 10-20.
69. Larsson, P. T.; Westermark, U.; Iversen, T., Determination of the cellulose I alpha allomorph content in a tunicate cellulose by CP/MAS C-13-NMR spectroscopy. *Carbohydrate Research* **1995,** *278* (2), 339-343.
70. Hallac, B. B.; Sannigrahi, P.; Pu, Y.; Ray, M.; Murphy, R. J.; Ragauskas, A. J., Biomass characterization of Buddleja davidii: a potential feedstock for biofuel production. *J Agric Food Chem* **2009,** *57* (4), 1275-1281.
71. Zhang, Y. H.; Lynd, L. R., Toward an aggregated understanding of enzymatic hydrolysis of cellulose: noncomplexed cellulase systems. *Biotechnol Bioeng* **2004,** *88* (7), 797-824.
72. Sannigrahi, P.; Miller, S. J.; Ragauskas, A. J., Effects of organosolv pretreatment and enzymatic hydrolysis on cellulose structure and crystallinity in Loblolly pine. *Carbohydr Res* **2010,** *345* (7), 965-970.
73. Zhu, L.; O'Dwyer, J. P.; Chang, V. S.; Granda, C. B.; Holtzapple, M. T., Structural features affecting biomass enzymatic digestibility. *Bioresour Technol* **2008,** *99* (9), 3817-3828.

74. Yoshida, M.; Liu, Y.; Uchida, S.; Kawarada, K.; Ukagami, Y.; Ichinose, H.; Kaneko, S.; Fukuda, K., Effects of cellulose crystallinity, hemicellulose, and lignin on the enzymatic hydrolysis of Miscanthus sinensis to monosaccharides. *Bioscience Biotechnology and Biochemistry* **2008,** *72* (3), 805-810.
75. Mittal, A.; Katahira, R.; Himmel, M. E.; Johnson, D. K., Effects of alkaline or liquid-ammonia treatment on crystalline cellulose: changes in crystalline structure and effects on enzymatic digestibility. *Biotechnology for biofuels* **2011,** *4*, 41-56.
76. Ioelovich, M.; Morag, E., Effect of cellulose structure on enzymatic hydrolysis. *Bioresources* **2011,** *6* (3), 2818-2835.
77. Pu, Y.; Ziemer, C.; Ragauskas, A. J., CP/MAS 13C NMR analysis of cellulase treated bleached softwood kraft pulp. *Carbohydr Res* **2006,** *341* (5), 591-597.
78. Puri, V. P., Effect of crystallinity and degree of polymerization of cellulose on enzymatic saccharification. *Biotechnology and Bioengineering* **1984,** *26* (10), 1219-1222.
79. Grethlein, H. E., The effect of pore-size distribution on the rate of enzymatic-hydrolysis of cellulosic substrates. *Bio-Technology* **1985,** *3* (2), 155-160.
80. Thompson, D. N.; Chen, H. C.; Grethlein, H. E., Comparison of pretreatment methods on the basis of available surface-area. *Bioresource Technology* **1992,** *39* (2), 155-163.
81. Cateto, C.; Hu, G.; Ragauskas, A., Enzymatic hydrolysis of organosolv Kanlow switchgrass and its impact on cellulose crystallinity and degree of polymerization. *Energy & Environmental Science* **2011,** *4* (4), 1516-1521.
82. Weimer, P. J.; French, A. D.; Calamari, T. A., Differential fermentation of cellulose allomorphs by ruminal cellulolytic bacteria. *Applied and Environmental Microbiology* **1991,** *57* (11), 3101-3106.
83. Ding, S. Y.; Himmel, M. E., The maize primary cell wall microfibril: A new model derived from direct visualization. *Journal of Agricultural and Food Chemistry* **2006,** *54* (3), 597-606.
84. Chundawat, S. P.; Bellesia, G.; Uppugundla, N.; da Costa Sousa, L.; Gao, D.; Cheh, A. M.; Agarwal, U. P.; Bianchetti, C. M.; Phillips, G. N., Jr.; Langan, P.; Balan, V.; Gnanakaran, S.; Dale, B. E., Restructuring the crystalline cellulose hydrogen bond

network enhances its depolymerization rate. *J Am Chem Soc* **2011,** *133* (29), 11163-11174.
85. Hall, M.; Bansal, P.; Lee, J. H.; Realff, M. J.; Bommarius, A. S., Cellulose crystallinity--a key predictor of the enzymatic hydrolysis rate. *The FEBS journal* **2010,** *277* (6), 1571-1582.
86. Klyosov, A. A.; Mitkevich, O. V.; Sinitsyn, A. P., Role of the activity and adsorption of cellulases in the efficiency of the enzymatic-hydrolysis of amorphous and crystalline cellulose. *Biochemistry* **1986,** *25* (3), 540-542.
87. Hong, J.; Ye, X. H.; Zhang, Y. H. P., Quantitative determination of cellulose accessibility to cellulase based on adsorption of a nonhydrolytic fusion protein containing CBM and GFP with its applications. *Langmuir* **2007,** *23* (25), 12535-12540.
88. Valjamae, P.; Sild, V.; Pettersson, G.; Johansson, G., The initial kinetics of hydrolysis by cellobiohydrolases I and II is consistent with a cellulose surface - erosion model. *European Journal of Biochemistry* **1998,** *253* (2), 469-475.
89. Pan, X.; Xie, D.; Kang, K. Y.; Yoon, S. L.; Saddler, J. N., Effect of organosolv ethanol pretreatment variables on physical characteristics of hybrid poplar substrates. *Applied Biochemistry and Biotechnology* **2007,** *137*, 367-377.
90. Pan, X. J.; Xie, D.; Yu, R. W.; Saddler, J. N., The bioconversion of mountain pine beetle-killed lodgepole pine to fuel ethanol using the organosolv process. *Biotechnology and Bioengineering* **2008,** *101* (1), 39-48.
91. Hallac, B. B.; Sannigrahi, P.; Pu, Y. Q.; Ray, M.; Murphy, R. J.; Ragauskas, A. J., Effect of Ethanol Organosolv Pretreatment on Enzymatic Hydrolysis of Buddleja davidii Stem Biomass. *Industrial & Engineering Chemistry Research* **2010,** *49* (4), 1467-1472.
92. Sinitsyn, A.P.; Gusakov, A.V.; Vlasenko, E.Y., Effect of structural and physico-chemical features of cellulosic substrates on the efficiency of enzymatic hydrolysis. Appl. Biochem. Biotechnol. **1991,** *30*, 43–59.
93. Zhang, Y. H. P.; Lynd, L. R., A functionally based model for hydrolysis of cellulose by fungal cellulase. *Biotechnology and Bioengineering* **2006,** *94* (5), 888-898.

94. Galbe, M.; Zacchi, G., Pretreatment of lignocellulosic materials for efficient bioethanol production. *Advances in biochemical engineering/biotechnology* **2007,** *108,* 41-65.
95. Sanchez, C., Lignocellulosic residues: biodegradation and bioconversion by fungi. *Biotechnology advances* **2009,** *27* (2), 185-194.
96. Ramos, L. P., The chemistry involved in the steam treatment of lignocellulosic materials. *Quim Nova* **2003,** *26* (6), 863-871.
97. Sun, Y.; Cheng, J. Y., Hydrolysis of lignocellulosic materials for ethanol production: a review. *Bioresource Technology* **2002,** *83* (1), 1-11.
98. Um, B. H.; Karim, M.; Henk, L., Effect of sulfuric and phosphoric acid pretreatments on enzymatic hydrolysis of corn stover. *Appl Biochem Biotechnol* **2003,** *105 -108,* 115-125.
99. Jensen, J. R.; Morinelly, J. E.; Gossen, K. R.; Brodeur-Campbell, M. J.; Shonnard, D. R., Effects of dilute acid pretreatment conditions on enzymatic hydrolysis monomer and oligomer sugar yields for aspen, balsam, and switchgrass. *Bioresour Technol* **2010,** *101* (7), 2317-2325.
100. Tian, S.; Zhu, W.; Gleisner, R.; Pan, X. J.; Zhu, J. Y., Comparisons of SPORL and dilute acid pretreatments for sugar and ethanol productions from aspen. *Biotechnol Prog* **2011,** *27* (2), 419-427.
101. Wyman, C. E.; Balan, V.; Dale, B. E.; Elander, R. T.; Falls, M.; Hames, B.; Holtzapple, M. T.; Ladisch, M. R.; Lee, Y. Y.; Mosier, N.; Pallapolu, V. R.; Shi, J.; Thomas, S. R.; Warner, R. E., Comparative data on effects of leading pretreatments and enzyme loadings and formulations on sugar yields from different switchgrass sources. *Bioresour Technol* **2011,** *102* (24), 11052-11062.
102. Zhang, J.; Ma, X.; Yu, J.; Zhang, X.; Tan, T., The effects of four different pretreatments on enzymatic hydrolysis of sweet sorghum bagasse. *Bioresour Technol* **2011,** *102* (6), 4585-4589.
103. Shi, J.; Pu, Y.; Yang, B.; Ragauskas, A.; Wyman, C. E., Comparison of microwaves to fluidized sand baths for heating tubular reactors for hydrothermal and dilute acid batch pretreatment of corn stover. *Bioresour Technol* **2011,** *102* (10), 5952-5961.

104. Ucar, G., Pretreatment of poplar by acid and alkali for enzymatic-hydrolysis. *Wood Science and Technology* **1990,** *24* (2), 171-180.
105. Zhu, Y. M.; Lee, Y. Y.; Elander, R. T., Optimization of dilute-acid pretreatment of corn stover using a high-solids percolation reactor. *Applied Biochemistry and Biotechnology* **2005,** *121*, 1045-1054.
106. Lee, Y. Y.; Wu, Z. W.; Torget, R. W., Modeling of countercurrent shrinking-bed reactor in dilute-acid total-hydrolysis of lignocellulosic biomass. *Bioresource Technology* **2000,** *71* (1), 29-39.
107. Taherzadeh, M. J.; Karimi, K., Enzyme-based hydrolysis processes for ethanol from lignocellulosic materials: a review. *Bioresources* **2007,** *2* (4), 707-738.
108. Chen, R. F.; Wu, Z. W.; Lee, Y. Y., Shrinking-bed model for percolation process applied to dilute-acid pretreatment hydrolysis of cellulosic biomass. *Applied Biochemistry and Biotechnology* **1998,** *70-2*, 37-49.
109. Sannigrahi, P.; Kim, D. H.; Jung, S.; Ragauskas, A., Pseudo-lignin and pretreatment chemistry. *Energy & Environmental Science* **2011,** *4* (4), 1306-1310.
110. Chum, H. L.; Johnson, D. K.; Black, S.; Baker, J.; Grohmann, K.; Sarkanen, K. V.; Wallace, K.; Schroeder, H. A., Organosolv pretreatment for enzymatic hydrolysis of poplars: I. Enzyme hydrolysis of cellulosic residues. *Biotechnol Bioeng* **1988,** *31* (7), 643-649.
111. Martinez, J. M.; Reguant, J.; Montero, M. A.; Montane, D.; Salvado, J.; Farriol, X., Hydrolytic pretreatment of softwood and almond shells. Degree of polymerization and enzymatic digestibility of the cellulose fraction. *Industrial & Engineering Chemistry Research* **1997,** *36* (3), 688-696.
112. Lloyd, T.; Wyman, C. E., Application of a depolymerization model for predicting thermochemical hydrolysis of hemicellulose. *Appl Biochem Biotechnol* **2003,** *105 -108*, 53-67.
113. Kabel, M. A.; Bos, G.; Zeevalking, J.; Voragen, A. G.; Schols, H. A., Effect of pretreatment severity on xylan solubility and enzymatic breakdown of the remaining cellulose from wheat straw. *Bioresour Technol* **2007,** *98* (10), 2034-2042.

114. Sun, Y.; Cheng, J. J., Dilute acid pretreatment of rye straw and bermudagrass for ethanol production. *Bioresour Technol* **2005,** *96* (14), 1599-606.
115. Schell, D. J.; Farmer, J.; Newman, M.; McMillan, J. D., Dilute-sulfuric acid pretreatment of corn stover in pilot-scale reactor: investigation of yields, kinetics, and enzymatic digestibilities of solids. *Appl Biochem Biotechnol* **2003,** *105 -108*, 69-85.
116. Hsu, T. C.; Guo, G. L.; Chen, W. H.; Hwang, W. S., Effect of dilute acid pretreatment of rice straw on structural properties and enzymatic hydrolysis. *Bioresour Technol* **2010,** *101* (13), 4907-4913.
117. Adel, A. M.; Abd El-Wahab, Z. H.; Ibrahim, A. A.; Al-Shemy, M. T., Characterization of microcrystalline cellulose prepared from lignocellulosic materials. Part I. Acid catalyzed hydrolysis. *Bioresour Technol* **2010,** *101* (12), 4446-4455.
118. Foston M and Ragauskas AJ (2010) Changes in lignocellulosic supramolecular and ultrastructure during dilute acid pretreatment of Populus and switchgrass. Biomass and Bioenergy 34:1885-1895
119. Kumar, R.; Mago, G.; Balan, V.; Wyman, C. E., Physical and chemical characterizations of corn stover and poplar solids resulting from leading pretreatment technologies. *Bioresour Technol* **2009,** *100* (17), 3948-3962.
120. Lloyd, T. A.; Wyman, C. E., Combined sugar yields for dilute sulfuric acid pretreatment of corn stover followed by enzymatic hydrolysis of the remaining solids. *Bioresour Technol* **2005,** *96* (18), 1967-1977.
121. Castro, E.; Diaz, M. J.; Cara, C.; Ruiz, E.; Romero, I.; Moya, M., Dilute acid pretreatment of rapeseed straw for fermentable sugar generation. *Bioresour Technol* **2011,** *102* (2), 1270-1276.
122. Stephens, C. H.; Whitmore, P. M.; Morris, H. R.; Bier, M. E., Hydrolysis of the amorphous cellulose in cotton-based paper. *Biomacromolecules* **2008,** *9* (4), 1093-1099.
123. Emsley, A. M.; Heywood, R. J.; Ali, M.; Eley, C. M., On the kinetics of degradation of cellulose. *Cellulose* **1997,** *4* (1), 1-5.
124. Zhao, X. B.; Wang, L.; Liu, D. H., Peracetic acid pretreatment of sugarcane bagasse for enzymatic hydrolysis: a continued work. *Journal of Chemical Technology and Biotechnology* **2008,** *83* (6), 950-956.

125. Debzi, E. M.; Chanzy, H.; Sugiyama, J.; Tekely, P.; Excoffier, G., The I-alpha- I-beta transformation of highly crystalline cellulose by annealing in various media. *Macromolecules* **1991,** *24* (26), 6816-6822.
126. Lindgren, T.; Edlund, U.; Iversen, T., A multivariate characterization of crystal transformations of cellulose. *Cellulose* **1995,** *2* (4), 273-288.
127. Osullivan, A. C., Cellulose: the structure slowly unravels. *Cellulose* **1997,** *4* (3), 173-207.
128. Hakansson, H.; Ahlgren, P.; Germgard, U., The degree of disorder in hardwood kraft pulps studied by means of LODP. *Cellulose* **2005,** *12* (3), 327-335.
129. Liu, C. G.; Wyman, C. E., The effect of flow rate of very dilute sulfuric acid on xylan, lignin, and total mass removal from corn stover. *Industrial & Engineering Chemistry Research* **2004,** *43* (11), 2781-2788.
130. Alvira, P.; Tomas-Pejo, E.; Ballesteros, M.; Negro, M. J., Pretreatment technologies for an efficient bioethanol production process based on enzymatic hydrolysis: A review. *Bioresour Technol* **2010,** *101* (13), 4851-4861.
131. VanWalsum, G. P.; Allen, S. G.; Spencer, M. J.; Laser, M. S.; Antal, M. J.; Lynd, L. R., Conversion of lignocellulosics pretreated with liquid hot water to ethanol. *Applied Biochemistry and Biotechnology* **1996,** *57-8*, 157-170.
132. Perez, J. A.; Gonzalez, A.; Oliva, J. M.; Ballesteros, I.; Manzanares, P., Effect of process variables on liquid hot water pretreatment of wheat straw for bioconversion to fuel-ethanol in a batch reactor. *Journal of Chemical Technology and Biotechnology* **2007,** *82* (10), 929-938.
133. Perez, J. A.; Ballesteros, I.; Ballesteros, M.; Saez, F.; Negro, M. J.; Manzanares, P., Optimizing Liquid Hot Water pretreatment conditions to enhance sugar recovery from wheat straw for fuel-ethanol production. *Fuel* **2008,** *87* (17-18), 3640-3647.
134. Hu, Z. J.; Ragauskas, A. J., Hydrothermal Pretreatment of Switchgrass. *Industrial & Engineering Chemistry Research* **2011,** *50* (8), 4225-4230.
135. Allen, S. G.; Schulman, D.; Lichwa, J.; Antal, M. J.; Laser, M.; Lynd, L. R., A comparison between hot liquid water and steam fractionation of corn fiber. *Industrial & Engineering Chemistry Research* **2001,** *40* (13), 2934-2941.

136. Laser, M.; Schulman, D.; Allen, S. G.; Lichwa, J.; Antal, M. J.; Lynd, L. R., A comparison of liquid hot water and steam pretreatments of sugar cane bagasse for bioconversion to ethanol. *Bioresource Technology* **2002,** *81* (1), 33-44.
137. Garrote, G.; Kabel, M. A.; Schols, H. A.; Falque, E.; Dominguez, H.; Parajo, J. C., Effects of Eucalyptus globulus wood autohydrolysis conditions on the reaction products. *J Agric Food Chem* **2007,** *55* (22), 9006-9013.
138. Vegas, R.; Kabel, M.; Schols, H. A.; Alonso, J. L.; Parajo, J. C., Hydrothermal processing of rice husks: effects of severity on product distribution. *Journal of Chemical Technology and Biotechnology* **2008,** *83* (7), 965-972.
139. Liu, C. G.; Wyman, C. E., The effect of flow rate of compressed hot water on xylan, lignin, and total mass removal from corn stover. *Industrial & Engineering Chemistry Research* **2003,** *42* (21), 5409-5416.
140. Liu, C. G.; Wyman, C. E., Partial flow of compressed-hot water through corn stover to enhance hemicellulose sugar recovery and enzymatic digestibility of cellulose. *Bioresource Technology* **2005,** *96* (18), 1978-1985.
141. Kim, Y.; Hendrickson, R.; Mosier, N.; Ladisch, M. R., Plug-flow reactor for continuous hydrolysis of glucans and xylans from pretreated corn fiber. *Energy & Fuels* **2005,** *19* (5), 2189-2200.
142. Gray, M. C.; Converse, A. O.; Wyman, C. E., Solubilities of oligomer mixtures produced by the hydrolysis of xylans and corn stover in water at 180 degrees C. *Industrial & Engineering Chemistry Research* **2007,** *46* (8), 2383-2391.
143. Yang, B.; Wyman, C. E., Characterization of the degree of polymerization of xylooligomers produced by flowthrough hydrolysis of pure xylan and corn stover with water. *Bioresource Technology* **2008,** *99* (13), 5756-5762.
144. Jacobsen, S. E.; Wyman, C. E., Xylose monomer and oligomer yields for uncatalyzed hydrolysis of sugarcane bagasse hemicellulose at varying solids concentration. *Industrial & Engineering Chemistry Research* **2002,** *41* (6), 1454-1461.
145. Bobleter, O., Hydrothermal degradation of polymers derived from plants. *Progress in Polymer Science* **1994,** *19* (5), 797-841.

146. Ando, H.; Sakaki, T.; Kokusho, T.; Shibata, M.; Uemura, Y.; Hatate, Y., Decomposition behavior of plant biomass in hot-compressed water. *Industrial & Engineering Chemistry Research* **2000,** *39* (10), 3688-3693.
147. Yu Y and Wu HW (2010) Significant Differences in the Hydrolysis Behavior of Amorphous and Crystalline Portions within Microcrystalline Cellulose in Hot-Compressed Water. Industrial & Engineering Chemistry Research 49:3902-3909
148. Xiao, L. P.; Sun, Z. J.; Shi, Z. J.; Xu, F.; Sun, R. C., Impact of hot compressed water pretreatment on the structural changes of woody biomass for bioethanol production. *Bioresources* **2011,** *6* (2), 1576-1598.
149. Weil, J.; Brewer, M.; Hendrickson, R.; Sarikaya, A.; Ladisch, M. R., Continuous pH monitoring during pretreatment of yellow poplar wood sawdust by pressure cooking in water. *Applied Biochemistry and Biotechnology* **1998,** *70-2*, 99-111.
150. Kim, T. H.; Kim, J. S.; Sunwoo, C.; Lee, Y. Y., Pretreatment of corn stover by aqueous ammonia. *Bioresour Technol* **2003,** *90* (1), 39-47.
151. Chundawat, S. P.; Vismeh, R.; Sharma, L. N.; Humpula, J. F.; da Costa Sousa, L.; Chambliss, C. K.; Jones, A. D.; Balan, V.; Dale, B. E., Multifaceted characterization of cell wall decomposition products formed during ammonia fiber expansion (AFEX) and dilute acid based pretreatments. *Bioresour Technol* **2010,** *101* (21), 8429-8438.
152. Taherzadeh, M. J.; Karimi, K., Pretreatment of lignocellulosic wastes to improve ethanol and biogas production: a review. *International journal of molecular sciences* **2008,** *9* (9), 1621-1651.
153. Alizadeh, H.; Teymouri, F.; Gilbert, T. I.; Dale, B. E., Pretreatment of switchgrass by ammonia fiber explosion (AFEX). *Appl Biochem Biotechnol* **2005,** *121-124*, 1133-1141.
154. Lee, J. M.; Jameel, H.; Venditti, R. A., A comparison of the autohydrolysis and ammonia fiber explosion (AFEX) pretreatments on the subsequent enzymatic hydrolysis of coastal Bermuda grass. *Bioresour Technol* **2010,** *101* (14), 5449-5458.
155. Teymouri F, Laureano-Perez L, Alizadeh H and Dale BE (2005) Optimization of the ammonia fiber explosion (AFEX) treatment parameters for enzymatic hydrolysis of corn stover. Bioresour Technol 96:2014-2018.

156. Balan, V.; Sousa Lda, C.; Chundawat, S. P.; Marshall, D.; Sharma, L. N.; Chambliss, C. K.; Dale, B. E., Enzymatic digestibility and pretreatment degradation products of AFEX-treated hardwoods (Populus nigra). *Biotechnol Prog* **2009,** *25* (2), 365-375.
157. Wyman, C. E.; Dale, B. E.; Elander, R. T.; Holtzapple, M.; Ladisch, M. R.; Lee, Y. Y., Comparative sugar recovery data from laboratory scale application of leading pretreatment technologies to corn stover. *Bioresour Technol* **2005,** *96* (18), 2026-2032.
158. Donohoe, B. S.; Decker, S. R.; Tucker, M. P.; Himmel, M. E.; Vinzant, T. B., Visualizing lignin coalescence and migration through maize cell walls following thermochemical pretreatment. *Biotechnol Bioeng* **2008,** *101* (5), 913-925.
159. Kristensen, J. B.; Thygesen, L. G.; Felby, C.; Jorgensen, H.; Elder, T., Cell-wall structural changes in wheat straw pretreated for bioethanol production. *Biotechnology for biofuels* **2008,** *1* (1), 5-21.
160. Chundawat, S. P. S.; Donohoe, B. S.; Sousa, L. D.; Elder, T.; Agarwal, U. P.; Lu, F. C.; Ralph, J.; Himmel, M. E.; Balan, V.; Dale, B. E., Multi-scale visualization and characterization of lignocellulosic plant cell wall deconstruction during thermochemical pretreatment. *Energy & Environmental Science* **2011,** *4* (3), 973-984.
161. Pingali, S. V.; Urban, V. S.; Heller, W. T.; McGaughey, J.; O'Neill, H.; Foston, M.; Myles, D. A.; Ragauskas, A.; Evans, B. R., Breakdown of cell wall nanostructure in dilute acid pretreated biomass. *Biomacromolecules* **2010,** *11* (9), 2329-2335.
162. Laureano-Perez, L.; Teymouri, F.; Alizadeh, H.; Dale, B. E., Understanding factors that limit enzymatic hydrolysis of biomass: characterization of pretreated corn stover. *Appl Biochem Biotechnol* **2005,** *121-124*, 1081-1099.
163. Gollapalli, L. E.; Dale, B. E.; Rivers, D. M., Predicting digestibility of ammonia fiber explosion (AFEX)-treated rice straw. *Appl Biochem Biotechnol* **2002,** *98-100*, 23-35.
164. Pingali, S. V.; Urban, V. S.; Heller, W. T.; McGaughey, J.; O'Neill, H.; Foston, M.; Myles, D. A.; Ragauskas, A.; Evans, B. R., Breakdown of cell wall nanostructure in dilute acid pretreated biomass. *Biomacromolecules* **2010,** *11* (9), 2329-2335.

165. Hansen, M. A.; Kristensen, J. B.; Felby, C.; Jorgensen, H., Pretreatment and enzymatic hydrolysis of wheat straw (Triticum aestivum L.)--the impact of lignin relocation and plant tissues on enzymatic accessibility. *Bioresour Technol* **2011,** *102* (3), 2804-2811.
166. Zhuang, X.; Yu, Q.; Wang, W.; Qi, W.; Wang, Q.; Tan, X.; Yuan, Z., Decomposition behavior of hemicellulose and lignin in the step-change flow rate liquid hot water. *Appl Biochem Biotechnol* **2012,** *168* (1), 206-218.
167. Holopainen-Mantila, U.; Marjamaa, K.; Merali, Z.; Kasper, A.; de Bot, P.; Jaaskelainen, A. S.; Waldron, K.; Kruus, K.; Tamminen, T., Impact of hydrothermal pre-treatment to chemical composition, enzymatic digestibility and spatial distribution of cell wall polymers. *Bioresour Technol* **2013,** *138*, 156-162.
168. Lima, M. A.; Lavorente, G. B.; da Silva, H. K.; Bragatto, J.; Rezende, C. A.; Bernardinelli, O. D.; Deazevedo, E. R.; Gomez, L. D.; McQueen-Mason, S. J.; Labate, C. A.; Polikarpov, I., Effects of pretreatment on morphology, chemical composition and enzymatic digestibility of eucalyptus bark: a potentially valuable source of fermentable sugars for biofuel production - part 1. *Biotechnology for biofuels* **2013,** *6* (1), 75-82.
169. Nitsos, C. K.; Matis, K. A.; Triantafyllidis, K. S., Optimization of hydrothermal pretreatment of lignocellulosic biomass in the bioethanol production process. *ChemSusChem* **2013,** *6* (1), 110-122.
170. Coletta, V. C.; Rezende, C. A.; da Conceicao, F. R.; Polikarpov, I.; Guimaraes, F. E., Mapping the lignin distribution in pretreated sugarcane bagasse by confocal and fluorescence lifetime imaging microscopy. *Biotechnology for biofuels* **2013,** *6* (1), 43-51.
171. Zhang, M.; Chen, G.; Kumar, R.; Xu, B., Mapping out the structural changes of natural and pretreated plant cell wall surfaces by atomic force microscopy single molecular recognition imaging. *Biotechnology for biofuels* **2013,** *6* (1), 147-157.
172. Hu, F.; Jung, S.; Ragauskas, A., Pseudo-lignin formation and its impact on enzymatic hydrolysis. *Bioresour Technol* **2012,** *117*, 7-12.
173. Studer, M. H.; DeMartini, J. D.; Davis, M. F.; Sykes, R. W.; Davison, B.; Keller, M.; Tuskan, G. A.; Wyman, C. E., Lignin content in natural Populus variants affects

sugar release. *Proceedings of the National Academy of Sciences of the United States of America* **2011,** *108* (15), 6300-6305.
174. Cao, S.; Pu, Y.; Studer, M.; Wyman, C.; Ragauskas, A. J., Chemical transformations of Populus trichocarpa during dilute acid pretreatment. *Rsc Advances* **2012,** *2* (29), 10925-10936.
175. Smith, P. K.; Krohn, R. I.; Hermanson, G. T.; Mallia, A. K.; Gartner, F. H.; Provenzano, M. D.; Fujimoto, E. K.; Goeke, N. M.; Olson, B. J.; Klenk, D. C., Measurement of protein using bicinchoninic acid. *Analytical biochemistry* **1985,** *150* (1), 76-85.
176. Alvira, P.; Negro, M. J.; Ballesteros, M., Effect of endoxylanase and alpha-L-arabinofuranosidase supplementation on the enzymatic hydrolysis of steam exploded wheat straw. *Bioresour Technol* **2011,** *102* (6), 4552-4558.
177. Palonen, H.; Tenkanen, M.; Linder, M., Dynamic interaction of Trichoderma reesei cellobiohydrolases Cel6A and Cel7A and cellulose at equilibrium and during hydrolysis. *Appl Environ Microbiol* **1999,** *65* (12), 5229-5233.
178. Hubbell, C. A.; Ragauskas, A. J., Effect of acid-chlorite delignification on cellulose degree of polymerization. *Bioresour Technol* **2010,** *101* (19), 7410-7415.
179. Froass, P. M.; Ragauskas, A. J.; Jiang, J., Nuclear magnetic resonance studies. 4. Analysis of residual lignin after kraft pulping. *Industrial & Engineering Chemistry Research* **1998,** *37* (8), 3388-3394.
180. Ghose, T. K., Measurement of cellulase activities. *Pure and Applied Chemistry* **1987,** *59* (2), 257-268.
181. Fulmer, G. R.; Miller, A. J. M.; Sherden, N. H.; Gottlieb, H. E.; Nudelman, A.; Stoltz, B. M.; Bercaw, J. E.; Goldberg, K. I., NMR Chemical Shifts of Trace Impurities: Common Laboratory Solvents, Organics, and Gases in Deuterated Solvents Relevant to the Organometallic Chemist. *Organometallics* **2010,** *29* (9), 2176-2179.
182. Jakobsons, J.; Hortling, B.; Erins, P.; Sundquist, J., Characterization of Alkali-Soluble Fraction of Steam Exploded Birch Wood. *Holzforschung* **1995,** *49* (1), 51-59.

183. Negro, M. J.; Manzanares, P.; Oliva, J. M.; Ballesteros, I.; Ballesteros, M., Changes in various physical/chemical parameters of Pinus pinaster wood after steam explosion pretreatment. *Biomass & Bioenergy* **2003,** *25* (3), 301-308.
184. Nguyen, Q. A.; Tucker, M. P.; Keller, F. A.; Eddy, F. P., Two-stage dilute-acid pretreatment of softwoods. *Applied Biochemistry and Biotechnology* **2000,** *84-6*, 561-576.
185. Sievers, C.; Marzialetti, T.; Hoskins, T. J. C.; Olarte, M. B. V.; Agrawal, P. K.; Jones, C. W., Quantitative solid state NMR analysis of residues from acid hydrolysis of loblolly pine wood. *Bioresource Technology* **2009,** *100* (20), 4758-4765.
186. Kim, J. Y.; Shin, E. J.; Eom, I. Y.; Won, K.; Kim, Y. H.; Choi, D.; Choi, I. G.; Choi, J. W., Structural features of lignin macromolecules extracted with ionic liquid from poplar wood. *Bioresour Technol* **2011,** *102* (19), 9020-9025.
187. Pavia, D.L., Lampman, G.M., Kriz, G.S., Vyvyan, J.R., 2009. Introduction to spectroscopy, fourth ed. Brooks-Cole, New York.
188. Teleman, A.; Lundqvist, J.; Tjerneld, F.; Stalbrand, H.; Dahlman, O., Characterization of acetylated 4-O-methylglucuronoxylan isolated from aspen employing 1H and 13C NMR spectroscopy. *Carbohydr Res* **2000,** *329* (4), 807-815.
189. Luijkx, G. C. A.; Vanrantwijk, F.; Vanbekkum, H., Hydrothermal formation of 1,2,4-benzenetriol from 5-hydroxymethyl-2-furaldehyde and d-fructose. *Carbohydrate Research* **1993,** *242*, 131-139.
190. Popoff, T.; Theander, O., Formation of aromatic-compounds from carbohydrates .1. Reaction of d-glucuronic acid, d-galacturonic acid, d-xylose, and l-arabinose in slightly acidic, aqueous-solution. *Carbohydrate Research* **1972,** *22* (1), 135-140.
191. Yamamoto, K.; Asada, T.; Nishide, H.; Tsuchida, E., The preparation of poly(dihydroxyphenylene) through the electro-oxidative polymerization of hydroquinone. *Bulletin of the Chemical Society of Japan* **1990,** *63* (4), 1211-1216.
192. Lynd, L. R.; Wyman, C. E.; Gerngross, T. U., Biocommodity Engineering. *Biotechnol Prog* **1999,** *15* (5), 777-793.
193. Girisuta, B.; Janssen, L.; Heeres, H. J., A kinetic study on the conversion of glucose to levulinic acid. *Chemical Engineering Research & Design* **2006,** *84* (A5), 339-349.

194. Hodge, D. B.; Karim, M. N.; Schell, D. J.; McMillan, J. D., Soluble and insoluble solids contributions to high-solids enzymatic hydrolysis of lignocellulose. *Bioresour Technol* **2008,** *99* (18), 8940-8948.
195. Kim, Y.; Ximenes, E.; Mosier, N. S.; Ladisch, M. R., Soluble inhibitors/deactivators of cellulase enzymes from lignocellulosic biomass. *Enzyme Microb Technol* **2011,** *48* (4-5), 408-415.
196. Bouajila, J.; Dole, P.; Joly, C.; Limare, A., Some laws of a lignin plasticization. *Journal of Applied Polymer Science* **2006,** *102* (2), 1445-1451.
197. Guigo, N.; Mija, A.; Vincent, L.; Sbirrazzuoli, N., Molecular mobility and relaxation process of isolated lignin studied by multifrequency calorimetric experiments. *Physical chemistry chemical physics : PCCP* **2009,** *11* (8), 1227-1236.
198. Selig, M. J.; Viamajala, S.; Decker, S. R.; Tucker, M. P.; Himmel, M. E.; Vinzant, T. B., Deposition of lignin droplets produced during dilute acid pretreatment of maize stems retards enzymatic hydrolysis of cellulose. *Biotechnology Progress* **2007,** *23* (6), 1333-1339.
199. Smith, P. K.; Krohn, R. I.; Hermanson, G. T.; Mallia, A. K.; Gartner, F. H.; Provenzano, M. D.; Fujimoto, E. K.; Goeke, N. M.; Olson, B. J.; Klenk, D. C., Measurement of Protein Using Bicinchoninic Acid. *Analytical biochemistry* **1985,** *150* (1), 76-85.
200. van Gool, M. P.; van Muiswinkel, G. C.; Hinz, S. W.; Schols, H. A.; Sinitsyn, A. P.; Gruppen, H., Two GH10 endo-xylanases from Myceliophthora thermophila C1 with and without cellulose binding module act differently towards soluble and insoluble xylans. *Bioresour Technol* **2012,** *119*, 123-132.
201. Gray, M. C.; Converse, A. O.; Wyman, C. E., Solubilities of oligomer mixtures produced by the hydrolysis of xylans and corn stover in water at 180 degrees C. *Industrial & Engineering Chemistry Research* **2007,** *46* (8), 2383-2391.
202. Pan, X. J.; Xie, D.; Gilkes, N.; Gregg, D. J.; Saddler, J. N., Strategies to enhance the enzymatic hydrolysis of pretreated softwood with high residual lignin content. *Applied Biochemistry and Biotechnology* **2005,** *121*, 1069-1079.

203. Zhao, H. B.; Kwak, J. H.; Wang, Y.; Franz, J. A.; White, J. M.; Holladay, J. E., Effects of crystallinity on dilute acid hydrolysis of cellulose by cellulose ball-milling study. *Energy & Fuels* **2006,** *20* (2), 807-811.
204. Marzialetti, T.; Olarte, M. B. V.; Sievers, C.; Hoskins, T. J. C.; Agrawal, P. K.; Jones, C. W., Dilute acid hydrolysis of Loblolly pine: A comprehensive approach. *Industrial & Engineering Chemistry Research* **2008,** *47* (19), 7131-7140.
205. Xiang, Q.; Kim, J. S.; Lee, Y. Y., A comprehensive kinetic model for dilute-acid hydrolysis of cellulose. *Appl Biochem Biotechnol* **2003,** *105 -108,* 337-352.
206. Saeman, J. F., Kinetics of wood saccharification - hydrolysis of cellulose and decomposition of sugars in dilute acid at high temperature. *Industrial and Engineering Chemistry* **1945,** *37* (1), 43-52.
207. Xiao, Z. Z.; Zhang, X.; Gregg, D. J.; Saddler, J. N., Effects of sugar inhibition on cellulases and beta-glucosidase during enzymatic hydrolysis of softwood substrates. *Applied Biochemistry and Biotechnology* **2004,** *113*, 1115-1126.
208. Kumar, R.; Wyman, C. E., Effect of Enzyme Supplementation at Moderate Cellulase Loadings on Initial Glucose and Xylose Release From Corn Stover Solids Pretreated by Leading Technologies. *Biotechnology and Bioengineering* **2009,** *102* (2), 457-467.
209. Rivard, C. J.; Adney, W. S.; Himmel, M. E.; Mitchell, D. J.; Vinzant, T. B.; Grohmann, K.; Moens, L.; Chum, H., Effects of Natural Polymer Acetylation on the Anaerobic Bioconversion to Methane and Carbon-Dioxide. *Applied Biochemistry and Biotechnology* **1992,** *34-5*, 725-736.
210. Kabel, M. A.; van den Borne, H.; Vincken, J. P.; Voragen, A. G. J.; Schols, H. A., Structural differences of xylans affect their interaction with cellulose. *Carbohyd Polym* **2007,** *69* (1), 94-105.
211. Kohnke, T.; Pujolras, C.; Roubroeks, J. P.; Gatenholm, P., The effect of barley husk arabinoxylan adsorption on the properties of cellulose fibres. *Cellulose* **2008,** *15* (4), 537-546.

212. Capanema, E. A.; Balakshin, M. Y.; Kadla, J. F., A comprehensive approach for quantitative lignin characterization by NMR spectroscopy. *J Agric Food Chem* **2004,** *52* (7), 1850-1860.
213. del Rio, J. C.; Rencoret, J.; Prinsen, P.; Martinez, A. T.; Ralph, J.; Gutierrez, A., Structural Characterization of Wheat Straw Lignin as Revealed by Analytical Pyrolysis, 2D-NMR, and Reductive Cleavage Methods. *Journal of Agricultural and Food Chemistry* **2012,** *60* (23), 5922-5935.
214. Yuan, T. Q.; Sun, S. N.; Xu, F.; Sun, R. C., Characterization of lignin structures and lignin-carbohydrate complex (LCC) linkages by quantitative 13C and 2D HSQC NMR spectroscopy. *J Agric Food Chem* **2011,** *59* (19), 10604-10614.
215. Hu, F.; Jung, S.; Ragauskas, A., Impact of Pseudolignin versus Dilute Acid-Pretreated Lignin on Enzymatic Hydrolysis of Cellulose. *ACS Sustainable Chemistry & Engineering* **2012,** *1* (1), 62-65.
216. Qing, Q.; Yang, B.; Wyman, C. E., Impact of surfactants on pretreatment of corn stover. *Bioresour Technol* **2010,** *101* (15), 5941-5951.
217. Roman-Leshkov, Y.; Chheda, J. N.; Dumesic, J. A., Phase modifiers promote efficient production of hydroxymethylfurfural from fructose. *Science* **2006,** *312* (5782), 1933-1937.
218. Mushrif, S. H.; Caratzoulas, S.; Vlachos, D. G., Understanding solvent effects in the selective conversion of fructose to 5-hydroxymethyl-furfural: a molecular dynamics investigation. *Physical chemistry chemical physics: PCCP* **2012,** *14* (8), 2637-2644.
219. Mancera, R. L.; Chalaris, M.; Refson, K.; Samios, J., Molecular dynamics simulation of dilute aqueous DMSO solutions. A temperature-dependence study of the hydrophobic and hydrophilic behaviour around DMSO. *Physical Chemistry Chemical Physics* **2004,** *6* (1), 94-102.
220. Kumar, R.; Hu, F.; Sannigrahi, P.; Jung, S.; Ragauskas, A. J.; Wyman, C. E., Carbohydrate derived-pseudo-lignin can retard cellulose biological conversion. *Biotechnol Bioeng* **2013,** *110* (3), 737-753.